

**AN APPROACH TO MODELING A STREAM-AQUIFER SYSTEM
FOR CONJUNCTIVE MANAGEMENT**

by

**H.J. Morel-Seytoux, Chuanmian Zhang
and R.A. Young**



Colorado Water

Resources Research Institute

Completion Report No. 170

**Colorado
State
University**

AN APPROACH TO MODELING A STREAM AQUIFER SYSTEM
FOR CONJUNCTIVE MANAGEMENT

Chuan-Mian Zhang and H.J. Morel-Seytoux
Department of Civil Engineering

Robert A. Young
Department of Agricultural and Resource Economics

May 1990

Grant No. 14-08-0001-G1411-04

The research on which this report is based was financed in part by the U.S. Department of the Interior, Geological Survey, through the Colorado Water Resources Research Institute. The contents of this publication do not necessarily reflect the views and policies of the U.S. Department of the Interior, nor does mention of trade names or commercial products constitute their endorsement by the United States Government.

COLORADO WATER RESOURCES RESEARCH INSTITUTE
Colorado State University
Fort Collins, Colorado 80523

Robert C. Ward, Director

ABSTRACT

A general methodology for modeling a groundwater system with complex boundary conditions by using the discrete kernel approach is developed. This methodology is applied in modeling a stream-aquifer system where the stream-aquifer relationship is in permanent hydraulic connection. Based on the fact that the interaction flux between stream and aquifer, i.e., return flow, is proportional to the difference between water levels in the river and in the aquifer, the stream-aquifer system is modeled as a boundary-value problem with a time-dependent third type boundary, which, in definition, is a kind of boundary condition where a linear combination of the piezometric head and its normal derivative is prescribed.

This stream-aquifer model includes two parts. The first part is a discrete kernel generator, which generates drawdown discrete kernels and return flow discrete kernels by a finite difference model for the case of homogeneous initial conditions and homogeneous boundary conditions of the third type. These discrete kernels are calculated only once and saved. They are the characteristic coefficients which represent the linear relationship between excitations and responses for a particular physical system. The second part is a simulator, which simulate the responses of the system due to any kind of activities imposed on the system, such as pumping, recharge, irrigation, non-equilibrium of the initial conditions and variation of river stages, in terms of the discrete kernels.

A numerical calculation procedure for the finite difference model is developed for the generation of discrete kernels in a groundwater system with different types of boundary conditions, such as prescribed head boundary and third type boundary. Techniques of "moving subsystem" and "sequential reinitialization" are further improved and used in the generation of discrete kernels and in the simulation procedures respectively, in order to increase the efficiency.

The computer codes have been developed for the finite difference model and for the simulation model. They have been thoroughly tested for accuracy, flexibility and cost. They have performed well in all categories.

Since the relationships between excitations and aquifer responses as well as return flow responses are explicit, the model can easily be used to couple a stream-aquifer system with any kind of policy evaluation or management model for simulation or mathematical optimization. The model has been applied to a part of the South Platte River Basin in Colorado from Denver to Greeley for the purpose of evaluating institutional alternatives for managing that highly interrelated stream-aquifer system from an economic standpoint while accounting for agronomic practices and legal constraints.

TABLE OF CONTENTS

<u>Chapter</u>	<u>Page</u>
ABSTRACT	iii
TABLE OF CONTENTS	iv
LIST OF TABLES	vii
LIST OF FIGURES	viii
1 INTRODUCTION	1
INTRODUCTION	1
REVIEW OF LITERATURE	3
Stream-Aquifer Interaction	3
Stream-Aquifer Simulation Suited for Management ..	6
SCOPE OF PRESENT STUDY	9
2 THE FUNDAMENTAL BOUNDARY VALUE PROBLEM	13
BACKGROUND	13
The Stream-Aquifer Relationship	13
Linear System Approaches	17
Principle of Superposition	17
Duhamel's Method	19
Green's Function Theory	19
Types of Boundary Conditions	20
PRESCRIBED HEAD BOUNDARY VALUE PROBLEM	21
Decomposition of the Problem	22
Convolution Form of the Solution	24
Discrete Form of the Solution	25
Artificial Pumping Rate Equivalent to	
Initial Conditions	26
Complete Solution	28
Determination of the Discrete Kernels	29
SOLUTION FOR A STREAM AQUIFER SYSTEM	30
Problem Decomposition.....	34
Discrete Kernel Generation	38
General Discrete Form Expression for Return Flow .	39
3 NUMERICAL PROCEDURES	42
FINITE DIFFERENCE MODEL FOR GENERATING DISCRETE KERNELS	42

TABLE OF CONTENTS (CONTINUED)

3	NUMERICAL PROCEDURES (CONT)	
	Discretization of a Stream-Aquifer System	43
	Formulation of the Finite Difference Equations ...	45
	Finite Difference Equations Applied to Different Cells	49
	Reach Cells	50
	Active Cells with Excitation	51
	Constant Head Cells	51
	No-Flow Cells	52
	Prescribed Head Cells	52
	Determination of the Drawdown Discrete Kernels	52
	Time Period and Time Step	53
	Solution for Return Flow Discrete Kernels	54
	Moving Subsystem	55
	SIMULATION MODEL	59
	Sequential Reinitialization	60
	Concept of Sequential Reinitialization	61
	Formulas for Sequential Reinitialization	63
	SUMMARY OF NUMERICAL PROCEDURES	67
	Flow Chart for General Two-Step Procedures	67
	Flow Chart for Discrete Kernel Generation Procedures	70
	Flow Chart for Simulation Procedures	70
4	ACCURACY AND EFFICIENCY OF THE METHODOLOGY AND OF THE	
	CALCULATION PROCEDURES	77
	COMPARISON OF RESULTS WITH AN EARLIER PROCEDURE	77
	Description of Test Case	78
	Comparison of the Discrete Kernels of Return Flow ...	78
	Comparison of the Discrete Kernels of Drawdowns	81
	Conclusion of Comparisons.....	86
	ACCURACY AND EFFICIENCY OF THE REINITIALIZATION TECHNIQUE.	87
	Description of Stream-Aquifer System for Accuracy Test	87
	Description of Two Distinct Procedures	87
	Comparison of the Results	89
	Description of Efficiency Test.....	89
	Delineation and Discretization of Stream-Aquifer System	91
	Aquifer Transmissivity	91
	Aquifer Effective Porosity	96
	River Reach Transmissivity	96
	Time Parameters	99
	Selection of Subsystem Size	99
	Initial Conditions	99
	River Stage Drawdowns	99
	Pumping Pattern	99
	Procedure without Reinitialization	101
	Procedure with Reinitialization Every 3 Periods..	101
	Procedure with Reinitialization Every Period ...	101
	Comparison of the Results	101

TABLE OF CONTENTS (CONTINUED)

5	APPLICATION TO A PORTION OF THE SOUTH PLATTE STREAM-AQUIFER SYSTEM	105
	PROBLEM STATEMENT	105
	OBJECTIVES OF STUDY	108
	DESCRIPTION OF THE STUDY AREA	109
	GENERATION OF THE RETURN FLOW DISCRETE KERNELS	111
	Aquifer and Stream Physical Parameters	111
	Determination of the Size of Subsystem	111
	Analysis of the Characteristics of the Return Flow Discrete Kernels	112
	SIMULATION OF RETURN FLOWS	124
	Initial Water Table Drawdowns in the Aquifer	125
	River Stage Drawdowns.....	125
	Net Uniform Withdrawal Rates	126
	Short-Time Simulation of Return Flows due to Natural Conditions	126
	River Mass Balance and Analysis	127
	Sensitivity Analysis in Simulation of Return Flows ..	130
	Long-Term Simulation of Return Flows for Different Management Scenarios	134
6	SUMMARY AND CONCLUSIONS	137
	SUMMARY	137
	CONCLUSIONS	139
	Contributions of This Study	139
	Applicabilities And Potential Uses of the Model	140
	Recommendation for Further Study	141
	REFERENCES	142

LIST OF TABLES

<u>Table</u>		<u>Page</u>
4.1	Comparison of Return Flow Discrete Kernels by Two Methods ($\Delta t_{\min} = \Delta t_{\max} = 1$ period). Uniform unit pulse of Withdrawal occurs in cell (2,2)	80
4.2	Comparison of Drawdown Discrete Kernels by Two Methods ($\Delta t_{\min} = \Delta t_{\max} = 1$ period)	83
4.3	Generation Cost of Discrete Kernels	86
4.4	River Reach Transmissivity and Other Parameters	98
4.5	Initial Water Table Drawdowns (in meters)	100
4.6	River Stage Drawdowns (in meters)	100
4.7	Comparison of Computer Time for Three Procedures ...	104
5.1	Comparison of the Accuracy and Computer Time in Generating Return Flow Discrete Kernels by Different Options for South Platte Study Area	113
5.2	Return Flow Discrete Kernels due to Pumping at Site Indexed 13	115
5.3	Mean Return Flow Discrete Kernel "Epsilon" Due to Pumping at Site 14	118
5.4	Mean Return Flow Discrete Kernel "Epsilon" Due to Pumping at Site 15.....	121
5.5	River Mass Balance	129
5.6	Sensitivity Analysis for Return Flow in m^3	131

LIST OF FIGURES

<u>Figure</u>		<u>Page</u>
2.1	Schematic View of a Stream in Hydraulic Connection with an Aquifer. Definition of Terminology	15
2.2	Finite Difference Grid System for Stream-Aquifer System	33
3.1	A Discretized Hypothetical Stream-Aquifer System.....	44
3.2	Illustration of Notations for Indices and Fluxes for a Finite Different Cell.....	46
3.3	Illustration of Moving Subsystem Concept.....	57
3.4	Illustration of the Spatial Propagation of the Zone of Influence of a Unit Pulse Excitation Beyond the No-Flow Boundary of Box by Sequential Reinitialization	64
3.5	Conceptual Flow Chart for General Two-Step Procedure...	69
3.6.a	Path of Information and of Calculations for Program KERGEIN	71
3.6.b	Path of Information and Calculations for Program KERGEIN.....	72
3.6.c	Path of Information and Calculations for Program KERGEIN.....	73
3.7.a	Procedures to Carry a Simulation by Program KERSIM.....	74
3.7.b	Procedures to Carry a Simulation by Program KERSIM.....	75
4.1	Stream-Aquifer Configuration and Grid System Used in Comparison of Two Procedures for Discrete Kernels Generation	79
4.2	Evolution of Return Flow Rates in Three Reaches due to a Unit Pulse of Pumping in Cell (2,2) of Stream-Aquifer System Shown in Figure 9	82

LIST OF FIGURES (CONT)

<u>Figure</u>		<u>Page</u>
4.3	Comparison of Drawdown Discrete Kernels by Two Methods of Generation	85
4.4	Hypothetical Stream-Aquifer System Used to Test Accuracy of the Reinitialization Technique.....	88
4.5	Comparison of Aquifer Return Flows by Three Procedures (without, with reinitialization every 3 periods, or every period)	90
4.6	Map of Transmissivity Contour Lines for the South Platte Study Area	92
4.7	Map of Saturated Thickness Contour Lines for South Platte Study Area	93
4.8	Map of Water Table Altitude Above Mean Sea Level	94
4.9	Delineation and Discretization of the Hypothetical Stream-Aquifer System	95
4.10	Average Transmissivities in $m^2/15$ days for Cells in Grid for South Platte Study	97
4.11	Comparison of Return Flows by 3 Procedures (without, with reinitialization every 3 periods or every period) for Reaches 3,4 and 5.....	102
4.12	Comparison of Return Flows by 3 Procedures (without, with reinitialization every 3 periods or every period) Reaches 6, 7 and 8	103
5.1	Illustration of Necessity to Estimate Return Flow in Space and in Time	107
5.2	The South Platte Valley from Henderson to Kersey and the Finite Difference Grid System	110
5.3	Five by Five Subsystem Centered at Pumping Site with Index 13	114
5.4	Time Evolution of Return Flows in 4 Reaches due to a Unit Pulse of Pumping in Cell 13	116
5.5	Temporal and Spatial Distribution of Return Flow Due to Pumping at Site 13	117
5.6	Five by Five Subsystem centered at Pumping Site 14 .	119

LIST OF FIGURES (CONT)

<u>Figure</u>		<u>Page</u>
5.7	Temporal and Spatial Distribution of Return Flow Due to Pumping at Site Indexed 14.....	120
5.8	Five by Five Subsystem centered at Pumping Site of Indexed 15	122
5.9	Distribution of Return Flows in Different Reaches Due to a Unit Pulse of Pumping at Site 15	123
5.10	Historical and Simulated Diversions for South Platte Basin During the 1968 Irrigation Season	132
5.11	Historical and Simulated Total Return Flows for Irrigation Season of 1968 in South Platte Basin	133
5.12	Long Term Cyclical Pattern of Seasonal Return Flows in the South Platte Basin	135

Chapter 1

INTRODUCTION

INTRODUCTION

With the development of industry, agriculture and the increase of the population, many places in the world are facing the problem of lack of water resources, especially those arid or semi-arid areas. One of the critically water scarce regions is the northeastern part of China. Studies have shown that the total amount of surface and ground waters is not enough for all the demand from cities and agricultural areas. Similar serious water resources problems both in quantity and quality are threatening many big cities along the east coast of China where the population, industries and business are highly concentrated.

Such critically increasing demand for a sufficient quantity and quality of water, properly distributed in time and space, has forced engineers and planners to propose more comprehensive and complex plans for water resources systems. Such plans include the regulation of natural water supplies and the transportation of water between watersheds, river basins, etc. One of the surface water regulation techniques is to build dams to hold water during the wet season (also prevent flood) and to release water during the dry periods. As needs grow and water supply remains constant, larger and larger storages are required. In many cases it is impossible to find proper dam sites and to obtain the large amount

of necessary capital. The environment concerns are also often difficult to resolve.

An alternative management strategy is to use aquifers, the natural underground reservoirs, which contain ten or hundred times more water than is held in storage in a river or in surface reservoirs. These underground reservoirs are naturally filtering water and regulating water to some degree. Large amounts of water from precipitation or irrigation percolate down into water table as an input to aquifer. The releases from the aquifer are either flow to a river as return flow or flow downstream in the aquifer. Since groundwater flow is much slower, aquifer does behave as a reservoir to hold water a relatively long time. However, while this kind of regulation is not following man's desire, it does show that the aquifer has the capability to regulate water, to redistribute water and to reuse water as long as we provide good management.

For arid or semi-arid areas, where the permanent hydraulic connection does exist between stream and aquifer, the interaction between surface and ground waters provides favorable conditions for development of the water resources. An aquifer is both a vast natural storage reservoir and a conveyance system, and ground water is an alternative water supply. However, without proper management of the stream-aquifer system, those advantages cannot be effectively exploited. The distinct characteristics of water in river and aquifer, which bring advantages to water resource development planning, also create difficulties in understanding their interaction and in simulation of this interaction. The difficulties are also due to the fact that there are so many problems associated with the regulation of water supplies. They are usually problems of hydrology, law,

economics and politics and must be resolved on the basis of broader decision making.

In the past two decades, many studies have been undertaken in the field of conjunctive management of surface and ground waters and great development have been achieved. However the demand for more efficient and cost effective tools still exist because the conjunctive management problems are always associated with a large scale physical system and a long time horizon. In addition, the demand of constant updating of methods still exist because of the variation of management purposes and operation levels.

REVIEW OF LITERATURE

The conjunctive management of surface and ground waters is a subject of great practical, economic and political importance in the field of water resources. Numerous developments associated with this subject have been obtained during last two decades. One of the major development is the technique of the response function approach (discrete kernel approach), which makes the distributed parameter groundwater management practically available. Among the other developments an important branch is the simulation technique of the interaction between stream and aquifer. In order to focus on the literature relevant to this study, this review will primarily cover two aspects: the stream-aquifer interaction and the modeling of stream-aquifer system suited for conjunctive management studies.

Stream-Aquifer Interaction

For the subject of stream-aquifer interaction, Illangasekare (1978) and Peters (1978) have already given an extensive literature review. For completion of this literature review a summarization is presented here for reader's convenience.

The earliest study on the interaction of river and aquifer was developed by Theis (1941). Theis derived an analytical solution for estimation of the flow from a stream to an aquifer caused by pumping near the stream. The ratio of flux from the river and the amount of water pumped from a single well was given under the ideal condition of a homogeneous and isotropic aquifer with an infinitely long straight and fully penetrating river. By placing an image recharge well of equal discharge on the opposite side of river with an equal distance, Theis considered river as a constant head boundary.

Glover and Balmer (1954) used the relationship derived by Carslaw (1921) between quantity pumped and aquifer drawdown to obtain an expression for the ratio of the flux from the river and the flux from the pump under an ideal condition similar to the condition for Theis solution. Glover's method has been used and further developed for many extensive applications.

Jenkins (1968) summarized the relations between the pumping time and stream depletion for an idealized system, which have been derived by several investigators (Theis, 1941; Conover, 1954; Glover and Balmer, 1954; Glover, 1960; Theis and Conover, 1963; and Hantush, 1964, 1965). He generated a set of dimensionless curves and tables which could be employed to estimate the rate of stream depletion. He introduced the stream depletion factor (sdf) which reflects the effects of the hydraulic

properties of the aquifer and the distance between the pumping well and stream. In his later study (1969) this descriptor *sdf* was evaluated for complex heterogeneous aquifers by using electric analog and finite difference digital models.

In all these studies, the changes in stage in the stream were not taken into consideration. Bouwer (1969) discussed the case of flow from a trapezoidal channel, underlain, but not extending to, an impermeable boundary. He calculated seepage by using the piezometric head difference of the channel and water table. The results indicate that the interaction flux between stream and aquifer is proportional to the head difference of the channel and the water table a few river widths away from the channel.

Hornberger (1970) numerically solved the problem of groundwater recession and groundwater flow in response to changes in stream stage in a simple system of a fully penetrating stream in an isotropic homogeneous aquifer. The Boussinesq's equation in one dimension was solved using a finite difference scheme. Zeta and Wiggert (1971) considered the stage change in the stream both in space and time. The dynamic equation describing one-dimensional open channel flow and the equation of one dimensional transient groundwater flow were solved numerically for a fully penetrating stream. Pinder and Sauer (1971) used a similar approach except the head in the aquifer was obtained by solving a two-dimensional transient horizontal flow equation. The differential equations of channel flow and aquifer flow were solved simultaneously, coupled by an expression for flow through the wetted perimeter. The coupling equation was the Darcy's law applied for flow across the thickness of wetted sediment for a partially penetrating rectangular stream.

These works are pioneering efforts in the simulation of stream-aquifer relations. The analytical solutions or numerical models are focused on simulation of the physical characteristics of the interaction between stream and aquifer. However, similar to many groundwater simulation models they are designed to predict the hydrologic behavior of the system in response to a particular set of numerical values of the excitation, such as pumping rates at a given well over several time periods or fluctuation in the river stage over several time periods, rather than provide a functional relation between the response and the excitation.

The increasing demand for managing groundwater system or stream-aquifer system found those groundwater simulation models are difficult to couple explicitly with management models especially for large scale problems with long time horizon. The necessity for simulation of stream-aquifer system suited for management has been gradually realized.

Stream-Aquifer Simulation Suited for Management

Maddock (1972) proposed an efficient method to generate a set of aquifer response functions under the condition that the aquifer system is nonhomogeneous and with irregularly shaped boundaries. He obtained drawdown of the aquifer by taking the convolution integration of input pumping rates through this set of response functions, which he called an "algebraic technological function".

With the introduction of response function to groundwater field, the distributed parameter groundwater modeling methods for management have been developed greatly. Groundwater policy evaluation models based on repeated simulation with response functions have been much more efficient

than using conventional groundwater hydraulic models. In addition, the explicit mathematical expression, as the system responses, have been able used to couple the physical system with the various formulation of management model for different purposes.

Maddock (1974) extended this response function concept to a combined stream-aquifer system and showed the applicability of the method to conjunctive use problems. He assumed that the interaction between the stream and the aquifer "to be such that the stream acts as a constant head boundary to the aquifer; i.e., there is sufficient flow in the stream at all times so that withdrawal directly from the stream or losses from the stream to the aquifer do not affect the head levels in the stream". He indirectly obtained the total volume of return flow during certain time period due to pumping by calculation of the difference between the accumulated quantity of water removed from aquifer storage and the accumulated quantity of water pumped from the wells.

Based on Maddock's work, Dreizin and Haimes (1977) developed a model with multiunit aquifers and interconnected streams. The system responds to pumpage or recharge in two ways: as drawdown in the aquifer or as flow between streams and aquifers. Correspondingly two sets of response functions are calculated. This model is applied to a conjunctive management of groundwater and surface water system with a network of streams and reservoirs all interacting with one another. In this model stream was still assumed as constant head boundary of the system, however to determine the stream-aquifer induced flow due to pumpage from wells, fraction functions relating infiltration to pumpage are developed.

Morel-Seytoux (Morel-Seytoux, et al. 1973) presented a similar procedure for stream-aquifer interaction where the response function was

named "discrete kernel". The reason was described by the paper (Morel-Seytoux, et al. 1980) that:

"Because the Green's function is generated at discrete points in time and space and because the Green's function is the kernel of the resolvent integral equation of the boundary value problem".

Morel-Seytoux and Daly (1975) presented a paper to demonstrate the discrete kernel approach in conjunctive management of stream and aquifer. The distinction of their work compared to Maddock's paper (Maddock, 1974) was, instead of treating stream as a constant head boundary of aquifer, they introduced the research result by Bouwer (1969) that return flow was proportional to the difference in the drawdowns in the stream's surface level and in the aquifer water table a few stream widths away from the stream. Therefore this stream-aquifer model is more reasonable, in terms of physical sense, in the simulation of interaction between stream and aquifer which have permanent hydraulic connection with each other. The further study on calculation of return flow by Peter (1978) showed that the result by this method had a reasonable agreement with the one by mass balance approach on the South Platte River, Colorado, U.S.A.

A combined model of water table and river stage evolution was presented by Morel-Seytoux (1975). By an integral equation it completely characterizes the interaction between a stream and an alluvial aquifer. Four physical characteristics were taken into account in this model. They were initial river drawdowns, initial aquifer drawdowns, upstream inflows and pumping rates. Both dynamics for river and aquifer were considered. The initial conditions for both stream and aquifer were taken into consideration as natural redistribution. Illangasekare (1978) in his dissertation, rederived all those influence coefficients. There are, in

all, 35 kinds of influence coefficients for a complete model of a stream-aquifer system. The major ideas were also described very clearly in the paper (Illangasekare and Morel-Seytoux, 1982) that the discrete kernel approach for an isolated aquifer and the discrete kernel approach for an isolated stream are combined to derive the influence coefficients for a combined stream-aquifer system. The isolated aquifer and the isolated stream are coupled by using a linear relationship for the stream-aquifer interaction.

SCOPE OF PRESENT STUDY

The primary purpose of this study is to develop a stream-aquifer model for the case in which stream and aquifer are in hydraulic connection. This model should be suited for cost-effective simulation or formal optimization in the study of conjunctive management of surface and ground waters.

For the purpose of conjunctive management, it has been realized that the response function approach must be adopted in this model. The significant meaning of generation of the response functions is not only because they represent the physical characteristics of an aquifer or a stream-aquifer system so that all kinds of simulation results may be obtained efficiently by simply using convolution integration through these response functions and any kinds of excitations. An other fundamental significance is that these response functions represent the explicit relationship between huge input and output vectors, so that the efficient tools of mathematical structure for optimization can be utilized for management of conjunctive use of surface and ground waters or coupling a hydrologic model with any social, economical, political or legal model.

It has been also realized that in the literature there are two typical ways in modeling the stream-aquifer interaction. One is to simply treat the stream as a constant head boundary to an aquifer (Maddock, 1974; Dreizin and Haimes, 1977). The other is to couple stream and aquifer by a linear relationship (Morel-Seytoux, et al. 1973; Morel-Seytoux and Daly, 1975; Morel-Seytoux, 1975; Peter, 1978; Illangasekare, 1978; Illangasekare and Morel-Seytoux, 1982). Comparing these two, the author thinks the treatment of stream as a constant head boundary is limited in certain cases. In practical problems, there are only probably very few big rivers, such as the Mississippi River in U.S.A. or the Yangtze River in China, which can be considered with sufficient flow at all times so that the interaction flux between stream and aquifer is not affected by the variation of river stage. Therefore this assumption is not suitable in most cases where rivers are usually wide and shallow, partially penetrating an aquifer. The second problem is, in the numerical model, the river is simulated by constant head cells (as in a finite difference model) (Dreizin and Haimes, 1977), the scale of which (usually 1 mile is detailed enough) are much larger than the real width of the river (several hundred feet) so that this simulation is not reasonable in scales. However with the assumption for river as constant head boundary, the solution of the problem is not complex.

A linear relationship between difference in the drawdowns in the stream level and in the aquifer water table is used to simulate the stream-aquifer interaction in the work of Morel-Seytoux and his colleagues. This relationship is based on physical characteristics in the stream-aquifer system. However the generation of so many influence coefficients makes the solution procedures of the problem not so easy.

In this study it has been found that the linear relationship between stream and aquifer is as same as the third type boundary condition in a bound-value problem in mathematics. Therefore a river is treated as a third type boundary to an aquifer. This treatment follows the physical characteristics of the stream-aquifer interaction but makes the solution procedures much easier. The solution is obtained directly by solving a boundary-value problem in two steps. First, two kinds of discrete kernels are generated, which are drawdown discrete kernels and return flow discrete kernels. They are only generated once. Then in the simulation stage, four types of external excitations to the system are considered. They are initial river drawdowns, initial aquifer drawdowns, variation of river stages and net withdrawals to the aquifer.

The objectives of this study are: (1) to develop the methodology for solutions of a boundary-value problem with different time-dependent boundary conditions; (2) to develop an efficient numerical procedures; (3) to develop a computer program; (4) to test the computer program for accuracy and cost; (5) to apply this model to a real system, a portion of the South Platte stream-aquifer system.

This dissertation consists of six chapters. Chapter 2 discusses different type boundary conditions including the stream-aquifer relationship. It also develops the general methodology for solutions for the fundamental boundary-value problem with different boundary conditions by discrete kernel approach, including solution for stream-aquifer system. The numerical procedures for generation of discrete kernels by a finite difference model, and for simulation are presented in Chapter 3. The accuracy and efficiency of the methodology and of the calculation procedures are presented in Chapter 4. In Chapter 5 the application to

a portion of the South Platte stream-aquifer system and its result are presented. The dissertation is completed with the summary and conclusions in the final chapter.

Chapter 2

THE FUNDAMENTAL BOUNDARY VALUE PROBLEM

The purpose of this chapter is to discuss the solution for the fundamental boundary-value problem by the discrete kernel approach in order to model a stream-aquifer system or any groundwater systems with complex boundary conditions. This chapter includes three sections. The first section is the background, which gives the background for the stream-aquifer relationship, the linear system approaches and the typical types of boundary conditions. The second section explains how to solve a complex boundary-value problem by principle of superposition and discrete kernels approach for a prescribed head boundary-value problem. The last section explains how this methodology is applied to a stream-aquifer system, which is conceptualized as a boundary-value problem with a third type boundary.

BACKGROUND

In order to model a system , it is important to have a thorough understanding about the physical characteristics of that system. The stream-aquifer relationship therefore is discussed before the discussion of the solution procedures.

The Stream-Aquifer Relationship

It is now a well recognized fact that surface and ground waters interact with each other. For example, consider a river in hydraulic connection with an alluvial aquifer. If the water level in the river is higher than in the aquifer, water will flow from the river into the aquifer and vice versa. By definition, baseflow in the stream is provided by depletion of the ground water storage.

The interactive relationship between a stream and an aquifer may display varied characteristics under different geographic or geologic conditions. The most common case is that of a river which partially penetrates the aquifer and is in permanent hydraulic connection with it, as shown in Figure 2.1. There is always water exchange between the river and the aquifer. This is qualitatively reasonable and the real question is: what is the physical law which governs this exchange? Bower (1969) has shown that the discharge at the interface between the river and the aquifer is proportional to the difference in the heads in the river and in the aquifer a few streams width away from the stream (e.g. Morel-Seytoux, 1985). Figure 2.1 illustrates this interaction schematically. This relationship, simply an integrated form of Darcy's law, can be expressed symbolically as:

$$Q_r = \Gamma (h - y) \quad (2.1)$$

where Q_r is the return flow between the stream and the aquifer. Q_r is algebraically defined as positive when the direction of the flow is from aquifer towards river and negative otherwise, h is the water table elevation in the aquifer, y is the stage in the river (both measured from

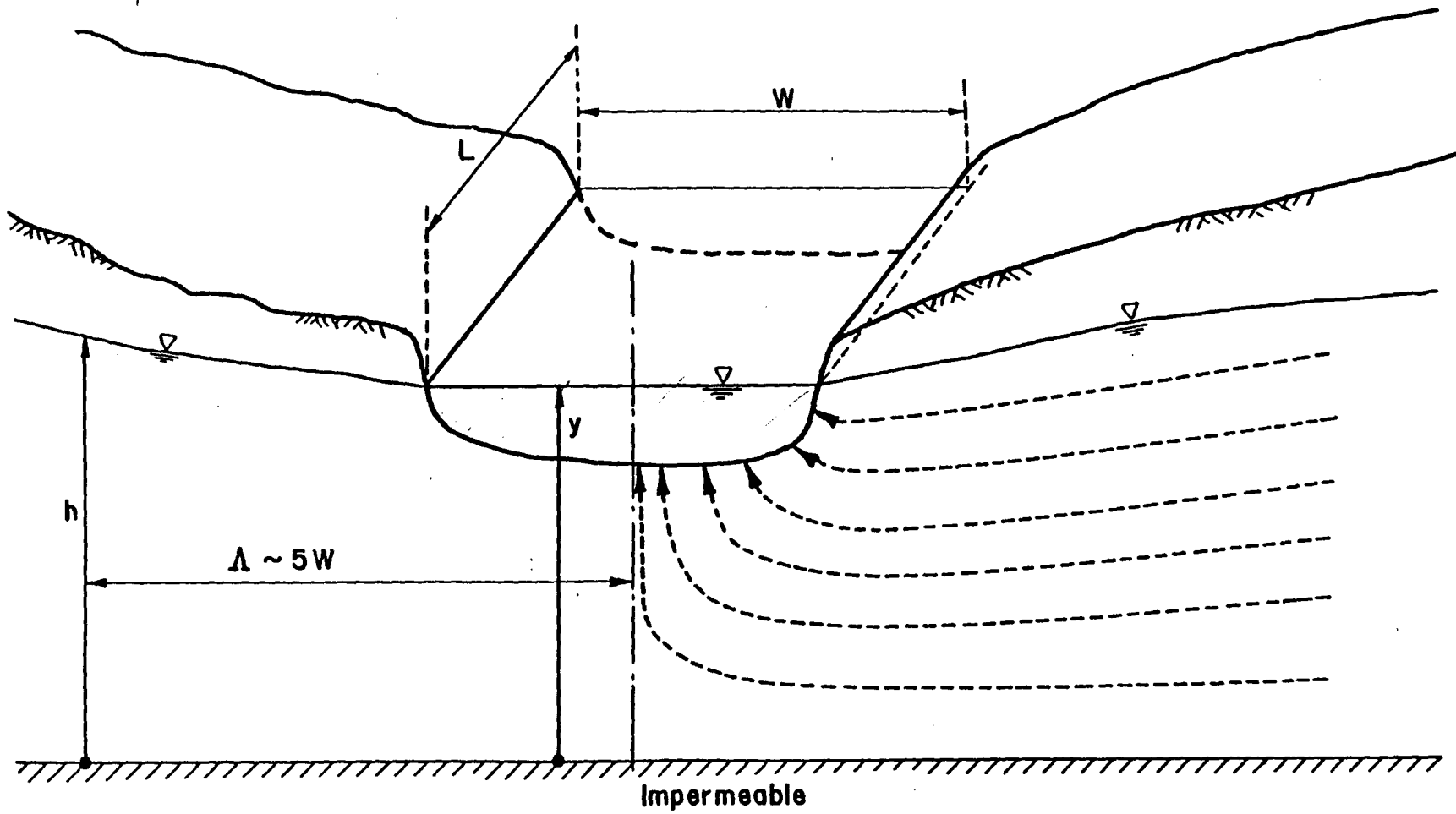


Figure 2.1 Schematic View of a Stream in Hydraulic Connection with an Aquifer. Definition of Terminology.

a common datum), and Γ , the coefficient of proportionality, is the river (or reach) transmissivity (area per unit time) which is a function of the fluid, aquifer and geometric river cross section properties. An approximate expression for Γ is obtained from the method of nets (e.g. Morel Seytoux, 1985):

$$\Gamma = \frac{T}{e} L \left[\frac{W_p + 2e}{e + 2\lambda} \right] \quad (2.2)$$

where L is the length of the reach, W_p is the wetted perimeter of the reach (in practice W_p is essentially the width of the reach, W), λ is the distance from the center of the river to the point where h is evaluated for use in Eq. (2.1). The theoretical and experimental work of Bouwer (1978) (e.g. Morel-Seytoux, 1985) has shown that λ should be of the order of $5W$. T is the local horizontal transmissivity and e is a mean saturated thickness within the distance of $5W_p$ on each side of the river center. Thus approximately the expression for the river transmissivity Γ is:

$$\Gamma = \frac{T}{e} L \left[\frac{W_p + 2e}{e + 10W_p} \right] = KL \left[\frac{W_p + 2e}{e + 10W_p} \right] \quad (2.3.a)$$

Equation (2.3.a) was derived under the assumption that the aquifer is isotropic. In many situations this is not the case and the hydraulic conductivity in the horizontal and vertical directions are quite different. Usually the horizontal conductivity K_H is much larger than the vertical one K_V . Under such conditions the method of flow nets yields the more general formula:

$$\Gamma = \frac{T_H}{e} L \left[\frac{W_p + 2e}{10W_p + \rho_{HV} e} \right] \quad (2.3.b)$$

where T_H is horizontal aquifer transmissivity (i.e. eK_H) and $\rho_{HV} = K_H/K_V$ is a measure of anisotropy. Eq. (2.3.b) reduces to Eq. (2.3.a) when $\rho_{HV} = 1$ (isotropic case). In addition the streambed is often clogged. Over a thickness z_c , the hydraulic conductivity is K_c . In such a situation a more general formula, again developed from the method of flow nets, yields:

$$\Gamma_c = \Gamma \frac{1}{1 + \frac{z_c \Gamma}{W_p L K_c}} \quad (2.3.c)$$

where in this equation Γ is given by Eq. (2.3.b). In the absence of a clogged layer, $z_c = 0$ and Eq. (2.3.c) reduces to $\Gamma_c = \Gamma$. On the other hand when the clogging is severe, K_c is very small and Γ_c reduces practically to $\frac{W_p L K_c}{z_c}$, which means that the entire hydraulic head drop occurs across the clogged layer. In the remainder of this report it is understood that T stands for T_H and the symbol T will be used exclusively for horizontal aquifer transmissivity.

Finally it may happen on occasions that the aquifer heads five widths away from river center are different on the left bank and on the right bank. In this case h in Eq. (2.1) represents the average of the two values.

Linear System Approaches

In this chapter the basic governing equation is linear (being a linearized form of an originally nonlinear equation) and time-invariant. Therefore linear system theory is applicable for the solution of the

problem. Before the discussion of the solutions, it is necessary to review the basic linear system theory.

Principle of Superposition. For a linear system, a powerful tool - the principle of superposition is applicable. As described by Bear (1979), the principle of superpositions states that if $\mu_1 = \mu_1(x,y,t)$ and $\mu_2 = \mu_2(x,y,t)$ are two general solutions of a homogeneous linear partial differential equation $L(\mu) = 0$, where L represents a linear operator, then their sum $\mu_1 + \mu_2$, or in general, any linear combination of μ_1 and μ_2

$$\mu = C_1\mu_1 + C_2\mu_2 \quad (2.4)$$

where C_1 and C_2 are constants, is also a solution of $L(\mu) = 0$. Or, in general, if $\mu_i = \mu_i(x,y,t)$, $i = 1, 2, \dots, n$, are particular solutions of $L(\mu) = 0$, then

$$\mu = \sum_{i=1}^n C_i \mu_i \quad (2.5)$$

where C_i 's are constants, is also a solution of this equation. The constants are determined by requiring that μ should also satisfy the prescribed boundary conditions and prescribed initial conditions. The solution μ in Eqs. (2.4) or (2.5), with coefficients determined so that the boundary conditions and initial conditions are satisfied, is called complete solution of the homogeneous equations.

The principle of superposition can be used to decompose a single complex system into several or many linear homogenous simple systems, the superposition of those solutions from simple systems is just the solution of the complex system. The interpretation of this principle is (1) the presence of one boundary condition does not affect the response produced

by the presence of other boundary conditions (and, of the initial conditions as well), and (2) there are no interactions among the responses produced by the different boundary conditions. Therefore, to determine the combined effect of a number of boundary conditions, it is possible to solve the effect of each individual boundary first and then combine the results. The advantage of the decomposition into subproblems is that the solution of each subproblem is simpler in general.

Duhamel's Method. Another useful tool is the Duhamel's method. As mentioned by Necati Özisik (1968) that Duhamel's method relates the solution of a boundary-value problem with time-dependent boundary conditions and/or sources to the solution of a similar problem with time-independent boundary conditions and/or sources by means of a simple relation. Since it is often easier to obtain the solution of the latter problem, Duhamel's method is a useful tool for obtaining the solution of a problem with time-dependent boundary conditions and/or sources whenever the solution of a similar problem with time-independent boundary conditions and/or sources is available.

Green's Function Theory. Green's function theory is a powerful theory in solution of boundary-value problem of linear system. It is used as a basic approach for this study. The basic idea of the Green's function theory is, as stated by Necati Özisik (1968):

"The solution of a boundary-value problem of heat conduction with distributed heat sources, nonhomogeneous boundary conditions and a prescribed initial condition can be represented in the integral form by means of a Green's function which is the solution of a similar problem for zero initial condition, homogeneous boundary conditions,

and an instantaneous heat source of unit strength situated at a single location within the region."

Discrete kernel is just the Green's function in a discrete form both in space and in time. A complex boundary-value problem of a linear and time-invariant system with distributed excitations can be solved in two steps. In a discrete form, first, to obtain the solution of a similar but homogeneous problem, which means, except a single unit excitation only during the first unit time period, either within the area or on the boundary, all other part of the area or boundary are with no excitations and the initial conditions are zero. This solution is called discrete kernel. Repeat this processes for as many times as needed, one can get all sets of discrete kernels. For the second step, using the principle of superposition and Duhamel's method to obtain the solution for the original complex problem in terms of discrete kernels and any combination of different time-dependent excitations.

Types Of Boundary Conditions

Mostly three types of boundary conditions occur naturally in ground water problems.

When an aquifer is in hydraulic connection with a major body of water such as a large size lake or reservoir, the lake imposes its head on the aquifer. The boundary condition is thus one of a prescribed head at the interface between the lake and the aquifer. If the lake level remains constant in time the prescribed head is constant.

At a boundary where the aquifer terminates as when, for example, a permeable alluvium encounters solid bedrock, the boundary condition at the interface is one of no flow. This natural boundary condition is a

particular case of the more general mathematical boundary condition which stipulates a prescribed flux at the boundary. An example of a prescribed flux as a boundary condition is that of injection of water from high pressure wells or through a recharge trench with very good permeability.

When a river intersects the aquifer, as illustrated in Figure 2.1, the boundary condition described by Eq. (2.1), is one that stipulates a linear relationship between the flux, Q_r , and the head, h , in the aquifer. This type of boundary condition is typical in the presence of a stream and is therefore called a "stream-aquifer" boundary condition. It is also known in the literature as either a boundary condition of the third type or a "radiation" boundary condition or a Fourier or a Cauchy boundary condition. Typically in ground water studies one is interested in only a part of an aquifer. Thus the boundary for the study is not a natural boundary but an artificial one which separates the part of the aquifer of interest from that which is of less interest. Typically, then, the division is artificial and at the boundary the condition cannot be one of a prescribed head or of a prescribed flux. The flux at this artificial interface will depend on what happens internally (i.e. in the aquifer part of interest) described by the head h in Eq. (2.1), and what happens externally (i.e. in the river or in the aquifer part of less interest) described by the stage y in Eq. (2.1). Under such artificial divisions the typical boundary condition will be of the third (or Fourier, or Cauchy, or radiation, or stream-aquifer) type.

PRESCRIBED HEAD BOUNDARY VALUE PROBLEM

To introduce the procedures for solution of the boundary value problem in the general case, it will be convenient to start with the

simplest case, that of a prescribed head over all boundaries. The governing equation is:

$$\phi \frac{\partial s}{\partial t} - \text{div}(TVs) = q(x,y,t) \quad (2.6)$$

where ϕ is effective porosity, s is drawdown, T is horizontal transmissivity and q is volumetric withdrawal rate per unit horizontal area. The domain of applicability of Eq. (2.6) is a spatial domain, D , with a boundary domain (which can be a surface or a line or a combination) denoted B . The boundary condition is a prescribed drawdown $s^B(x,y,t)$ on B . Initially the drawdown in the domain is a spatial function, $s^i(x,y)$.

Decomposition of the Problem.

The principle of superposition provides a convenient method to construct solutions to complex problems from simple solutions to elementary problems. The original boundary value problem, namely:

$$\phi \frac{\partial s}{\partial t} - \text{div}(TVs) = q \quad \text{in } D \quad (2.7.a)$$

subject to boundary condition:

$$s(x,y,t) = s^B(x,y,t) \quad \text{on } B \quad (2.7.b)$$

and initial condition:

$$s(x,y,0) = s^i(x,y) \quad \text{in } D \quad (2.7.c)$$

is decomposed into several subproblems. For each subproblem, there is only one non-homogeneous term.

For the first subproblem the governing equation is:

$$\phi \frac{\partial s}{\partial t} - \text{div}(T\nabla s) = q \quad \text{in } D \quad (2.8.a)$$

subject to the boundary condition:

$$s(x,y,t) = 0 \quad \text{on } B \quad (2.8.b)$$

and initial condition:

$$s(x,y,0) = 0 \quad \text{in } D \quad (2.8.c)$$

The subproblem system is strictly excited by the sink term q , only. For this reason the subproblem will be referred to as the "pure sink" - excitation problem. The classical Theis solution is the simple solution of that subproblem when there is only one well present in the system and the rate of pumping is steady.

For the second subproblem, the governing equation is of the homogeneous type (i.e. has no right-hand side forcing term) namely:

$$\phi \frac{\partial s}{\partial t} - \text{div}(T\nabla s) = 0 \quad \text{in } D \quad (2.9.a)$$

with boundary condition:

$$s(x,y,t) = s^B(x,y,t) \quad \text{on } B \quad (2.9.b)$$

and initial condition:

$$s(x,y,0) = 0 \quad \text{in } D \quad (2.9.c)$$

This is a "pure boundary" - excitation problem (initially the system is at rest and there are no sink terms). A typical problem of this type is one of a lake-aquifer system initially at rest and the lake level starts to fluctuate. One wishes to study the aquifer response to the lake level fluctuations.

For the third subproblem the governing equation is of the homogeneous type again (i.e. no sink term):

$$\phi \frac{\partial s}{\partial t} - \text{div} (\nabla s) = 0 \quad \text{in } D \quad (2.10.a)$$

with boundary condition:

$$s(x,y,t) = 0 \quad \text{on } B \quad (2.10.b)$$

but initial condition:

$$s(x,y,0) = s^i(x,y) \neq 0 \quad \text{in } D \quad (2.10.c)$$

This is a "pure initial condition" - excitation problem (or "pure relaxation" problem). Were the aquifer initially at rest nothing would happen. Ultimately if no external excitations were to be imposed (pumping wells or change in head at boundaries) the system would return to rest (i.e. relax).

One can verify readily that the sum of the solutions to the three subproblems (i.e. the "pure sink"- solution, the "pure boundary" solution and the "pure relaxation" - solution) is a solution to the original complex problem.

Convolution Form of the Solution

Let $k^B(x,y;\xi,\eta;t)$ be a very special solution to the "pure boundary" - excitation problem, where the prescribed drawdown on the boundary is uniformly a unit impulse in time along the boundary (a uniform unit impulse drawdown excitation on the entire boundary). Then it is known from linear system theory (i.e. Green's functions, Duhamel's theorem) that for a general prescribed drawdown on the boundary, s^B , the drawdown solution everywhere, expressed in terms of the unit impulse boundary response (or kernel) function is:

$$s(x,y,t) = \int_B \int_0^t s^B(\xi,\eta;\tau) k^B(x,y;\xi,\eta;t-\tau) d\tau d\xi d\eta \quad (2.11)$$

Similarly the general solution to a "pure sink" - excitation problem can be expressed in terms of a special solution, the response (kernel) to a unit impulse withdrawal excitation at the location of the sinks, in the convolution form:

$$s(x,y,t) = \int_D \int_0^t Q(\xi,\eta;\tau) k^W(x,y;\xi,\eta;t-\tau) d\tau d\xi d\eta \quad (2.12)$$

In Eq. (2.12) $k^W()$ is the unit-impulse kernel of drawdown response at location of coordinates (x,y) due to volumetric withdrawal rate excitation $Q(\tau)$ at singular withdrawal location of coordinates (ξ,η) .

Discrete Form of the Solution

By superposition of solutions given by Eqs. (2.11) and (2.12) and discretization in time and in space (Morel-Seytoux and Daly, 1975) one obtains for drawdown at a location indexed g (which may refer to a point or to an area, e.g. a typical cell in a finite-difference discretization) the expression:

$$s_g(n) = \sum_{p=1}^P \sum_{\nu=1}^n \delta_{gp}^W(n-\nu+1) Q_p(\nu) + \sum_{b=1}^{N_B} \sum_{\nu=1}^n \delta_{gb}^B(n-\nu+1) s_b^B(\nu) \quad (2.13)$$

In Eq. (2.13) $s_g(n)$ is the drawdown at location indexed g at the end of time period n , δ_{gp}^W is the drawdown discrete kernel at cell g due to withdrawal at location indexed p (with dimension of length per discharge), $Q_p(\nu)$ is the mean pumping rate at location p during time period ν , $\delta_{gb}^B()$

is the drawdown discrete kernel at location g (a point or a cell) due to prescribed drawdown at boundary location b (which is dimensionless), $s_b^B(\nu)$ is the mean prescribed drawdown at boundary site b during time period ν . p is the number of total withdrawal sites, and N_B is the total number of boundary sites with prescribed drawdown.

Artificial Pumping Rate Equivalent to Initial Conditions

The "pure initial condition" - excitation problem is different from the other two subproblems. There is no time-dependent external excitation included in this subproblem. The only excitation is the prescribed initial drawdown in the aquifer. Due to the existing head gradients in the domain, water tends to flow. The effect of this flow due to the prescribed initial head gradients can also be considered due to an equivalent "pumping rate" under the homogeneous initial conditions. This equivalent "pumping rate" can be called artificial pumping rate. The relationship of this equivalence can be expressed as:

$$-\text{div} (T\nabla s^i) = q^a(x,y) \quad (2.14)$$

where $q^a(x,y)$ is the artificial pumping rate. Since s^i is known everywhere the values of $q^a(x,y)$ can be obtained by solving Eq. (2.14) .

Substraction of Eq.(2.14) from Eq.(2.10.a) yields:

$$\phi \frac{\partial}{\partial t} (s-s^i) - \text{div} [T\nabla(s-s^i)] = -q^a \quad (2.15.a)$$

noticing that $\phi \frac{\partial s^i}{\partial t}$ is a dummy item which equals zero. The boundary value problem for $(s-s^i)$ is homogeneous with respect to the initial condition because at time zero, very evidently, $s-s^i \equiv 0$. However it is not homogeneous with respect to the boundary condition or the sinks. Problem (2.10) is therefore deduced into Eq.(2.15.a), Eq.(2.15.b) and Eq.(2.15.c) as following.

$$s - s^i = -s^i \quad \text{on B} \quad (2.15.b)$$

$$s - s^i = 0 \quad \text{in D} \quad (2.15.c)$$

Problem (2.15) can be further decomposed into two subproblems, one as a "pure sink" - excitation problem with the artificial pumping as the only excitation term, and the other including the non-homogenous boundary condition as a "pure boundary" - excitation problem. The solution for $(s-s^i)$, and thus s , is deduced from Eqs. (2.11) and (2.12) for $s-s^i$ with a boundary condition $(-s^i)$ and sink distribution $(-Q^a)$ or explicitly:

$$s(x,y,t) = s^i + \int_D \int_0^t k^w(x,y;\xi,\eta;t-\tau) [-Q^a(\xi,\eta)] d\tau d\xi d\eta + \int_B \int_0^t k^B(x,y;\xi,\eta;t-\tau) [-s^i(\xi,\eta)] d\tau d\xi d\eta \quad (2.16)$$

The discrete form of Eq. (2.16) is:

$$\xi(n) = s_g^i - \sum_{\gamma=1}^G \sum_{\nu=1}^n \delta_{g\gamma}^w(n-\nu+1) Q_\gamma^a - \sum_{b=1}^{N_B} \sum_{\nu=1}^n \delta_{gb}^B(n-\nu+1) s_b^i \quad (2.17)$$

where Q_γ^a is the artificial pumping rate at location γ , and s_b^i , prescribed initial drawdown at location b .

Complete Solution

By superposition the complete solution is of the form:

$$\begin{aligned}
 s_g(n) = & \sum_{p=1}^P \sum_{\nu=1}^n \delta_{gp}^w(n-\nu+1) Q_p(\nu) + \sum_{b=1}^{N_B} \sum_{\nu=1}^n \delta_{gb}^B(n-\nu+1) s_b^B(\nu) \\
 & + s_g^i - \sum_{\gamma=1}^G \sum_{\nu=1}^n \delta_{g\gamma}^w(n-\nu+1) Q_\gamma^a - \sum_{b=1}^{N_B} \sum_{\nu=1}^n \delta_{gb}^B(n-\nu+1) s_b^i
 \end{aligned} \tag{2.18}$$

On the right hand side of this equation, the first term is the drawdown due strictly to pumping, the second term is the incremental drawdown due strictly to the prescribed drawdown on the boundary, and the last three terms represent the drawdown contribution strictly due to relaxation. One can notice that if the prescribed drawdown is constant (independent of time), $s_b^B = s_b^i$, the second term and the last term will cancel each other. Of course Eq. (2.18) can be written in the more concise and meaningful form:

$$\begin{aligned}
 s_g(n) = & s_g^i + \sum_{\gamma=1}^G \sum_{\nu=1}^n \delta_{g\gamma}^w(n-\nu+1) [Q_\gamma(\nu) - Q_\gamma^a] \\
 & + \sum_{b=1}^{N_B} \sum_{\nu=1}^n \delta_{gb}^B(n-\nu+1) [s_b^B(\nu) - s_b^i]
 \end{aligned} \tag{2.19}$$

Determination of the Discrete Kernels

The only unknowns for the general solution are the discrete kernels $\delta_{\xi p}^w(\cdot)$, $\delta_{\xi b}^b(\cdot)$ and $\delta_{\xi \gamma}^w(\cdot)$. Each of these looks different from the other, but actually as long as p , b or γ represent the same site in a finite difference model, they are the same or easily deduced from each other. The beauty of the discrete kernels approach (a discrete application of Green's functions) lies essentially in this remark! No matter what kinds of pumping pattern, what kinds of outer region drawdown patterns or initial conditions, the discrete kernels need to be calculated only once for only one single auxiliary problem, which is time-independent, with homogeneous initial conditions and with homogeneous boundary conditions of the proper type (i.e. the same as for the system of concern). This auxiliary boundary-value problem is:

$$\phi \frac{\partial s}{\partial t} - \text{div}(TVs) = D_{\delta}(x,y;\xi,\eta;t) \quad \text{in } D \quad (2.20.a)$$

$$s(x,y,0) = 0 \quad \text{in } D \quad (2.20.b)$$

$$s(x,y,t) = 0 \quad \text{on } B \quad (2.20.c)$$

where $D_{\delta}(\cdot)$ is the Dirac delta function singular at $x=\xi$, $y=\eta$ and $t=0$. The analytical solution of this problem is the Green's function or unit-impulse kernel function $k^w(x,y;\xi,\eta;t)$. Physically this Green's function is the drawdown response of the aquifer at (x,y,t) due to a unit impulse of pumping at singular site of coordinates (ξ,η) at time zero.

Due to the heterogeneous nature of the aquifer, its finite extent and complex boundary shape, it is difficult to find the Green's function by analytical approaches. The numerical technique can be used to generate the discrete form of Green's function -- the so-called "discrete kernel".

The physical significance of the drawdown discrete kernel, $\delta_{gp}^w(n)$, is the response of drawdown of the aquifer at cell g at time n due to a unit pulse of pumping at site p during the first time period. The formulation of the finite difference model for this auxiliary problem as well as the numerical procedures for the calculations are given in the next chapter.

SOLUTION FOR A STREAM-AQUIFER SYSTEM

As seen previously the boundary condition of a stream-aquifer is of the third type (Fourier). The third type boundary condition is defined as one for which neither the head nor the flux but a linear relationship between them is prescribed. As described by Carslaw and Jaeger (1959), if the normal outward flux across the boundary q_n is proportional to the head difference between the boundary and the surrounding medium, so that it is given by

$$q_n = C (h - h_0) \quad (2.21)$$

where h_0 is the water level in the surrounding medium (which can be an aquifer, a river or a lake, etc.), h is the water level right on the aquifer side of the boundary of the flow domain (or in its close neighborhood), and C is a constant. The quantity C can be called "outer" conductivity or "outer" conductance, and it has the dimension of transmissivity. In the limit as C tends to 0, q_n tends to 0 and the third type boundary condition reduces to the no flow boundary condition. In the limit as C tends to ∞ , $(h - h_0)$ tends to 0, and the third type boundary condition reduces to the prescribed head boundary condition.

Comparing Eq. (2.1) with Eq. (2.21) shows that the stream-aquifer relationship is of course a third type (Fourier) boundary condition,

except that Q_r , return flow, is a flux from aquifer to river from both sides of river, and the river need not be at the boundary. Of course one must now develop a better understanding of the term boundary. A boundary is any site where a boundary condition is applied. It must not be understood in the restricted layman sense of outer limit of a domain. The stream-aquifer interaction problem can be solved by solving a two-dimensional boundary value problem treating the stream as a special time-dependent "boundary" of the third type.

The mutual interaction means that river stages and water levels in the aquifer depend on each other. The river stage is a function of return flow and the water level of the aquifer is also a function of return flow. The return flow is an important link between the surface and subsurface systems which will tend to equalize the water levels.

The complete stream-aquifer model should include the dynamics of both conveyance systems (river and aquifer) and their mutual interactions, especially for a stream with limited discharge. However at the current level of model development, the assumption is (temporarily) made that the river exerts full control over the aquifer. In other words river stage is a function of time and space but independent of aquifer water level. The river imposes a boundary condition on the groundwater and the dynamics of the river are not considered.

The influence of the river with a prescribed stage is described by a third type boundary condition for the aquifer. The methodology for solving a boundary-value problem can be directly used for a stream-aquifer system.

Considering an aquifer domain with a stream passing through it (as shown in Figure 2.2), given initial drawdowns of the aquifer, the drawdown

of the river stages are prescribed with time and the pumping rates also vary in time. The special boundary conditions for the aquifer shown in Figure 2.2 are no flow ones on the left and right sides of the aquifer. The conditions on the upper and lower boundaries are not specified at this point. In a finite difference model, the flow domain is divided into cells and the river is divided into reaches according to cells, as shown in Figure 2.2. The mathematical description of the problem is:

$$\phi \frac{\partial s}{\partial t} - \text{div}(\nabla s) = q \quad \text{in } D \quad (2.22.a)$$

$$s(x,y,0) = s^i(x,y) \quad \text{in } D \quad (2.22.b)$$

$$Q_r + \Gamma s = \Gamma \sigma \quad \text{on stream} \quad (2.22.c)$$

$$L(s) = f(x,y,t) \quad \text{on external boundary} \quad (2.22.d)$$

where σ is the drawdown of the river stage relative to the same high datum as aquifer drawdown, Γ is the reach transmissivity, Q_r is the return flow (discharge) between aquifer and river. In Figure 2.2, the river is inside the domain. It could be on the boundary or partially on the boundary. $L(s) = f(x,y,t)$ is any kind of linear boundary condition on the external boundary of the aquifer. In order to concentrate on the solution of the stream-aquifer problem, a discussion of the external boundary condition is postponed until the section on the numerical procedures.

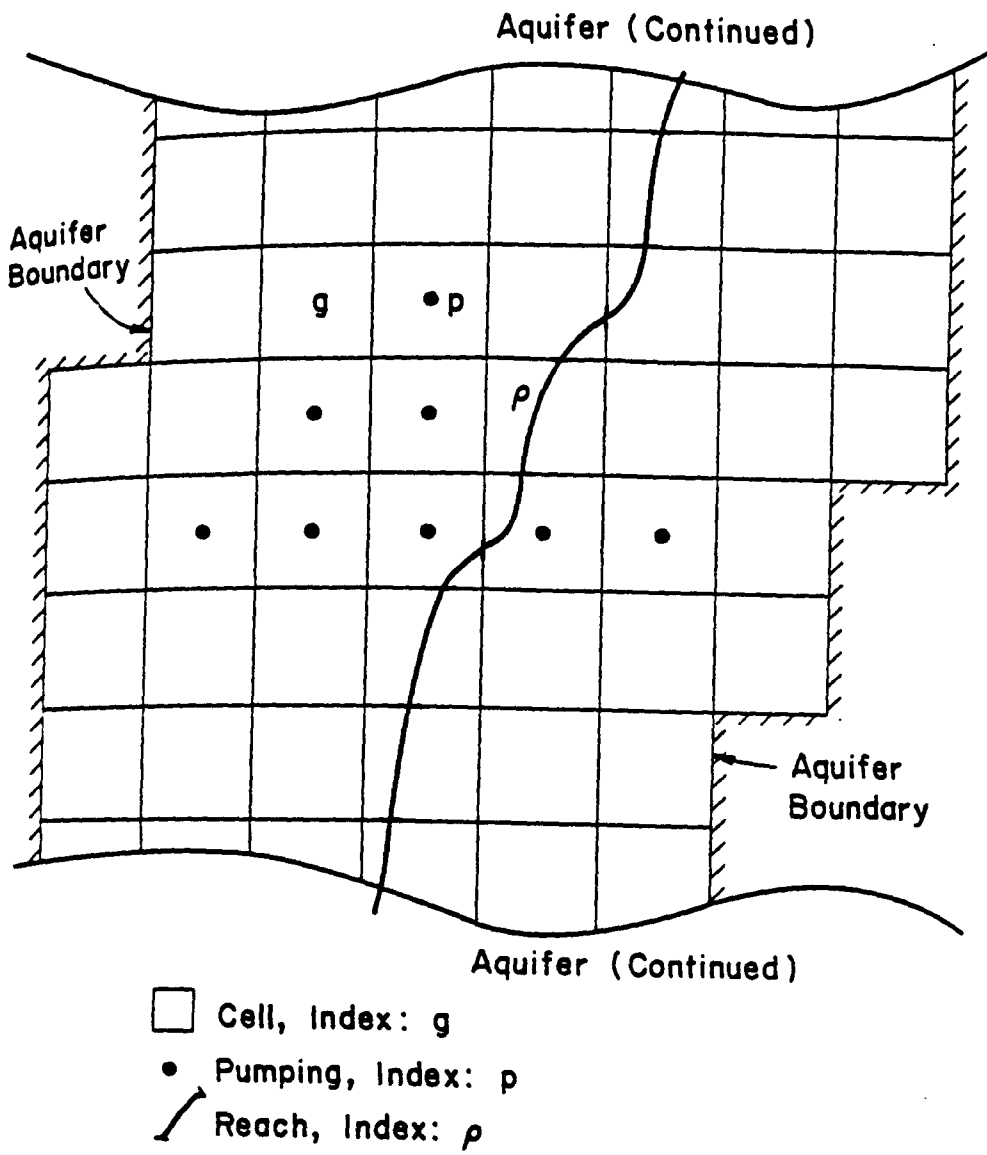


Figure 2.2 Finite Difference Grid System for Stream-Aquifer System

aquifer. The discrete kernel form of the solution to this latter "pure sink"-excitation problem, including the stream-aquifer interaction, is:

$$s_s(n) = \sum_{p=1}^P \sum_{\nu=1}^n \delta_{sp}^w (n-\nu+1) Q_p(\nu) \quad (2.26)$$

where $\delta_{sp}^w()$ is the pumping (withdrawal) drawdown discrete kernel (including the stream-aquifer interaction effect).

For the second subproblem ("pure stream"-problem), the governing equation is homogeneous:

$$\phi \frac{\partial s}{\partial t} - \text{div}(TVs) = 0 \quad \text{in } D \quad (2.27.a)$$

the initial condition is homogeneous:

$$s(x,y,0) = 0 \quad \text{in } D \quad (2.27.b)$$

the only excitation is the stream stage fluctuation:

$$Q_r + \Gamma s = \Gamma \sigma \quad \text{on stream} \quad (2.27.c)$$

One could also treat the return flow as a sink, then the governing equation can be written in the form:

$$\phi \frac{\partial s}{\partial t} - \text{div}(TVs) = q_r \quad (2.28)$$

or, given the nature of q_r :

$$\phi \frac{\partial s}{\partial t} - \text{div}(TVs) + \Gamma' s = \Gamma' \sigma \quad (2.29)$$

Problem Decomposition

Following the decomposition method previously described, the stream-aquifer problem can be similarly decomposed into three subproblems. For the first subproblem ("pure sink"-problem), the governing equation is:

$$\phi \frac{\partial s}{\partial t} - \text{div} (TVs) = q \quad \text{in } D \quad (2.23.a)$$

the initial condition is homogeneous:

$$s(x,y,0) = 0 \quad \text{in } D \quad (2.23.b)$$

and so is the stream boundary condition:

$$Q_r + \Gamma s = 0 \quad \text{on stream} \quad (2.23.c)$$

One could treat the return flow as a sink and instead of specifying a boundary condition along the stream, write the governing equation as:

$$\phi \frac{\partial s}{\partial t} - \text{div} (TVs) = q + q_r \quad (2.24)$$

(q_r is return flow per unit stream horizontal plane area), or instead, given the relation between return flow and drawdown, Eq. (2.24) takes the alternative form:

$$\phi \frac{\partial s}{\partial t} - \text{div} (TVs) + \Gamma' s = q \quad (2.25)$$

where Γ' is reach transmissivity per unit horizontal area. One may notice that on the left-hand side one more item appears, that means the governing equation has included the effect of interaction between stream and

Equation (2.29), is the same as Eq. (2.25) by identification of the sink term q as $\Gamma\sigma$. Consequently the solution for the "pure stream"-excitation problem, including the stream-aquifer interaction, is:

$$s_s(n) = \sum_{\rho=1}^R \sum_{\nu=1}^n \delta_{s\rho}^w(n-\nu+1) \Gamma_{\rho} \sigma_{\rho}(\nu) \quad (2.30)$$

where $\delta_{s\rho}^w()$ is the drawdown discrete kernel due to withdrawal at site ρ (in this case a reach site). These $\delta()$ are the same as in Eq. (26) except for specific sites involved.

It remains to discuss the subproblem for the nonhomogeneous initial conditions in aquifer drawdowns.

$$\phi \frac{\partial s}{\partial t} - \text{div}(\nabla s) = 0 \quad \text{in } D \quad (2.31.a)$$

$$s(x,y,0) = s^i(x,y) \quad \text{in } D \quad (2.31.b)$$

$$Q_r + \Gamma s = 0 \quad \text{on stream} \quad (2.31.c)$$

One should pay more attention to the difference between the equivalent transformation of initial conditions with or without the presence of the stream. If without the presence of the river, such as problem (2.10), the only excitation of the system is the flow due to initial non-equilibrium of the aquifer. However, with the presence of the river, the difference between the initial aquifer drawdown and river stage drawdown ($\sigma = 0$ in this subproblem) will cause additional internal excitation -- return flow, which can be calculated by Eq.(2.31.c):

$$Q_r^a = -\Gamma s^i \quad \text{on stream} \quad (2.32)$$

Therefore in a stream-aquifer problem, the initial conditions are equivalent to two kinds of artificial discharge rates: (1) artificial pumping rate, and (2) artificial return flow rate. The derivation of the solution is as following. Treat the return flow as a sink term and put it at the left-hand side in the governing equation, so that:

$$\phi \frac{\partial s}{\partial t} - \text{div}(TVs) + \Gamma' s = 0 \quad (2.33)$$

Subtraction of Eqs. (2.14) and (2.32) from Eq. (2.33) yields:

$$\phi \frac{\partial (s-s^i)}{\partial t} - \text{div} [TV(s-s^i)] + \Gamma' (s-s^i) = -q^a + q_r^a \quad (2.34.a)$$

with the corresponding change in initial and boundary conditions:

$$s - s^i = 0 \quad (2.34.b)$$

$$Q_r - Q_r^a + \Gamma(s - s^i) = 0 \quad (2.34.c)$$

Problem (2.34) is equivalent to problem (2.31). The initial condition and the boundary condition are all homogeneous in problem (2.34), the only excitation is $(Q_r^a - Q^a)$. Therefore the solution in a discretized form will be:

$$s_g(n) = s_g^i + \sum_{\gamma=1}^G \sum_{\nu=1}^n \delta_{g\gamma}^w(n-\nu+1) \{ -Q_\gamma^a + Q_{r\gamma}^a \} \quad (2.35)$$

By superposition of solutions for these three subproblems, Eqs. (2.26), (2.30) and (2.35), the solution to the original stream-aquifer problem is:

$$s_g(n) = s_g^i + \sum_{\gamma=1}^G \sum_{\nu=1}^n \delta_{g\gamma}^w(n-\nu+1) \{ Q_\gamma(\nu) + \Gamma_\gamma \sigma_\gamma(\nu) - Q_\gamma^a + Q_{r\gamma}^a \} \quad (2.36)$$

Discrete Kernel Generation

The only discrete kernels that need to be generated are the $\delta_{g\gamma}^w(n)$. For simplicity in writing the superscript W will be dropped. These discrete kernels represent the drawdowns at site g due to a unit pulse of withdrawal at site γ in a finite difference solution of Eq. (2.25) with homogeneous initial and boundary conditions.

In the case of a stream-aquifer system, the discrete kernels of return flows are also of interest. It is necessary to find the return flow discrete kernel, $\epsilon_{\rho,p}(n)$, which, by definition, is the mean return flow rate in reach ρ during time period n due to a unit pulse of pumping at cell p. When $\sigma(t) = 0$ on the stream boundary, the return flow at time t is simply, in this special case, $-I_s(t)$. In most cases, the return flow volume during each time period is needed. Thus the return flow discrete kernel during time period n for reach ρ due to a unit pulse of pumping at cell p is:

$$\epsilon_{\rho,p}(n) = \frac{\sum_{i=1}^{M(n)} Q_{r,\rho,p}(t_i) \Delta t_i}{\sum_{i=1}^{M(n)} \Delta t_i} = -\Gamma_{\rho} \frac{\sum_{i=1}^{M(n)} s_{g(\rho),p}(t_i) \Delta t_i}{\sum_{i=1}^{M(n)} \Delta t_i} \quad (2.37)$$

where Δt_i is the time interval for time step i , $M(n)$ is the total number of time steps within the n th time period, $Q_{r,\rho,p}(t_i)$ is the point return flow in reach ρ at time t_i due to pumping at p . $s_{g(\rho),p}(t_i)$ is the point drawdown at cell g , which contains reach μ , at time t_i due to unit pulse of pumping at p , and Γ_{ρ} is the reach transmissivity of reach ρ .

From Eq. (2.37) one can see that the calculation of the return flow discrete kernels follows the integrated form of Darcy's law. The absence of the river stage drawdown is due to the fact that the river stage drawdown is always zero in the auxiliary problem. The calculation of the return flow discrete kernels is done simultaneously with the calculation of the drawdown discrete kernels. As it was the case for the drawdown discrete kernels, the return flow discrete kernels need only be calculated once.

One has to notice that there is difference between these two kinds of discrete kernels. The drawdown discrete kernel is a point value at the end of the time period, while the return flow discrete kernel is the return flow volume increment during the time period. For this reason, use of Eq. (2.37) will give more accurate results than the simpler approximation: $\epsilon_{\rho,p}(n) = -\Gamma_{\rho} \delta_{g(\rho),p}(n)$.

General Discrete Form Expression for Return Flows

By definition the mean return flow rate in reach j is:

$$Q_{rj}(n) = \Gamma_j [\sigma_j(n) - s_j(n)] \quad (2.38)$$

The drawdown $s_j(n)$ is deduced from Eq. (2.37) with $g = j$, thus, with $\gamma(j)$ being the index of the cell in which reach j is located,

$$Q_{rj}(n) = \Gamma_j [\sigma_j(n) - s_{j(0)}^i] - \Gamma_j \sum_{\gamma=1}^G \sum_{\nu=1}^n \delta_{j,\gamma} (n-\nu+1) \{Q_\gamma(\nu) + \Gamma_\gamma \sigma_\gamma(\nu) - Q_\gamma^a + Q_{r,\gamma}^a\} \quad (2.39)$$

For the case of a unit pulse of pumping at site indexed γ and homogeneous conditions Eq. (2.39) reduces to:

$$Q_{rj}(n) = -\Gamma_j \delta_{j,\gamma} (n) = \epsilon_{j,\gamma} (n) \quad (2.40)$$

In terms of the $\epsilon()$ Eq. (2.39) can be written as:

$$Q_{rj}(n) = \Gamma_j \sigma_j(n) - \Gamma_j s_{j(0)}^i + \sum_{\gamma=1}^G \sum_{\nu=1}^n \epsilon_{j,\gamma} (n-\nu+1) [Q_\gamma(\nu) + \Gamma_\gamma \sigma_\gamma(\nu) - Q_\gamma^a + Q_{r,\gamma}^a] \quad (2.41)$$

The physical significance of Eq. (2.36) is that the drawdown at cell g at the end of time period n is a superposition of several influences coming from: initial drawdown at cell g , drawdown due to net withdrawal $Q_\gamma(\nu)$, drawdown due to river stage variation $\sigma_\gamma(\nu)$ and drawdown due to the non-equilibrium initial condition ($Q_{r,\gamma}^a - Q_\gamma^a$).

The physical significance of Eq. (2.41) is that the return flow at reach j during time period n is simply equal to:

$$Q_{rj}(n) = \Gamma_j [\sigma_j(n) - s_{j(0)}(n)] \quad (2.41.a)$$

where $g(j)$ represents cell g which contains reach j . Since $s_{g(j)}(n)$ is caused by three kinds of possible excitations, the return flow as given by Eq. (2.41) reflects this fact.

Chapter 3
NUMERICAL PROCEDURES

The simulation of the behavior of a stream-aquifer system is secured in two stages. First a finite difference model generates the discrete kernels by solving an auxiliary problem with homogeneous initial conditions and homogeneous boundary conditions. Second a simulation model combines the discrete kernels and the relevant excitations for the problem at hand to compute the solution.

FINITE DIFFERENCE MODEL FOR GENERATING DISCRETE KERNELS

The auxiliary problem is described by the governing equation where $U(\xi, \eta; t)$ is a unit pulse of volume withdrawal rate per unit horizontal area at location (ξ, η) :

$$\phi \frac{\partial s}{\partial t} - \text{div}(T\nabla s) = U(\xi, \eta; t) \quad \text{in domain D} \quad (3.1.a)$$

with initial condition

$$s(x, y, 0) = 0 \quad \text{in domain D} \quad (3.1.b)$$

stream boundary condition

$$Q_r + \Gamma s = 0 \quad \text{along the stream} \quad (3.1.c)$$

and boundary conditions

$$s = 0 \text{ or } q_n = 0 \quad \text{on the outer boundary of the domain} \quad (3.1.d)$$

In practical cases, the aquifer and river parameters vary in space, and the boundary configurations are irregular. Numerical methods must be employed to obtain approximate solutions. A fully implicit finite difference scheme is used to solve the problem.

Discretization of a Stream-Aquifer System.

Figure 3.1 shows a spatial discretization of a hypothetical stream-aquifer system into cells and reaches. A rectangular or square mesh system (Figure 3.1 illustrates only the case of squares) is superimposed on a hypothetical stream-aquifer system. To conform with computer array conventions, an i, j coordinate system is used, where i is the row index, $i=1,2,\dots,N_R$, j is the column index, $j=1,2,\dots,N_C$, (N_R represents the number of rows and N_C represents the number of columns). The width of the cells along rows is designated as Δx_j and the width of the cells along the columns is designated as Δy_i . The size of the cells is not necessarily the same for all the cells. The value of drawdown s or the aquifer hydraulic properties such as T , transmissivity, and ϕ , effective porosity, associated with the index of each cell, in concept, represent average values over the extent of the cell. A unit pulse of withdrawal excitation corresponds to a withdrawal of a unit volume, withdrawn uniformly from a single cell during the first time period only, and no excitations in any other cells at any time.

The river is discretized by the finite difference cells into reaches. Another set of indices, $\rho = 1,2,3,\dots$, represents the river reach system. Thus in a cell that contains a reach, there are two indices. For example in Figure 3.1 cell (2,3), i.e. cell for which $i=2$ and $j=3$, contains

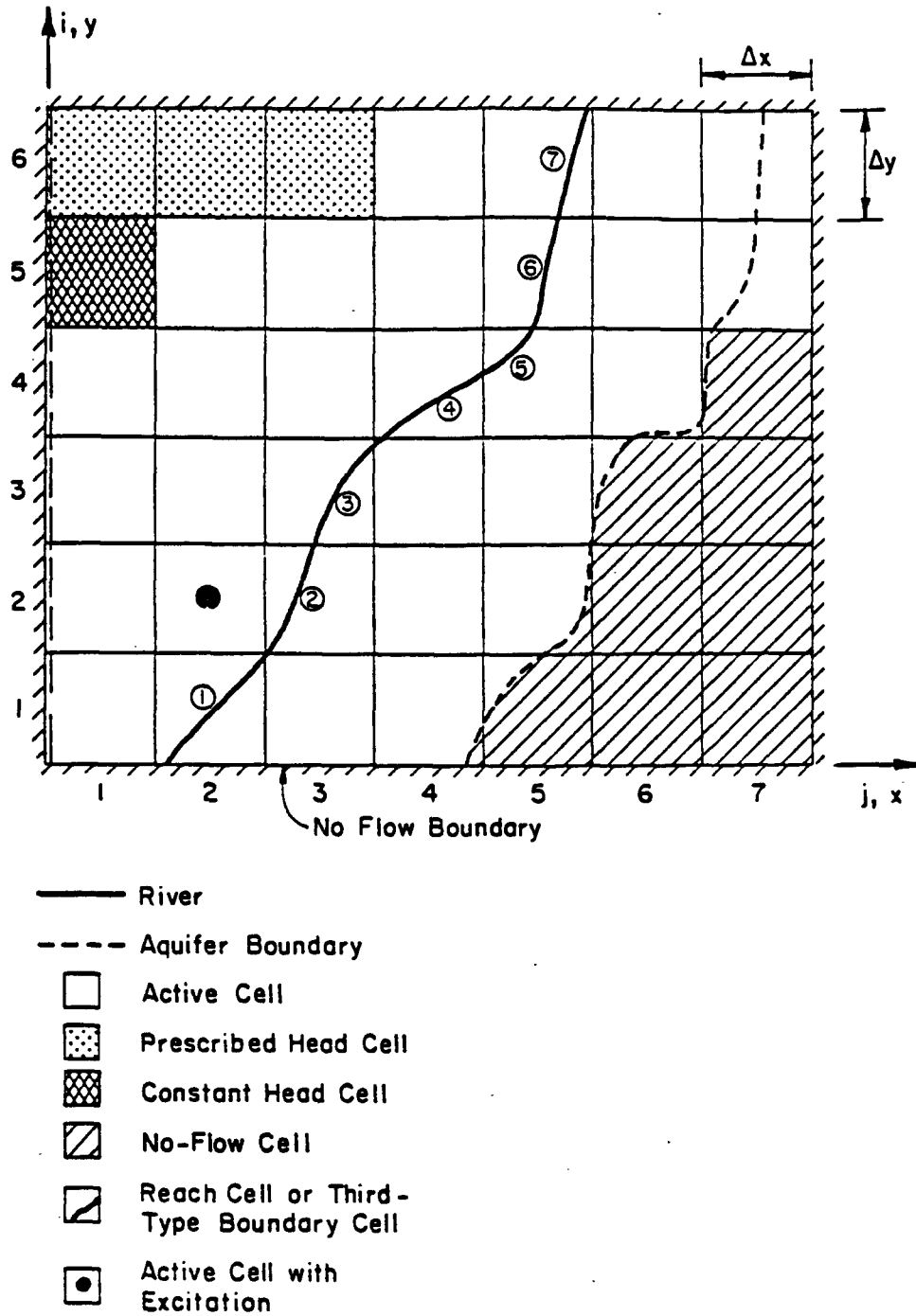


Figure 3.1 A Discretized Hypothetical Stream-Aquifer System

reach(2). The river stage drawdown σ and the reach transmissivity I represent average values for the reach.

For illustrative purposes all types of boundary condition cells are included in this hypothetical system. They are classified as active cells, prescribed head cell, constant head cells, no-flow cells, reach cells or third type boundary cells and active cells with (withdrawal) excitation. Notice that prescribed flux cells are not mentioned because they are essentially as same as active cells with withdrawal excitation. For this reason, the prescribed flux boundary condition will not be particularly mentioned in the rest text.

Formulation of the Finite Difference Equations.

From the mass balance principle, the sum of all flows into and out of a cell must be equal to the rate of change of storage within the cell. Symbolically, if we consider a cell as a control volume, such as cell (i,j) in Figure 3.2, then:

$$QW - QE + QS - QN = -\phi \frac{\Delta s}{\Delta t} \Delta x \Delta y \quad (3.2)$$

where QW is the flow rate into the cell from the west side, QS is the flow rate into the cell from the south side, QN is the flow rate out of the cell from the north side, QE is the flow rate out of the cell from the east side, Δx and Δy are spatial distances of the cell, Δt is the calculation time step, Δs is the change in average drawdown in the cell over the time interval Δt and ϕ is the average effective porosity of the cell.

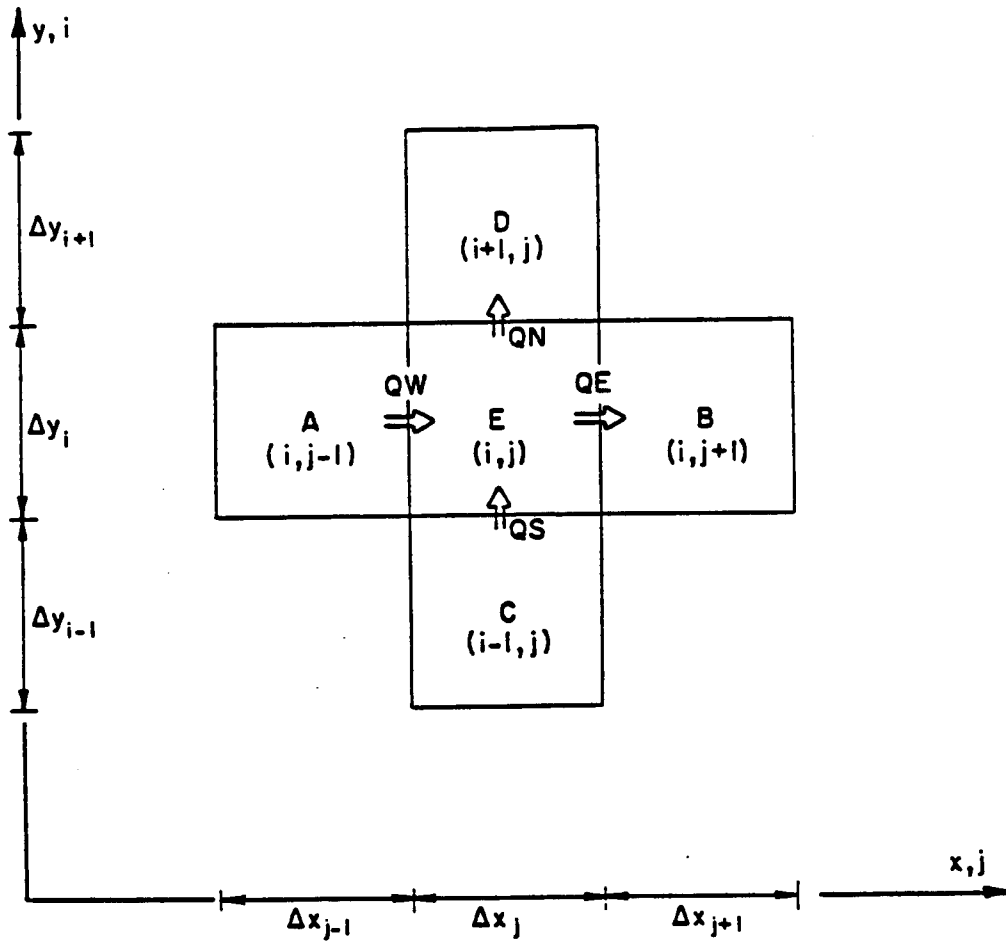


Figure 3.2 Illustration of Notations for Indices and Fluxes for a Finite Different Cell.

Considering cell (i,j) which is an active cell without excitation, the flows into or out of the cell, are approximately given by the expression:

$$QW = Q_{ij-1/2} = -T_{ij-1/2} \frac{(s_{i,j-1} - s_{i,j}) \Delta y_i}{\frac{(\Delta x_{j-1} + \Delta x_j)}{2}} \quad (3.3.a)$$

$$QE = Q_{ij+1/2} = -T_{ij+1/2} \frac{(s_{i,j} - s_{i,j+1}) \Delta y_i}{\frac{(\Delta x_j + \Delta x_{j+1})}{2}} \quad (3.3.b)$$

$$QS = Q_{i-1/2,j} = -T_{i-1/2,j} \frac{(s_{i-1,j} - s_{i,j}) \Delta x_j}{\frac{(\Delta y_i + \Delta y_{i-1})}{2}} \quad (3.3.c)$$

$$QN = Q_{i+1/2,j} = -T_{i+1/2,j} \frac{(s_{i,j} - s_{i+1,j}) \Delta x_j}{\frac{(\Delta y_i + \Delta y_{i+1})}{2}} \quad (3.3.d)$$

where $T_{ij-1/2}$, $T_{ij+1/2}$, $T_{i-1/2,j}$, $T_{i+1/2,j}$ are interblock transmissivities for each side of cell (i,j).

Using a fully-implicit finite difference scheme and applying Eq. (3.2) to cell (i,j), with the substitution of the expressions for the Q from Eqs. (3.3.a), (3.3.b), (3.3.c) and (3.3.d) into Eq. (3.2) yields after change in sign:

$$\begin{aligned} & \frac{2T_{ij-1/2} (s_{ij-1}^v - s_{ij}^v) \Delta y_i}{\Delta x_{j-1} + \Delta x_j} \quad \frac{2T_{ij+1/2} (s_{ij}^v - s_{ij+1}^v) \Delta y_i}{\Delta x_{j+1} + \Delta x_j} \\ & \frac{2T_{i-1/2,j} (s_{i-1,j}^v - s_{i,j}^v) \Delta x_j}{\Delta y_{i-1} + \Delta y_i} \quad \frac{2T_{i+1/2,j} (s_{i,j}^v - s_{i+1,j}^v) \Delta x_j}{\Delta y_{i+1} + \Delta y_i} \\ = & \phi_{ij} \frac{s_{ij}^v - s_{ij}^o}{\Delta t} \Delta x_j \Delta y_i \end{aligned}$$

where s' is the average drawdown at the end of a time step (new value) and s° is the average drawdown at the beginning of a time step (old value).

By placing all the unknowns on the left-hand side and the known quantities on the right hand side, the previous equation takes the form:

$$\begin{aligned}
 & - A_{ij}s'_{ij-1} - B_{ij}s'_{ij+1} - C_{ij}s'_{i-1j} - D_{ij}s'_{i+1j} \\
 & + (A + B + C + D + E)_{ij}s'_{ij} = E_{ij}s^\circ_{ij}
 \end{aligned} \tag{3.4}$$

where

$$A_{ij} = \frac{2T_{ij-1/2}\Delta y_i}{\Delta x_j + \Delta x_{j-1}} \tag{3.4.a}$$

$$B_{ij} = \frac{2T_{ij+1/2}\Delta y_i}{\Delta x_j + \Delta x_{j+1}} \tag{3.4.b}$$

$$C_{ij} = \frac{2T_{i-1/2j}\Delta x_j}{\Delta y_i + \Delta y_{i-1}} \tag{3.4.c}$$

$$D_{ij} = \frac{2T_{i+1/2j}\Delta x_j}{\Delta y_i + \Delta y_{i+1}} \tag{3.4.d}$$

$$\text{and } E_{ij} = \frac{\phi_{ij}\Delta x_j\Delta y_i}{\Delta t} \tag{3.4.e}$$

Equation (3.4) is the final form of the finite difference equation for an interior point. It is a fully-implicit finite difference equation containing five unknowns: s'_{ij-1} , s'_{ij+1} , s'_{ij} , s'_{i+1j} and s'_{i-1j} .

An equation of this type is written for each active cell in the system. The total number of unknowns is equal to the total number of equations. In the system of equations each equation may contain as much as 5 unknowns and the equations must be solved simultaneously.

The coefficients A, B, C, and D are functions of the interblock transmissivities and of the size of the cells. They are calculated once for all to define the system of equations.

The interblock transmissivities may be calculated in several ways. With the harmonic averaging procedure the interblock transmissivity has the form:

$$T_{ij-1/2} = \frac{2(T_{ij})(T_{ij-1})}{T_{ij} + T_{ij-1}} \quad \begin{array}{l} i = 1, 2, \dots, N_R \\ j = 1, 2, \dots, N_C \end{array}$$

whereas with the geometric averaging procedure the expression is:

$$T_{ij-1/2} = \sqrt{T_{ij}T_{ij-1}} \quad \begin{array}{l} i = 1, 2, \dots, N_R \\ j = 1, 2, \dots, N_C \end{array}$$

where N_R is the total number of rows and N_C is the total number of columns in the finite difference model.

Finite Difference Equations Applied to Different Cells.

Equations have to be written for all the active cells in the study domain. Basically there are six types of cells used to represent various types of boundary conditions, as shown in Figure 3.1.

An (interior) active cell is a cell in which the drawdown varies but includes no boundary. A reach cell is a cell which contains a reach. The drawdown difference between river and aquifer causes a return flow. A constant head cell is a cell with drawdown prescribed to remain zero all

the time. A no-flow cell is an inactive cell, actually outside the aquifer. The transmissivity of a no-flow cell is zero. An active cell with excitation is a cell where withdrawal may potentially occur, or flux may be prescribed. The physical nature of the excitation may be ignored. Actually the excitation may result from withdrawal (sink), return flow, prescribed flux. A prescribed head cell is a cell with drawdown prescribed in time.

For noninterior cells, i.e. cells within which a boundary condition is to be imposed, Eq. (3.4) does not apply strictly in that form. Different finite difference equations should be properly written for different cells.

Reach Cells. The finite difference equation for reach cells (or third type boundary cells) requires the presence of the return flow on the right hand side of the finite difference form of Eq. (3.4). However, because this return flow depends upon the unknown drawdown ($Q_r = \Gamma s$), that term is actually placed on the left hand side, namely:

$$- A_{ij} s_{ij-1}^v - B_{ij} s_{ij+1}^v - C_{ij} s_{i-1,j}^v - D_{ij} s_{i+1,j}^v \quad (3.5)$$

$$+ (A + B + C + D + E)_{ij} s_{ij}^v + \Gamma_{ij} s_{ij}^v = E_{ij} s_{ij}^o$$

In some cases if the time step Δt is not small enough, then using average return flow during a time step, namely

$$\bar{Q}_r = - 1/2 \Gamma (s_v + s^o) \quad (3.6)$$

on the right hand side would be better. Hence an alternative equation for a reach cell is:

$$\begin{aligned}
& - A_{ij} s_{ij-1}^v - B_{ij} s_{ij+1}^v - C_{ij} s_{i-1,j}^v - D_{ij} s_{i+1,j}^v \\
& + (A + B + C + D + E)_{ij} s_{ij}^v + 1/2 \Gamma_{ij} s_{ij}^v = E_{ij} s_{ij}^o - 1/2 \Gamma_{ij} s_{ij}^o
\end{aligned} \tag{3.7}$$

Equation (3.7) is no longer a purely fully-implicit finite difference equation, since the average return flow during the time step is expressed via a Crank-Nicolson type scheme. If there are third type boundary cells, beside the reach cells, in the study area, the finite difference equations are the same as Eq. (3.7) except that the symbol Γ refers to the appropriate conductance for the boundary. Equations (3.5) and (3.7) are for the reach cells where there is no potential external excitations.

Active Cells with Excitation. In a cell that contains a sink excitation, the finite difference equation (for the generation of the discrete kernels) includes a unit pulse on the right-hand side, thus is of the form:

$$\begin{aligned}
& - A_{ij} s_{ij-1}^v - B_{ij} s_{ij+1}^v - C_{ij} s_{i-1,j}^v - D_{ij} s_{i+1,j}^v \\
& + (A + B + C + D + E)_{ij} s_{ij}^v = E_{ij} s_{ij}^o + U(n)
\end{aligned} \tag{3.8}$$

where $U(n)$ is a pulse function (i.e. of value one for $0 \leq n \leq 1$ and zero for $n > 1$) and n is the number of time periods.

Constant Head Cells. For a constant drawdown cell (at value zero) the general interior equation, Eq. (3.4), can be used with the special trick (Trescott, et al., 1976) of assigning a very large value to the effective porosity, say $\phi_{ij} = 1.0E+20$ (to represent $\phi_{ij} \rightarrow \infty$, so that $E_{ij} \rightarrow \infty$), in order to keep $s_{ij}^v = s_{ij}^o$. This will cause the drawdown in the cell to

remain unchanged. There is flow exchange with the adjacent cells but $s_{ij}^{\nu} = s_{ij}^0 = 0$.

No-Flow Cells. For a no-flow cell the general interior equation applies but the interblock transmissivities are equal to zero in a no-flow cell. The coefficients A,B,C,D in Eq. (3.4) will have values zero. Thus there is no flow exchange with the surrounding cells. If on one or two sides of a cell there is a no-flow boundary, such as cell (1,1), then some terms are dropped automatically in Eq. (3.4). For cell (1,1) in Figure 3.1, since left and bottom sides of the cell are no flow boundaries, the coefficients A and C would be equal to zero ($T_{1,1/2} = 0$, $T_{1/2,1} = 0$).

Prescribed Head Cells. For a prescribed head cell the general interior equation Eq.(3.4) is applied,

$$\begin{aligned}
 & - A_{ij} s_{ij-1}^{\nu} - B_{ij} s_{ij+1}^{\nu} - C_{ij} s_{i-1,j}^{\nu} - D_{ij} s_{i+1,j}^{\nu} \\
 & + (A + B + C + D + E)_{ij} s_{ij}^{\nu} = E_{ij} s_{ij}^0
 \end{aligned} \tag{3.4}$$

However, if cell (i,j) is the excitation cell, the drawdowns s_{ij} at both time 0 and ν remain value of 1.0 for the first time period, and zero for all the rest time periods. And in all the other prescribed head cells drawdown keeps zero all the time.

Determination of the Drawdown Discrete Kernels

In a finite difference model, different finite difference equations are applied on different cells. According to the definition, the drawdown discrete kernels, are the solutions for a system of finite difference equations under such an excitation pattern that every time there is only one unit pulse of pumping in one cell during the first time period and no

pumping in any other cells all the time. If this unit pulse of pumping happens at reach cell, $U(n)$ should be added at the right-hand-side of Eq. (3.5) or (3.7). It must be mentioned that for a prescribed head cell, the unit pulse of excitation is a unit depth of drawdown. That means the drawdown in that particular cell keeps one for the first time period and zero for all rest time periods, and the drawdowns in all other prescribed head cells keep zero all the time. Changing the excitation pattern to have a unit pulse of pumping in another cell, another set of drawdown discrete kernels are obtained. According to the need, a unit pulse excitation can be imposed on any cell which might have any kind of physical activities previously discussed (e.g. sink, reach, etc.).

There are many techniques for solving a system of linear equations. Here the subroutine UDU, developed by Erik Thompson, professor of Civil Engineering at CSU, is used to solve the system of finite difference equations.

Time Period and Time Step

Before the calculation of the discrete kernels, a time period must be selected. The time period should be chosen according to the simulation or optimization purpose. Usually, the time period is chosen as one week, two weeks or one month because the groundwater flow in the aquifer is pretty slow. The time period selected for the discrete kernels should be the same as the desired simulation output interval.

In the solution of the finite difference equations the time step Δt is selected to meet specified requirements of accuracy. Since the excitation applied to the system is a unit pulse, the discrete kernels within the first two time periods are much more sensitive to the time step

than during the later periods. When the excitation is applied and immediately after it is stopped, the system responds dramatically, whereas after that the system responds more gradually, relaxing itself into an equilibrium condition. For this reason, a small time step, Δt_{\min} , is used for the first step calculation. A time step multiplying factor K_t is chosen. The subsequent time steps are increased by the multiplying factor K_t ($\Delta t_{n+1} = K_t \Delta t_n$) until a maximum time step Δt_{\max} is reached. This procedure is used for the first two periods. A full period is used as the time step for the remaining periods of calculation. The time step is defined as a dimensionless parameter, which is always equal to a certain fraction of one time period, such as 0.01, 0.2, To avoid confusion the symbol DT is used to represent the time step as a fraction of one time period.

Solution for Return Flow Discrete Kernels

The calculation of the return flow discrete kernels is carried out at the same time as the calculation of the drawdown discrete kernels. In the auxiliary problem, the river stage drawdown in each reach cell stays zero all the time. Where there is a unit pulse of excitation in one of the cells, the return flow in any reach is only a function of the response drawdown in that cell which contains the reach, i.e.,

$$Q_{r,\rho}(t) = -\Gamma_{\rho} \sigma_{\rho}(t) \quad (3.9)$$

where ρ is the index of the reach. The average return flow during the m^{th} time step, ending at time t_m and of duration DT_m , is:

$$\bar{Q}_{r,\rho}(t_m) = -1/2 \Gamma_{\rho} [s_{[i,j](\rho)}(t_m - DT_m) + s_{[i,j](\rho)}(t_m)] \quad (3.10)$$

where $[i,j](\rho)$ is the index pair of the cell that contains reach ρ , t_m is time relative to beginning of period expressed in units of periods.

The return flow discrete kernel during a time period or in reach ρ , included in cell (i,j) , is the cumulative volume of return flow during the whole time period, symbolically:

$$\epsilon_{\rho}(n) = \sum_{m=1}^{M(n)} Q_{r,\rho}(t_m) DT_m = -\Gamma_{\rho} \sum_{m=1}^{M(n)} s_{[i,j](\rho)}(t_m) DT_m \quad (3.11)$$

where $M(n)$ is the number of time steps within the time period n , t_m is time at the end of time step m , $t_m = \sum_{\lambda=1}^{M(n)} DT_{\lambda}$, $Q_{r,\rho}(t_m)$ is the point value of return flow at reach ρ at time t_m and $s_{[i,j](\rho)}(t_m)$ is the point value of drawdown in cell (i,j) at time t_m .

The mean return flow discrete kernel during time period n in reach ρ is:

$$\epsilon_{\rho}(n) = -1/2 \Gamma_{\rho} \sum_{m=1}^{M(n)} [s_{[i,j](\rho)}(t_m) + s_{[i,j](\rho)}(t_m - DT_m)] DT_m \quad (3.12)$$

Unlike the drawdown discrete kernels $\delta()$ which have to be calculated for all the active cells, the return flow discrete kernels need only be calculated for the cells that contain reaches.

Moving Subsystem

Based on the fact that the responses (aquifer drawdown or return flow) due to a unit pulse of excitation at one cell are significant only

within a relatively small region around the excitation (a much larger region for confined aquifers), the moving subsystem procedure is introduced in the generation of the discrete kernels in the case of an unconfined aquifer.

The size of the subsystem is determined by the aquifer properties and the total number of time periods for generation. The principle is that during the calculation horizon the responses outside of the subsystem should be practically zero. The size of the subsystem can be decided by trial tests or by an approximate formula (Verdin, et al., 1981). Since the unit pulse excitation must be located at the center of the subsystem, the number of cells in a subsystem is always odd, such as 3 by 3 cells, 5 by 5 cells and so on. To avoid a mass balance error, the external boundary condition for the subsystem is a no-flow boundary.

Figure 3.3 illustrates the manner in which the moving subsystem concept works. Having chosen a 3 by 3 subsystem size, based on the aquifer properties, if there is a unit pulse of pumping at cell (2,2) then the subsystem covers the surrounding 9 cells as shown in Figure 3.3. If there is another unit pulse of pumping at cell (4,3), then the subsystem with its 9 cells will be centered at cell (4,3).

For each subsystem, the number of finite difference equations is equal to the number of cells within the subsystem. Let us consider a system of interest with 400 cells. For each set of discrete kernels (that is for all the responses due to a unit pulse of pumping), a system of 400 finite difference equations must be solved simultaneously if a moving

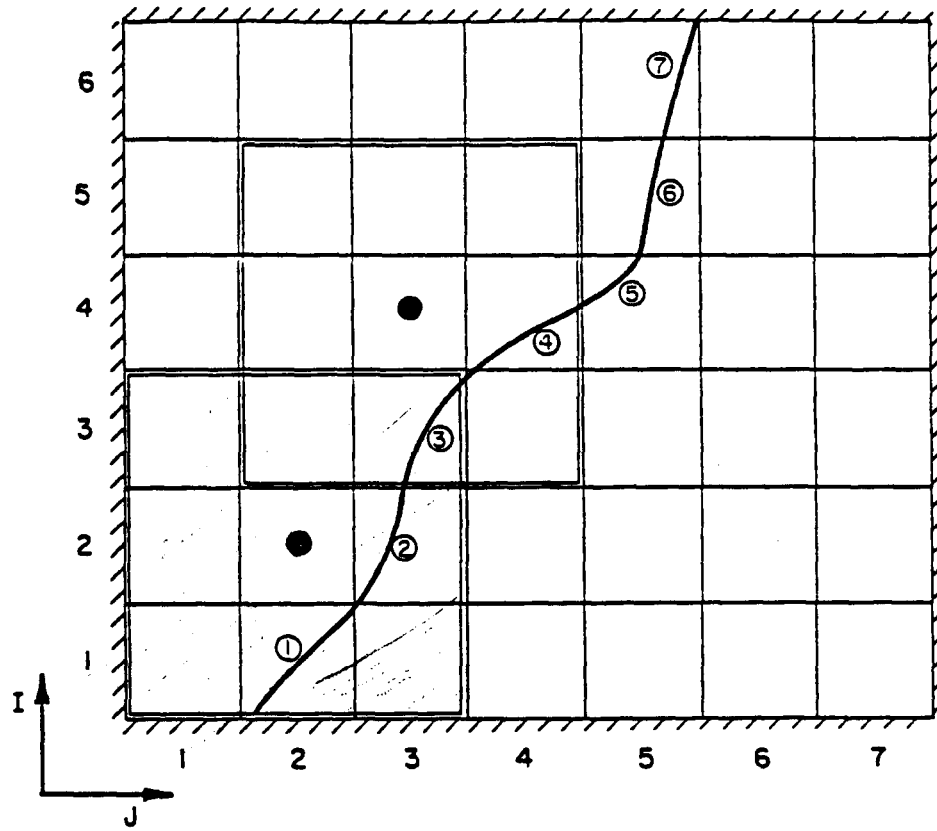


Figure 3.3. Illustration of Moving Subsystem Concept.

subsystem is not used. On the other hand for a 3 by 3 moving subsystem, only 9 finite difference equations need to be solved simultaneously. Only the 9 drawdown discrete kernels which are practically non-zero are regenerated for each time period. At the same time return flow discrete kernels are calculated. The number of return flow discrete kernels in a subsystem is equal to the number of reaches in it.

After the discrete kernels in one subsystem for all the time periods required are generated, the subsystem is moved to the center of the next cell. One after another, the moving subsystem has to be centered to all the active cells with potential excitations. It is important to note that if the initial conditions will be taken care during simulation, all the active cells must be treated as active cells with potential withdrawal excitations. Again let the total number of cells in the system be 400. The discrete kernels can be generated for the system as a whole or by using the moving subsystem procedure. Using the system as a whole $(400)^2$ drawdown discrete kernels for one time period must be generated while with the moving subsystem procedure only 9 (400) drawdown discrete kernels need to be generated.

The conclusion is quite clear that with the moving subsystem, the cost for the generation of the discrete kernels is reduced tremendously, especially for a large-scale system. However, two points must be made. First, for a confined aquifer, since the response to an excitation is felt almost instantaneously throughout the aquifer, it is not suitable to use a moving subsystem except a large one. Second, since the moving subsystem is only proper to generate the discrete kernels for a limited time horizon, during long time simulations, the sequential reinitialization

technique must be used, together with the generation of the discrete kernels using the moving subsystem procedure, for practical problems.

SIMULATION MODEL

Once all the discrete kernels have been generated and saved, major investigations can be pursued by running the simulation model under a variety of different circumstances and with various patterns and types of excitations.

The simulation model is based on a series of algebraic formulae. The equation for calculation of drawdown in the aquifer was developed previously as Eq. (2.36) which represents a linear superposition over space and time for different excitations. The drawdown of aquifer in cell g at the end of the time period n due to all kinds of excitations in an (i,j) system is:

$$s_g(n) = s_g^i + \sum_{i=1}^{N_R} \sum_{j=1}^{N_C} \sum_{\nu=1}^n \delta_{g,ij}(n-\nu+1) [Q_{ij}(\nu) + \Gamma_{ij}\sigma_{ij}(\nu) + Q_{r,ij}^a - Q_{ij}^a] \quad (3.13)$$

where g is an index for a particular cell, which can be characterized alternatively by pair of indices (α, β) representing the cell center coordinates. In Eq. (3.13), the discrete kernels $\delta_{g,ij}(\cdot)$ are already obtained from the generation model. The initial drawdown of the aquifer s_g^i , the pumping rate $Q_{ij}(\cdot)$ and the river stage $\sigma_{ij}(\cdot)$ are provided as inputs. The artificial pumping rates are calculated by an integrated finite difference form of the steady-state governing equation:

Application of Eq. (3.13) for period 3 and beyond is not possible since $\delta(3)$ and $\delta(4)$ are not known. However taking $s_g(2)$ as the new initial drawdown and in addition recalculating the artificial pumping rate Q_{ij}^a and the artificial return flow rate $Q_{r,ij}^a$ since they depend upon the initial conditions which are now different at time 2 than they were at time zero, Eq. (3.13) can be reused for calculation of drawdowns for period 3 and 4, and so on. That means limited number of discrete kernels can be used for unlimited number of time periods (as long as the system is time-invariant) through sequential reinitialization technique.

The propagation in space can also be explained by some illustrative examples. One may wonder how it is possible to make a simulation for a large scale area, such as several hundreds of cells, by using the discrete kernels generated within a limited "moving subsystem" such as 3 by 3 cells. One can argue very reasonably that within a certain number of time periods such as two months, the drawdowns outside of the subsystem due to pumping at the center may practically be zero. However it is certainly not true after 10 years! This argument is correct and it is accounted for by the reinitialization technique because there is spatial propagation beyond the boundaries of the moving subsystem.

Consider the example of the stream-aquifer system shown in Figure 3.4. During the generation procedure, all the cells in it are considered as potential excitation cells. Using a finite difference model, 25 sets of drawdown and return flow discrete kernels are generated for only one time period, by moving a subsystem of 3 by 3 cells from cell (1,1) up to cell (5,5). In the simulation, the initial aquifer and river stage drawdowns everywhere, for this example, are assumed to be zero. The only

excitation is a lone pumping in cell (4,2) for the first time period. After that there are no excitations at all.

The responses at the end of the first time period are certainly limited within the subsystem indicated on Figure 3.4 by the dashed line. In the case of Figure 3.4 the $s(I,J,1)$, drawdowns in cell of coordinates I and J , at time period 1, are different from zero only for $I \geq 3$ and for $J \leq 3$. Similarly the return flows $Q_r(\rho,1)$ in reach ρ during period 1 are different from zero only for $\rho=3$ and 4. Even though pumping has stopped after the first period, the drawdowns at the end of the first period will cause a flow out of the 3 by 3 box. This is due to the fact that artificial pumping rate is a function of the drawdowns of the four neighboring cells. After the first period, for example, the artificial pumping rate in cell (2,3), which is outside the box, is not zero, because one of the neighboring drawdowns, such as drawdown in cell (3,3), is no longer zero. Thus during the second period, cell (2,3) is excited by a Q^* in that very cell and a Q^* in cell (2,2), (3,2), (3,3) and (3,4). Therefore in all the cells, except the bottom right corner cell (1,5), the responses, either drawdowns or return flows are different from zero at the end of the second period.

One can see that in this way, a large scale system can be simulated by those discrete kernels generated within many small "moving subsystems". This is the essential reason for the cost effectiveness of the whole calculation procedures. From these two examples, one may develop an intuitive feeling about the propagation in time and in space for the approach behind the name "sequential reinitialization."

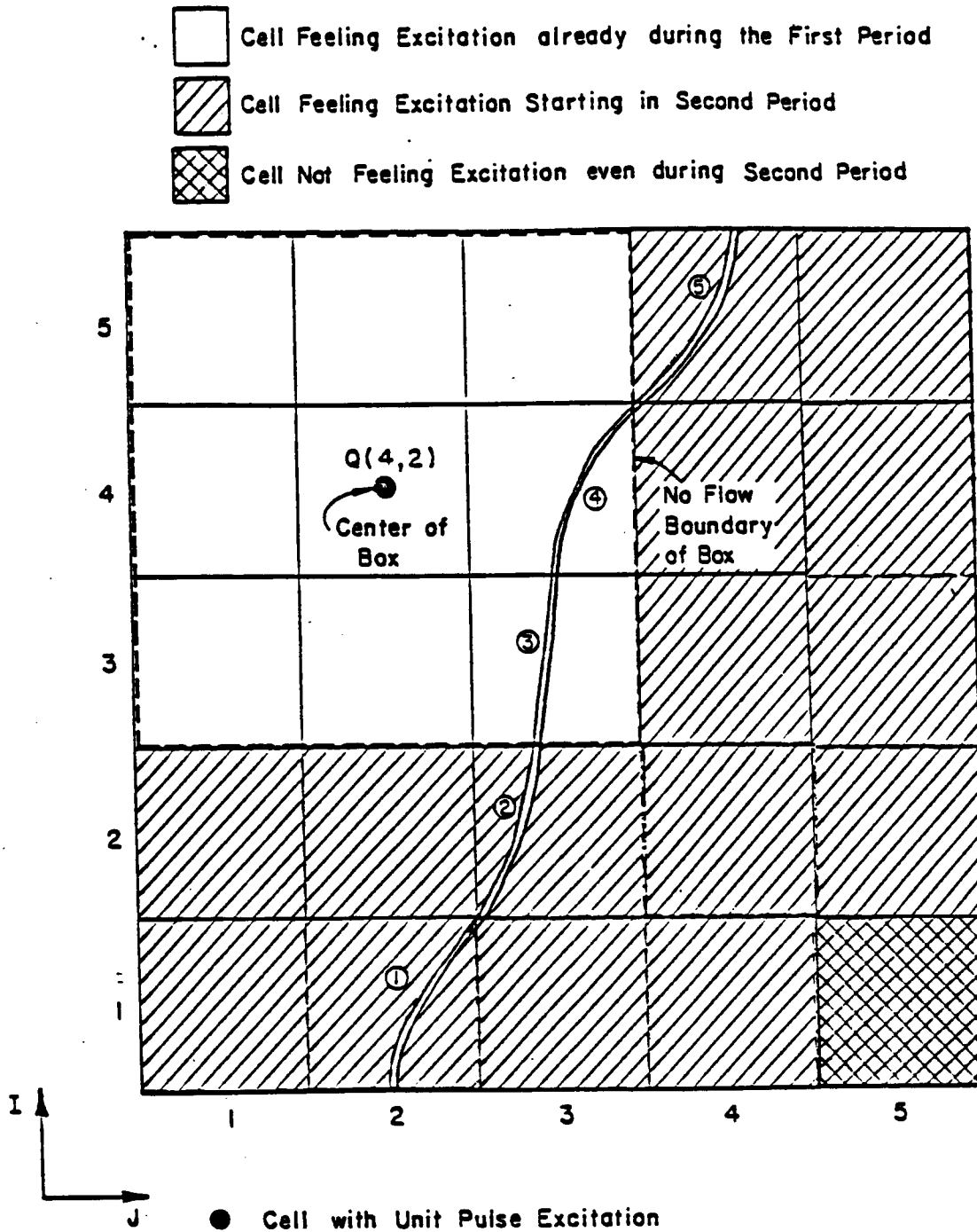


Figure 3.4 Illustration of the Spatial Propagation of the Zone of Influence of a Unit Pulse Excitation Beyond the No-Flow Boundary of the Box by Sequential Reinitialization

Formulas for Sequential Reinitialization. The basic procedures of sequential reinitialization is to predict drawdowns using Eq. (3.13), for as many periods as there are discrete kernels available from the generation step. Let us say that a total of N discrete kernels i.e. $\delta(1)$, $\delta(2)$, ..., $\delta(N)$ are available. Then with Eq. (3.13) drawdowns can be predicted at period times 1, 2, ..., N . At time N one has run out of discrete kernels to proceed further. However, the predicted drawdowns at time N can be thought of as initial drawdowns for the future times. Then Eq. (3.13) can be used again. However since the initial conditions are different at time N than they were at time zero, the artificial withdrawal rates must be recalculated. Once done, it suffices to use Eq. (3.13) to predict drawdowns for another stretch of N periods, etc. Let $Q^a(Nk)$ refers to the value of that rate after k reinitializations have occurred. Thus at time zero and during the first N periods $k=0$. After the first reinitialization $k=1$, etc... Let $s_g(Nk)$ denote the initial drawdown after k reinitializations have occurred. The generalization of Eq. (3.13) for the stretch of time from $Nk+1$ to $N(k+1)$ is:

$$s_g(Nk+n) = s_g(Nk) + \sum_{i=1}^{N_R} \sum_{j=1}^{N_C} \sum_{\nu=1}^n \delta_{g,ij} (n-\nu+1) \{Q_{ij}(Nk+\nu) - Q_{ij}(Nk) + \Gamma_{ij} \sigma_{ij}(Nk+\nu) + Q_{ij}(Nk)\} \quad (3.17)$$

valid for $n=1,2,\dots,N$ and $k=0,1,2,\dots$

Even though many discrete kernels may be available one may wish to reinitialize before one runs out of kernels. More correctly then, N represents the number of periods within a "reinitialization stretch." It

cannot exceed the number of available discrete kernels. One could conceive of reinitialization stretches of different sizes. In Eq. (3.17) it would suffice to replace every product Nk by $t(k)$ defined as:

$$t(k) = \sum_{\kappa=0}^k N(\kappa) \quad (3.18)$$

where $N(\kappa)$ is the number of periods within the κ^{th} reinitialization stretch and $t(k)$ is the moment at which the k^{th} reinitialization occurs. The stretch before reinitialization first occurs is the zeroth stretch. Again $s_g^i(Nk)$ represents the initial condition for the k^{th} reinitialization stretch. It represents the real initial condition only for $k = 0$. Similarly, $Q_{r,ij}^a(Nk)$ and $Q_{ij}^a(Nk)$ are the artificial return flow rates and artificial pumping rates during the k^{th} reinitialization stretch. Therefore all these initial conditions have to be updated at the beginning of each new reinitialization period. Equation (3.17) shows that the drawdowns at any period time can be computed by using previously computed drawdowns as initial conditions and the same set of discrete kernels can be used over and over again. Similarly the reinitialization formula for return flows can be obtained by modifying Eq. (3.16) in the form:

$$Q_{r,\rho}(Nk+n) = -\Gamma_{\rho} s_{g(\rho)}(Nk) + \Gamma_{\rho} \sigma_{\rho}(Nk+n) \\ + \sum_{i=1}^{N_R} \sum_{j=1}^{N_C} \sum_{\nu=1}^n \epsilon_{\rho,ij}(n-\nu+1) [Q_{ij}(Nk+\nu) + Q_{r,ij}^a(Nk) + \Gamma_{ij} \sigma_{ij}(Nk+\nu) - Q_{ij}^a(Nk)] \quad (3.19)$$

for $n=1,2,\dots, N$ and $k=0,1,2,\dots$

The reinitialization formulae given by Eqs. (3.17) and (3.19) provide a very useful tool in simulation for a large-scale and long time horizon

problem. First, with reinitialization, only a few discrete kernels need to be generated while the total simulation horizon can be as long as desired. The computations are very cost-effective. Secondly, because the generation of the discrete kernels within a moving subsystem is limited in space, it is also limited in time. After several time periods, the responses due to any kind of excitation will not be confined within the borders of the subsystem. The reinitialization technique is the necessary tool to propagate responses over space (across the boundary of the moving subsystem) and to extend the responses over time, i.e., to achieve the natural redistribution. This effect can be seen clearly from the examples. In most cases the moving subsystem procedure and the reinitialization technique must be used together unless the moving subsystem is selected large enough and the simulation time horizon is not too long.

One should notice that whenever the moving subsystem and the sequential reinitialization are used, the discrete kernels must be generated with a unit pulse withdrawal excitation for all the active cells, one after another.

SUMMARY OF NUMERICAL PROCEDURES

In order to summarize the numerical procedures, several flow charts are provided. One is the conceptual flow chart for the general two-step procedure. The other two are the procedures for the generation of the discrete kernels and the procedures for the simulation, respectively. The computer programs for generation, KERGEN, and for simulation, KERSIM, are developed following the flow charts.

Flow Chart for General Two-Step Procedure

The flow chart for the general procedure (Figure 3.5) only reflects one of the ways to conduct a conjunctive management study, which is evaluation by simulation. It shows that as long as the discrete kernels are generated and saved, one can evaluate results of the policy variation by repeated simulations in terms of those discrete kernels and the relevant excitations.

In a stream-aquifer system, there are usually three kinds of excitations, which might cause aquifer drawdowns and return flows. The first kind of excitation is direct withdrawal understood in an algebraic sense from the aquifer, as may be caused by pumping, irrigation, artificial recharge, precipitation,.... The algebraic summation of these rates from different causes is called the net withdrawal rate.

The second kind of excitation is the fluctuation in river stage. The drawdowns of the river stage in different reaches will usually vary during different time periods. If one visualizes a river reach as a long and narrow "pumping ditch," then effect of a drawdown in river stage is equivalent to that of pumping. Therefore it seems logical that this excitation of river stage variation can be converted to an equivalent one of net withdrawal.

The third excitation is caused by the initial non-equilibrium conditions. If the initial drawdowns of the aquifer and the initial drawdowns of the river are not zero everywhere relative to steady state,

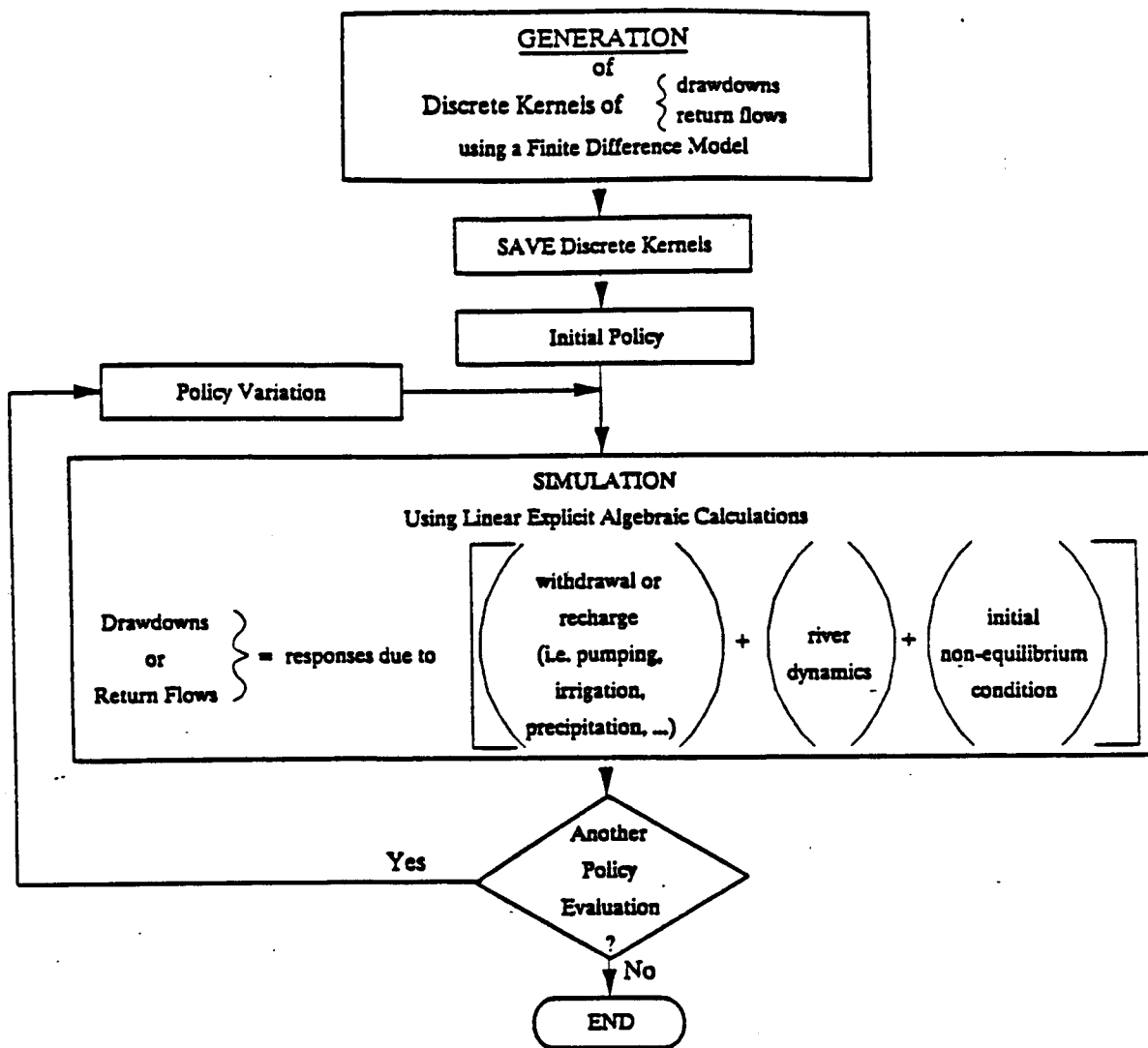


Figure 3.5 Conceptual Flow Chart for General Two-Step Procedure.

even if there are no external excitations, the water table everywhere will change. These non-zero initial drawdowns will cause evolution of drawdowns and return flows. The influence of the non-equilibrium initial conditions excitation types can also be viewed as that resulting from equivalent net withdrawal rates by a proper correspondence.

Since the three kinds of excitations can be replaced by equivalent net withdrawal excitation types, only the generation of the discrete kernels for that type of excitation is necessary. They are generated once and saved. During the simulation, the overall response of the system to various kinds of excitations, reduced to one equivalent kind, is obtained by superposition in time and in space.

Flow Chart for Discrete Kernel Generation Procedures

The flow chart for the discrete kernel generation procedure shows the structure of the computer program KERGEN, which is developed by the author. There are several options available in the computer program. One option (Figure 3.6) is that the program can be used either for a stream-aquifer system or for an isolated aquifer. Another computer code option can generate the discrete kernels with the moving subsystem procedure (for an unconfined aquifer) or not using it (e.g. for a confined aquifer).

Flow Chart for Simulation Procedures

The flow chart for simulation procedures in Figure 3.7 shows the structure of the computer program KERSIM, which is also developed by the author. It shows the procedures for using the sequential reinitialization techniques for a stream-aquifer system.

Procedures for optimization will depend on the kind of mathematical programming selected for use and upon the type of objective function and constraints pertinent to the problem at hand.

FLOW CHART SHOWING DISCRETE KERNEL GENERATION PROCEDURES

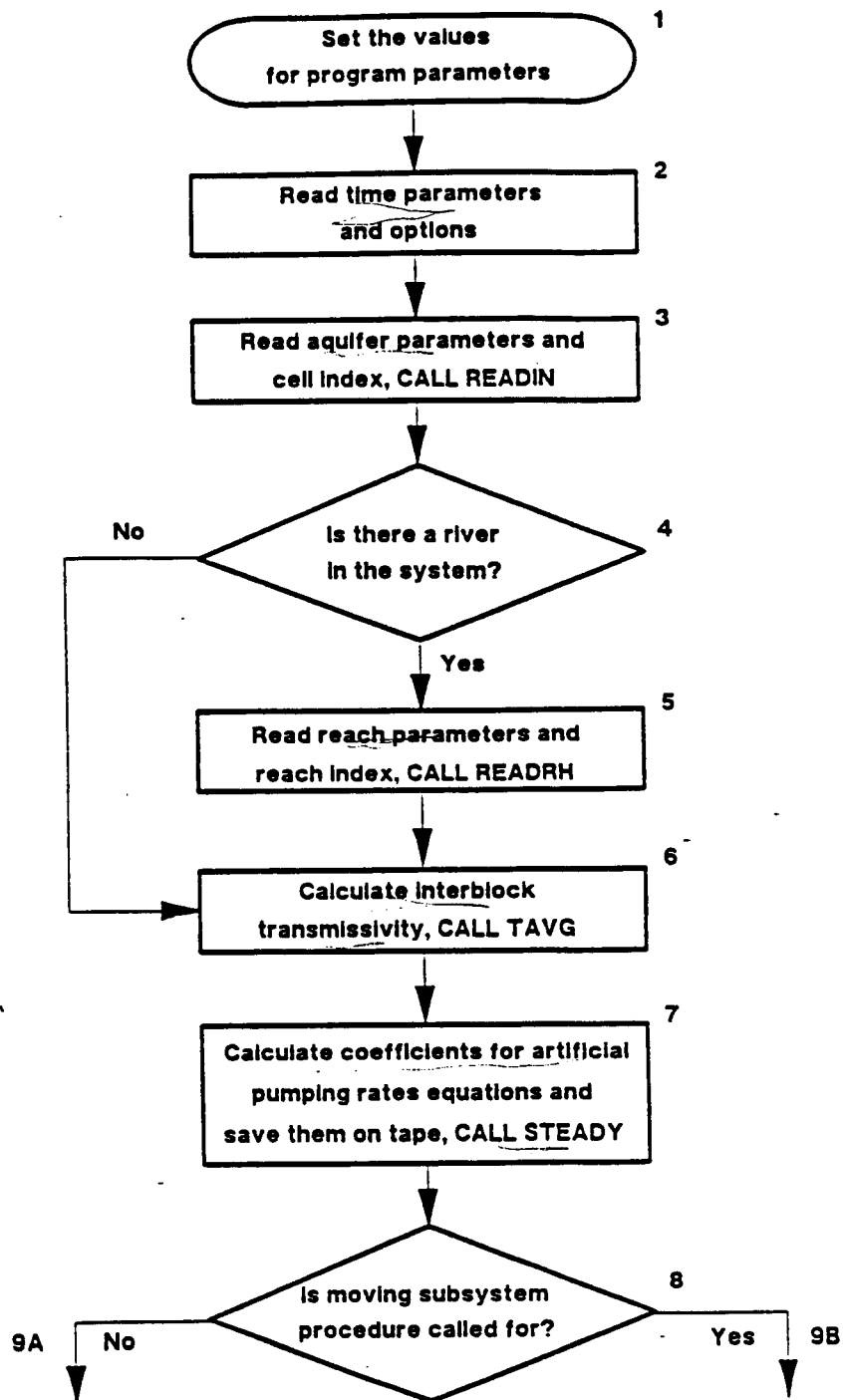


Figure 3.6.a Path of Information and Calculations for Program KERGEN.

FLOW CHART SHOWING DISCRETE KERNEL GENERATION PROCEDURES

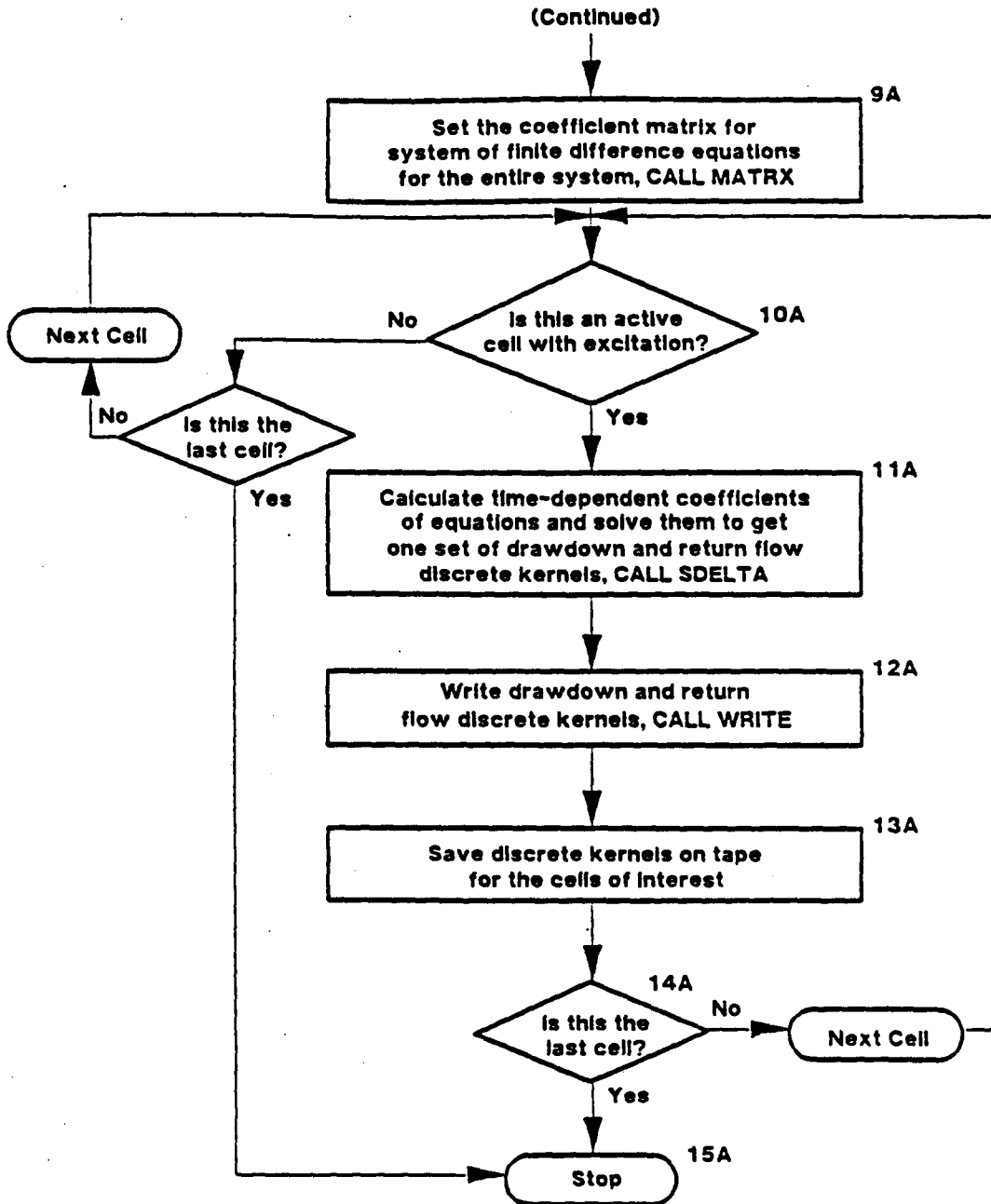


Figure 3.6.b. Path of Information and Calculations for Program KERGEN.

FLOW CHART SHOWING DISCRETE KERNEL GENERATION PROCEDURES

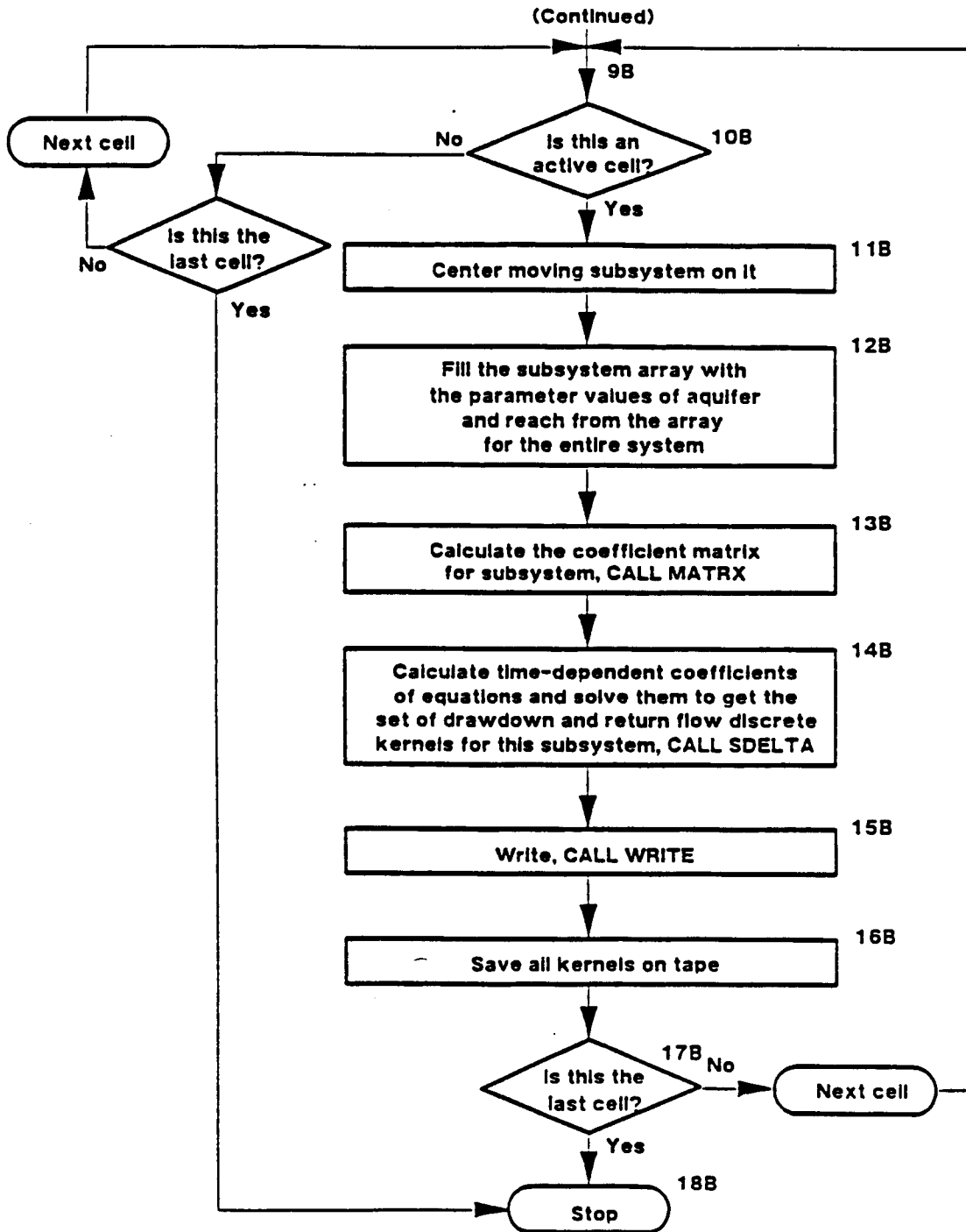


Figure 3.6.c. Path of Information and Calculations for Program KERGEN.

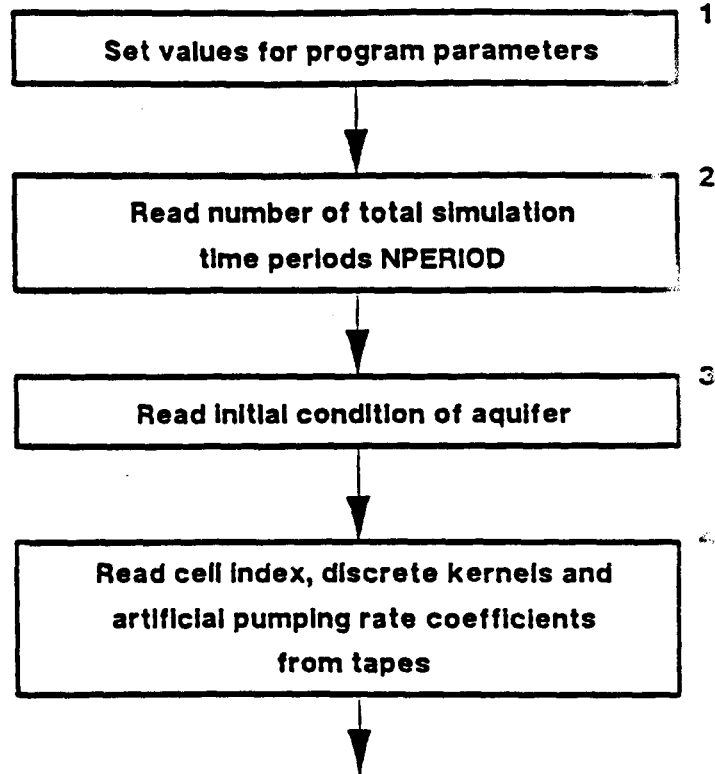
FLOW CHART SHOWING SIMULATION PROCEDURES

Figure 3.7.a. Procedures to Carry a Simulation by Program KERSIM.

FLOW CHART SHOWING SIMULATION PROCEDURES

(Continued)

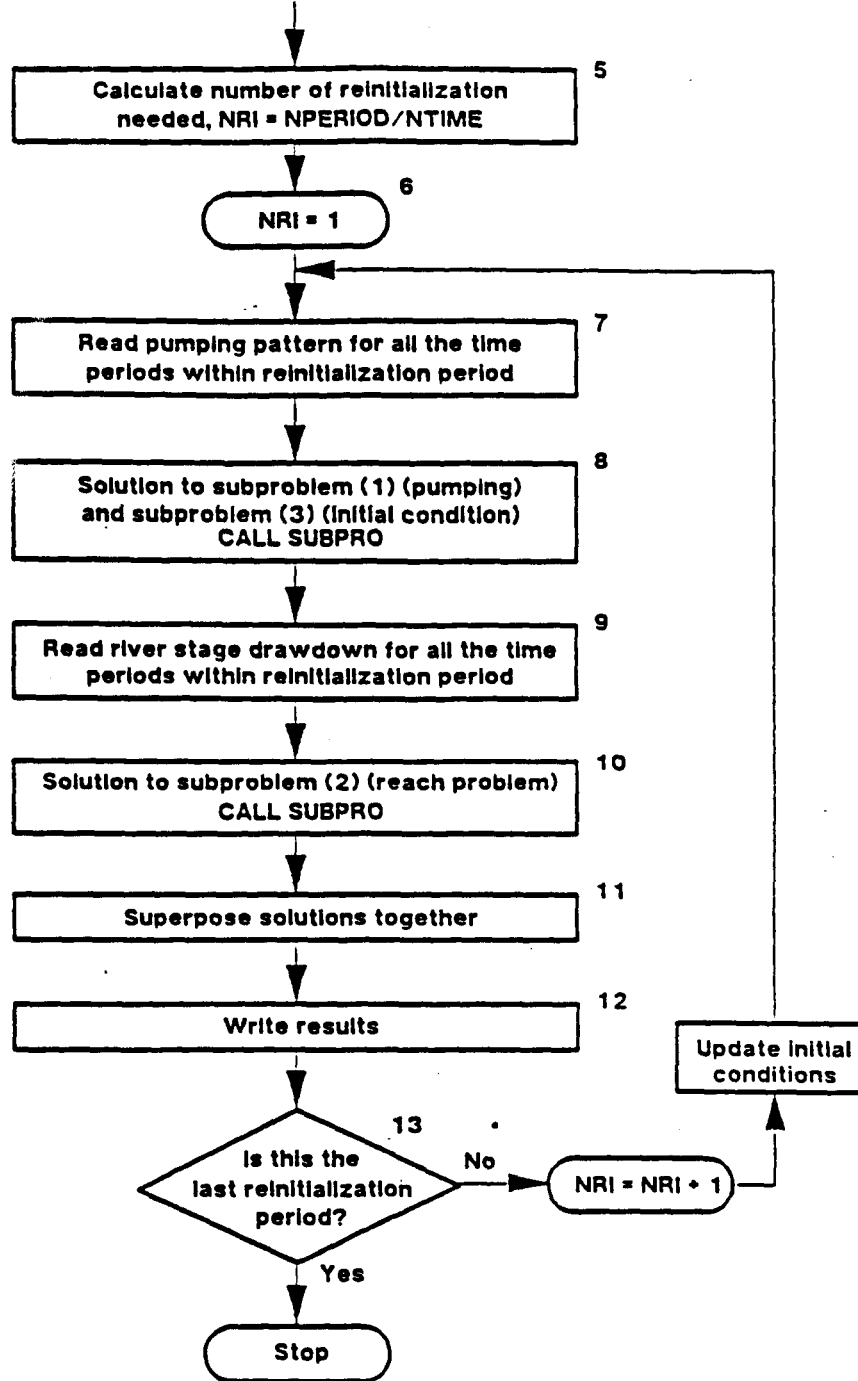


Figure 3.7.b. Procedures to Carry a Simulation by Program KERSIM.

Chapter 4

ACCURACY AND EFFICIENCY OF THE METHODOLOGY AND OF THE CALCULATION PROCEDURES

The purposes of the methodology tests were to check the correctness of the methodology and computer codes and to demonstrate their efficiency. The tests are based on two very simple hypothetical cases and one more realistic hypothetical case. The computer codes KERNEL, KERGEN AND KERSIM are developed by the author. The procedures for use of these computer codes are described in a separate report (Zhang and Morel-Seytoux, 1989).

COMPARISON OF RESULTS WITH AN EARLIER PROCEDURE

In the early work of Morel-Seytoux (Morel-Seytoux et al., 1973; Morel-Seytoux, 1975; Morel-Seytoux and Daly, 1975) the procedure for the generation of the discrete kernels of drawdown and of return flows was different than the one presented in this report. In this early procedure the discrete kernels of drawdown were first generated without the presence of the stream. Then in a second step the presence of the stream was considered and the discrete kernels of return flow generated, and if desired, the discrete kernels of drawdown, including the influence of the stream, are calculated. Because the calculation procedures are different but the results should be the same, the comparison verifies the correctness of the new procedure presented in this research.

Description of Test Case

Figure 4.1 displays the hypothetical stream-aquifer configuration and the grid system used for the comparison. The cell size is uniform with $\Delta x = \Delta y = 1600$ m. The aquifer transmissivity has value $50,000 \text{ m}^2/\text{period}$. The effective porosity has value 0.2. The river passing through the area is divided into five reaches. The river reach transmissivity is uniform of value equal to $100,000 \text{ m}^2/\text{period}$. The number of periods selected for the generation of the discrete kernels is four with the month being the period. There is pumping in only one cell of coordinates (2,2). The boundary condition is one of no flow along the four sides and initially the water table is horizontal.

Comparison of the Discrete Kernels of Return Flow

The comparison is made by running two different programs KERNEL (for the early procedure) and KERGEN (for the new procedure). Two runs are made for two sets of time parameters, that is the initial calculation time step Δt_{\min} , the multiplication time step factor K_t and the maximum time step Δt_{\max} . In one run $\Delta t_{\min} = \Delta t_{\max} = 1$ period = 1 month. The comparison for that run is displayed in Table 4.1. The results are exactly the same. This indicates that the two methods are strictly equivalent (which is a theoretical result) even as numerically implemented. This comparison indicates that the new procedure was programmed correctly for the computer.

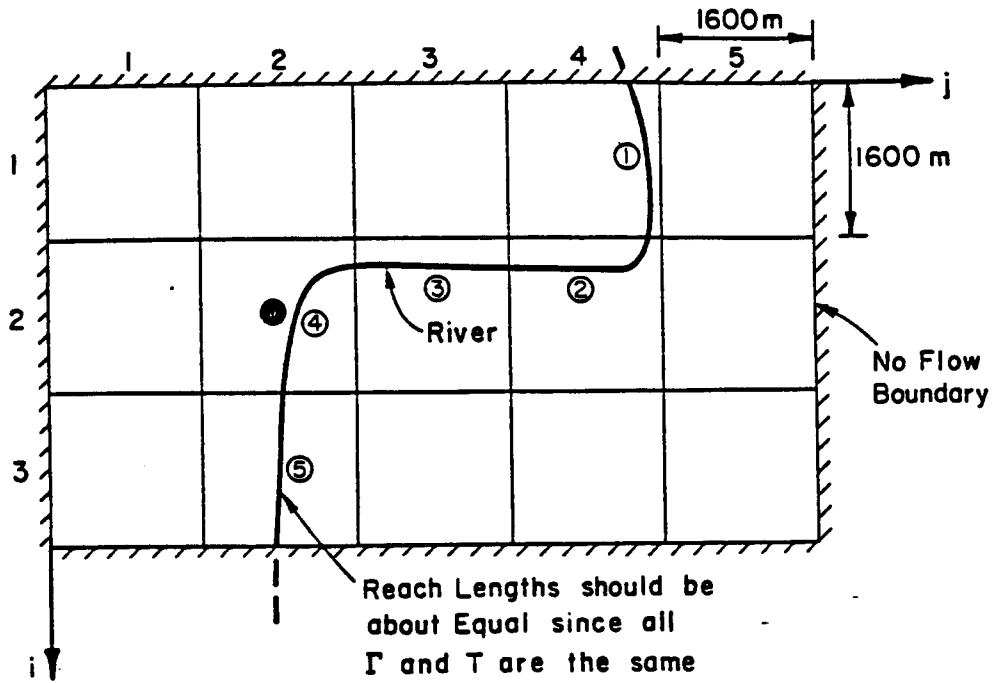


Figure 4.1. Stream-Aquifer Configuration and Grid System Used in Comparison of Two Procedures for Discrete Kernels Generation.

Table 4.1

Comparison of Return Flow Discrete Kernels by Two Methods

$$(\Delta t_{\min} = \Delta t_{\max} = 1 \text{ period})$$

Uniform Unit Pulse of Withdrawal Occurs in Cell (2,2)

a) Early Procedure (e.g. Morel-Seytoux and Daly, 1975)

Reach	Period				
	1	2	3	4	
1	-0.00007	-0.00028	-0.00056	-0.00085	
2	-0.0031	-0.00090	-0.00138	-0.0068	
3	-0.00451	-0.01025	-0.01138	-0.0167	
4	-0.06691	-0.10925	-0.06988	-0.0405	
5	-0.00481	-0.01113	-0.01270	-0.0122	

(b) New Procedure

	Time = 1	Time = 2	Time = 3	Time = 4
REACH 1	-.00007	-.00028	-.00056	-.00085
REACH 2	-.00031	-.00090	-.00138	-.00168
REACH 3	-.00451	-.01025	-.01138	-.01067
REACH 4	-.06691	-.10925	-.06988	-.04605
REACH 5	-.00481	-.01113	-.01270	-.01222

In a second run Δt_{\min} was set at a value of 0.01, Δt_{\max} at 0.10 and K_1 was equal to 1.5. Figure 4.2 displays the time response of return flow rates due to a unit pulse of pumping in cell (2,2) for reaches 3, 4 and 5. There is very little difference between the procedures, the differences being due to differences in numerical errors of the two procedures.

Comparison of the Discrete Kernels of Drawdowns

The same aquifer configuration (see Figure 4.1) is used with the same aquifer and stream parameter values. In one run the time parameters are $\Delta t_{\min} = \Delta t_{\max} = 1$ period = 1 month. The results are shown in Table 4.2. The results are identical, again as they theoretically should be. This comparison provides further assurance that the new procedure implementation on the computer is correct.

In a second run the time parameters were: $\Delta t_{\min} = 0.01$, $\Delta t_{\max} = 0.10$ and k_1 (AFAC in computer code) = 1.5. Figure 4.3 shows the results for cells (1,2), (2,2) and (3,2). Figure 4.3 also shows the drawdown response due to a unit pulse of pumping without the presence of the stream, denoted the isolated aquifer discrete kernels. Again there are no differences between the two methods. The drawdowns when the river is present are less than when it is not, the river providing a partial replacement for the water taken out of aquifer storage by pumping.

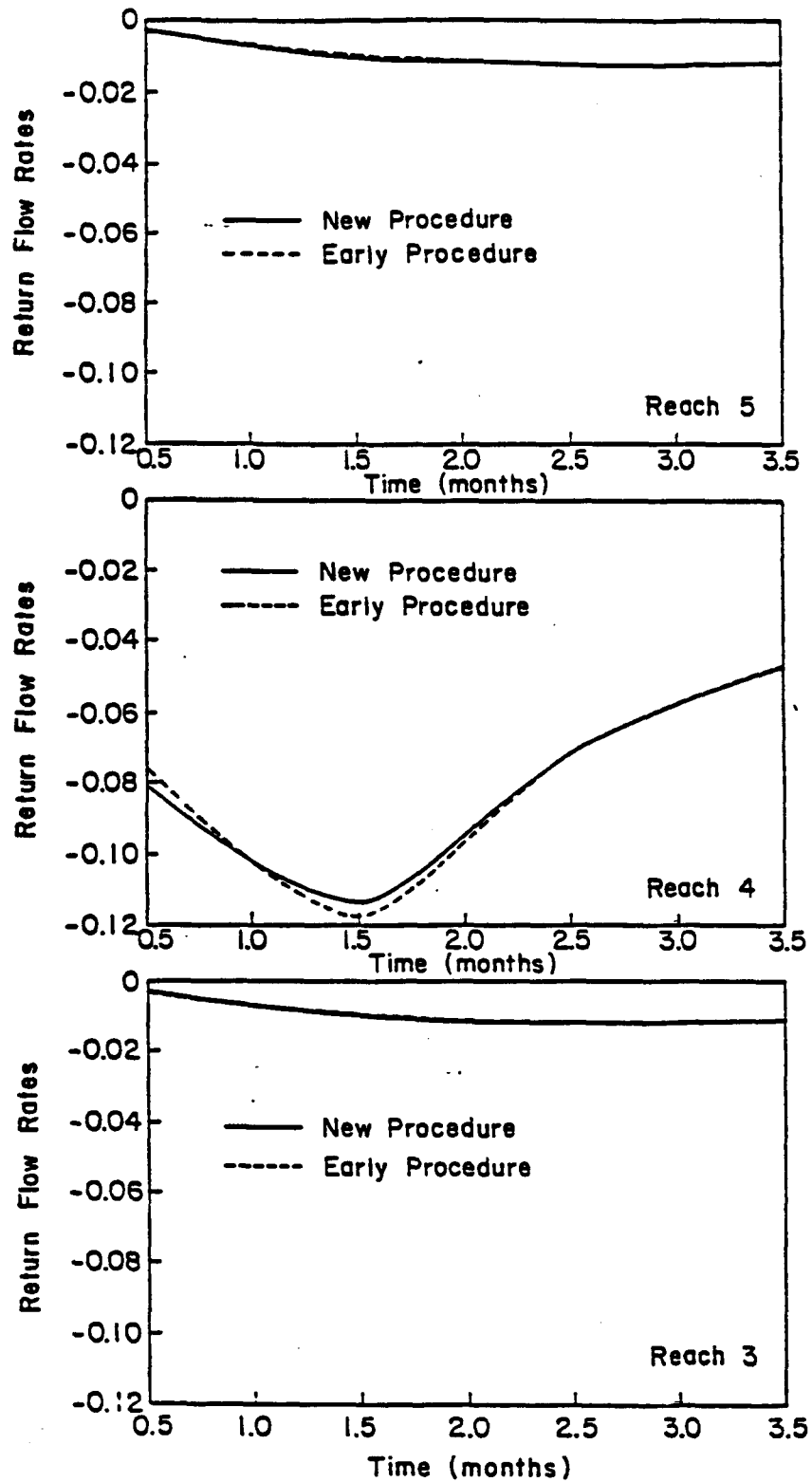


Figure 4.2. Evolution of Return Flow Rates in Three Reaches due to a Unit Pulse of Pumping in Cell (2,2) of Stream-Aquifer System Shown in Figure 4.1.

Table 4.2.

Comparison of Drawdown Discrete Kernels by Two Methods $(\Delta t_{\min} = \Delta t_{\max} = 1 \text{ period})$

(a) Early Procedure

Period Time = 1

	J= 1	J= 2	J= 3	J= 4	J= 5
I= 1	.16915E-07	.10346E-06	.14731E-07	.14772E-08	.16061E-09
I= 2	.10358E-06	.13381E-05	.90105E-07	.61429E-08	.48866E-09
I= 3	.16315E-07	.96112E-07	.14182E-07	.15477E-08	.16637E-09

Period Time = 2

	J= 1	J= 2	J= 3	J= 4	J= 5
I= 1	.3857E-07	.14928E-06	.31660E-07	.40589E-08	.57768E-09
I= 2	.14971E-06	.84677E-06	.11499E-06	.11913E-07	.13673E-08
I= 3	.36211E-07	.12645E-06	.29534E-07	.43733E-08	.60818E-09

Period Time = 3

	J= 1	J= 2	J= 3	J= 4	J= 5
I= 1	.59316E-07	.16501E-06	.45990E-07	.70578E-08	.12596E-08
I= 2	.16598E-06	.55087E-06	.11264E-06	.15750E-07	.24439E-08
I= 3	.54268E-07	.12746E-06	.41567E-07	.78132E-08	.13468E-08

Period Time = 4

	J= 1	J= 2	J= 3	J= 4	J= 5
I= 1	.76826E-07	.16564E-06	.56437E-07	.99434E-08	.21581E-08
I= 2	.16731E-06	.37013E-06	.10070E-06	.17785E-07	.35733E-08
I= 3	.68628E-07	.11699E-06	.49443E-07	.11297E-07	.23417E-08

Table 4.2 (continued)

(b) New Procedure

Location of Pumping is: I = 2 J = 2

Period Time = 1

	J= 1	J= 2	J= 3	J= 4	J= 5
I= 1	.16915E-07	.10346E-06	.14731E-07	.14772E-08	.16061E-09
I= 2	.10358E-06	.13381E-05	.90105E-07	.61429E-08	.48866E-09
I= 3	.16315E-07	.96112E-07	.14182E-07	.15477E-08	.16637E-09

Period Time = 2

	J= 1	J= 2	J= 3	J= 4	J= 5
I= 1	.38578E-07	.14928E-06	.31660E-07	.40589E-08	.57768E-09
I= 2	.14971E-06	.84677E-06	.11499E-06	.11913E-07	.13673E-08
I= 3	.36211E-07	.12645E-06	.29534E-07	.43733E-08	.60818E-09

Period Time = 3

	J= 1	J= 2	J= 3	J= 4	J= 5
I= 1	.59316E-07	.16501E-06	.45990E-07	.70579E-08	.12596E-08
I= 2	.16598E-06	.55087E-06	.11264E-06	.15750E-07	.24439E-08
I= 3	.54268E-07	.12746E-06	.41567E-07	.78132E-08	.13468E-08

Period Time = 4

	J= 1	J= 2	J= 3	J= 4	J= 5
I= 1	.76826E-07	.16564E-06	.56437E-07	.99434E-08	.21581E-08
I= 2	.16731E-06	.37012E-06	.10070E-06	.17785E-07	.35733E-08
I= 3	.68628E-07	.11699E-06	.49443E-07	.11297E-07	.23417E-08

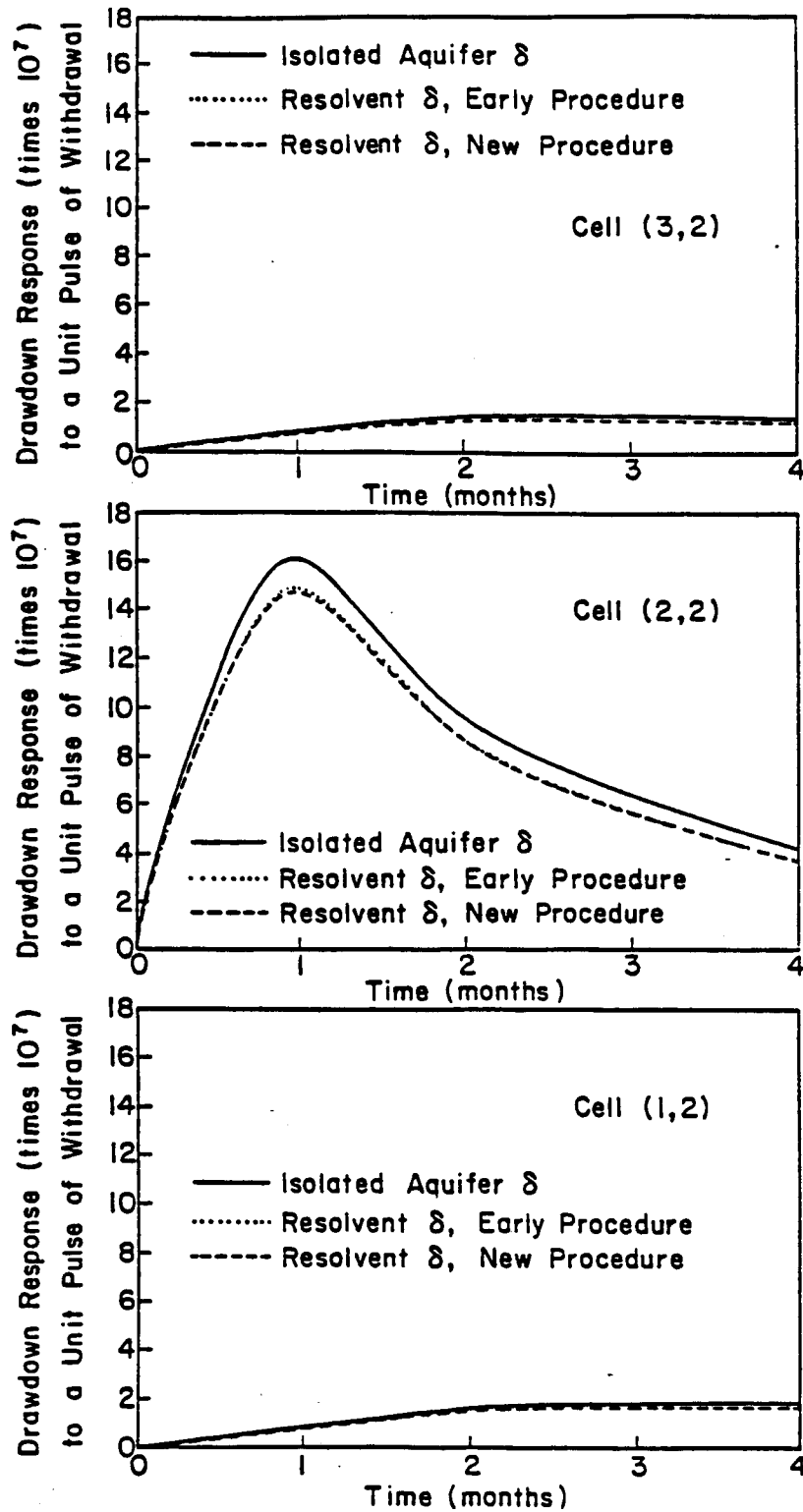


Figure 4.3. Comparison of Drawdown Discrete Kernels by Two Methods of Generation

Conclusion of Comparisons

The new procedure has been implemented correctly as it yields the same results as for the early procedure. The new procedure is simpler as it requires only one step: generation of discrete kernels by a finite difference procedure. In the early procedure, following the first step, which generates drawdown discrete kernels as if the aquifer was isolated, two systems of linear equations must be solved to obtain the discrete kernels of return flows and then of drawdowns in the presence of the stream. The new procedure is also more cost effective as shown by the comparison given in Table 4.3.

Table 4.3

Generation Cost of Discrete Kernels

Time Parameter	Early Procedure	New Procedure
$\Delta t_{\min} = \Delta t_{\max} = \text{month}$	0.589 cp sec.	0.251 cp sec.
$\Delta t_{\min} = 0.01, \Delta t_{\max} = 0.10$	1.188 cp sec.	0.358 cp sec.

Also the new procedure requires somewhat less storage.

ACCURACY AND EFFICIENCY OF THE REINITIALIZATION TECHNIQUE

For a given stream-aquifer system, the results of two procedures to predict return flows are compared. In one case the reinitialization technique and the moving subsystem procedures are not used, whereas in the second case they both are.

Description of Stream-Aquifer System for Accuracy Test

Figure 4.4 provides the description of the geometry of the stream-aquifer system as well as the grid system and the boundary conditions, used for this test. The aquifer is homogeneous with a transmissivity value of 50,000 $m^2/month$ and effective porosity value of 0.20. There are seven river reaches and one pumping site in the system. The reach transmissivity in each reach is the same, of value 100,000 $m^2/month$. The aquifer and river drawdowns are initially all zero.

Description of Two Distinct Procedures. The procedure without reinitialization simply generates the drawdown and return flow discrete kernels for 9 periods (9 months) due to a unit pulse of pumping at cell (3,3) for the entire system by program KERGEN, selecting the option "no moving subsystem." The procedure with reinitialization requires two steps. In a first step the drawdown and return flow discrete kernels are generated only for one time period within a 3 by 3 moving subsystem by program KERGEN, selecting the option "with moving subsystem." In an alternative first step, the discrete kernels are generated for three periods.

The moving subsystem center moves from one cell to another for all the active cells. Every time, when the subsystem is centered in an

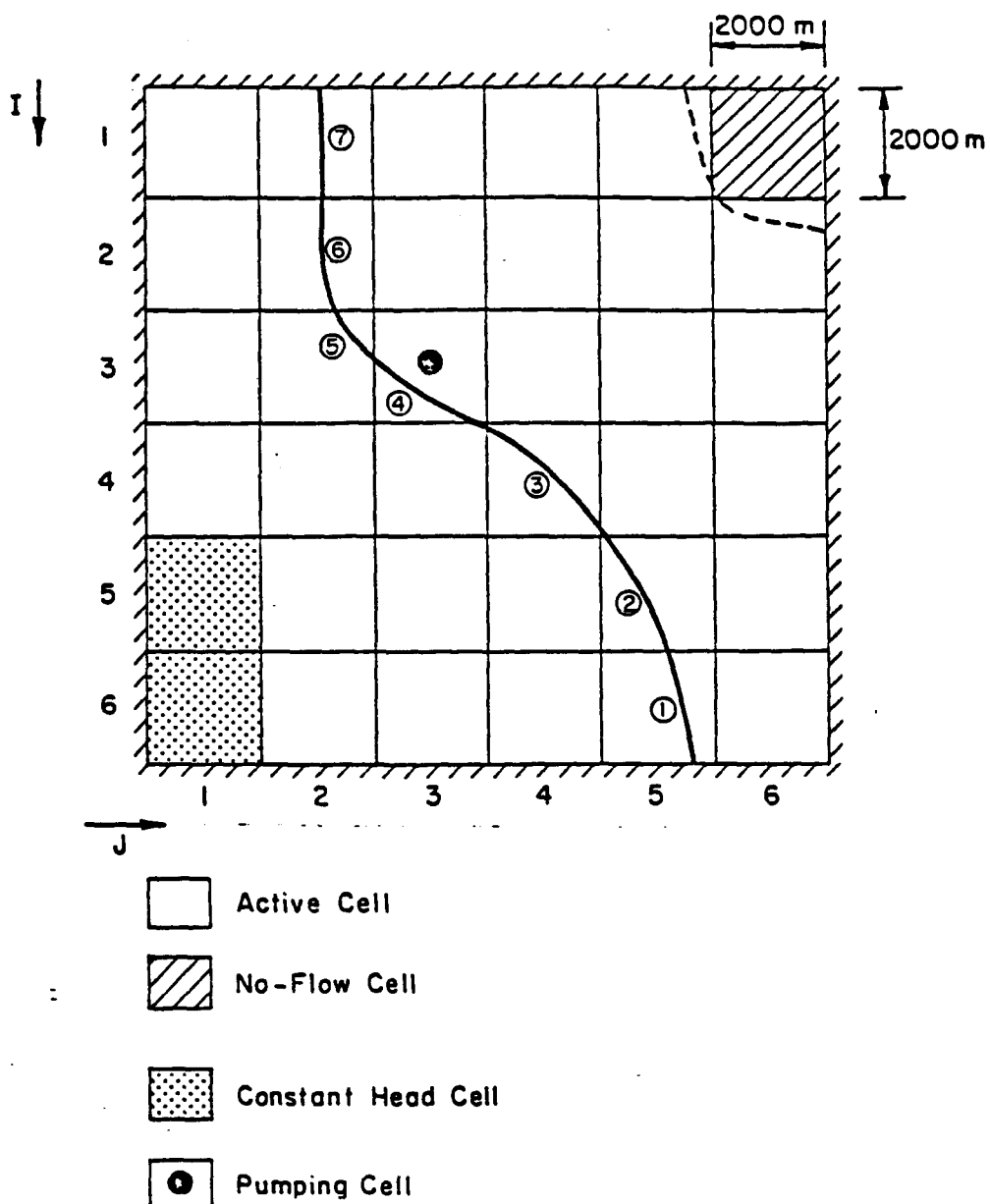


Figure 4.4. Hypothetical Stream-Aquifer System Used to Test Accuracy of the Reinitialization Technique.

active cell, a set of discrete kernels will be generated for 9 cells for one or three time periods. In total 33 sets of drawdown and return flow discrete kernels are generated for the future need of reinitialization in the simulation stage. In the second step, simulation is performed by program KERSIM, with zero initial drawdowns everywhere and for a unit volume of pumping only at cell (3,3) during the first time period. The procedure with reinitialization was run twice. In one run, reinitialization occurs after every 3 time periods. In another run reinitialization is performed every time period.

Comparison of the Results. Since the boundary conditions and initial conditions are exactly the same, the results by the different procedures should also be the same. The return flows in reaches 3, 4 and 5, for 9 time periods are shown in Figure 4.5. Clearly the results are very close. Actually it is not known for sure which of the 3 results is the most accurate one. Since none of the solutions are analytical, all are subject to various errors (rounding, truncation, etc.)

Description of Efficiency Test

A small area of the South Platte River basin is chosen for this efficiency test. (The area is small but all the data are from the real case). The purpose of the study is to demonstrate the steps involved in applying the model to a real stream-aquifer system, to show the efficiency of using the reinitialization technique and to analyze the results. The emphasis in the study is on the calculations of the return flows due to the net withdrawals and the natural non-equilibrium conditions over one irrigation season.

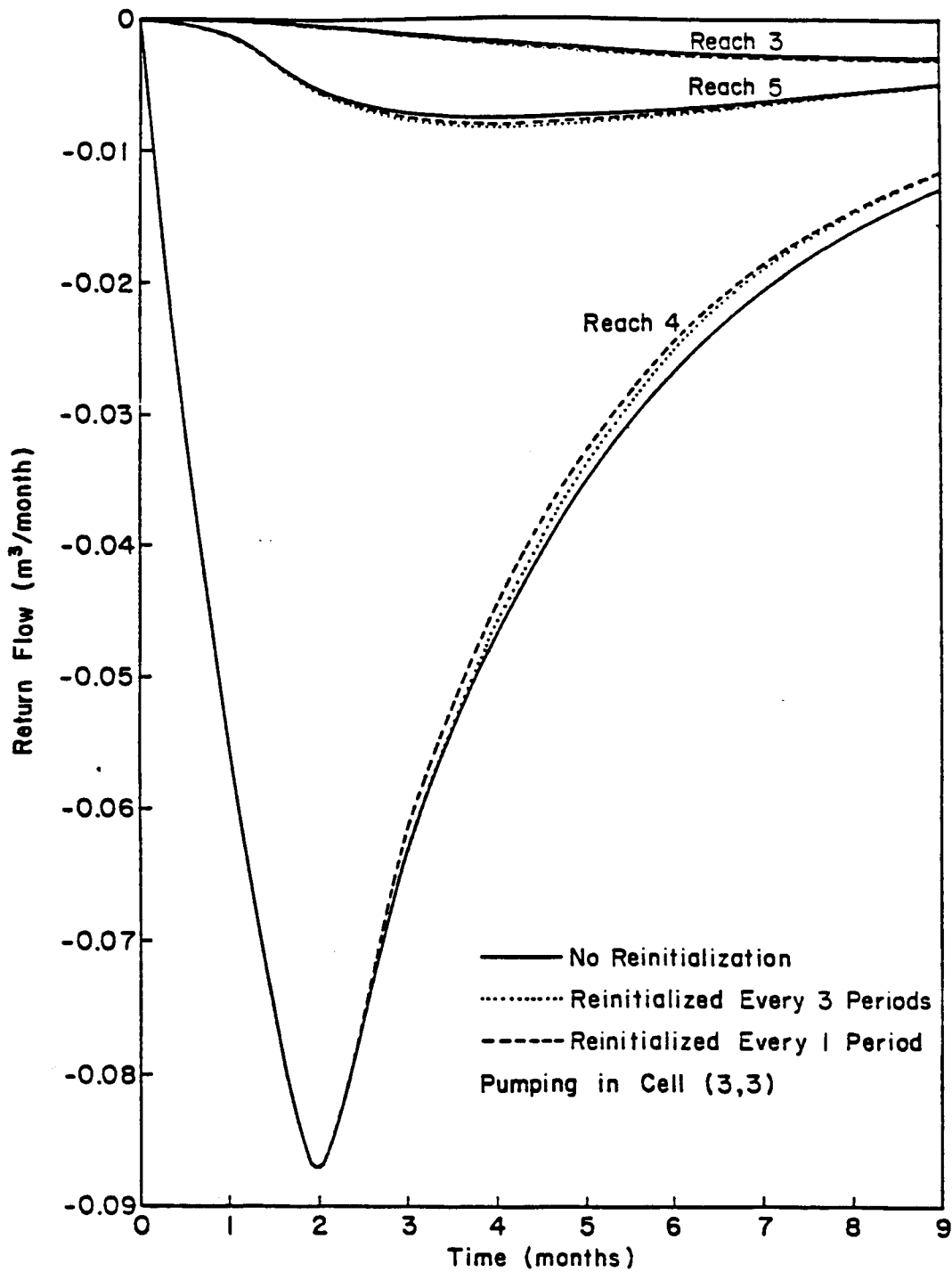


Figure 4.5. Comparison of Aquifer Return Flows by Three Procedures (without, with reinitialization every 3 periods, or every period).

The area of concern extends from the Henderson gaging station to the city of Brighton along the South Platte River. The geographical features and aquifer properties of this area are shown in Figures 4.6, 4.7, and 4.8 which are copied from the U.S. Geological Survey maps compiled by Donald R. Albin and R. Theodore Hurr (1972)(transmissivity), and Paul A. Schneider, Jr. (1972) (saturated thickness and water table altitude).

Delineation and Discretization of the Stream-Aquifer System.

The delineation and discretization of the stream-aquifer system are shown in Figure 4.9. The location of the river reach and boundary of the aquifer are copied from USGS maps. A grid size of one mile by one mile is selected. The overall rectangular domain shape is required by program KERGEIN and as a result some inactive cells are included in the study area. The cells outside of the real aquifer boundary, cross-hatched, are treated as no-flow cells. The reaches are numbered from 1 to 8 from upstream to downstream. The rest of the reaches are ignored (i.e. are in no hydraulic connection with the aquifer). The boundaries on the east and west sides are basically along the natural aquifer boundaries. The boundaries at the upstream and downstream ends are artificial boundaries. For simplicity, they are treated as constant head boundaries. The number of total grids is 9 (number of rows) time 7 (number of columns) = 63, and the number of total active cells is 32.

Aquifer Transmissivity - An average value of aquifer transmissivity read from Figure 4.6 is assigned to each cell. For a no-flow cell, the transmissivity is zero. The values are shown in Figure 4.10. The values in gallon per day per foot units were converted to square meters per 15

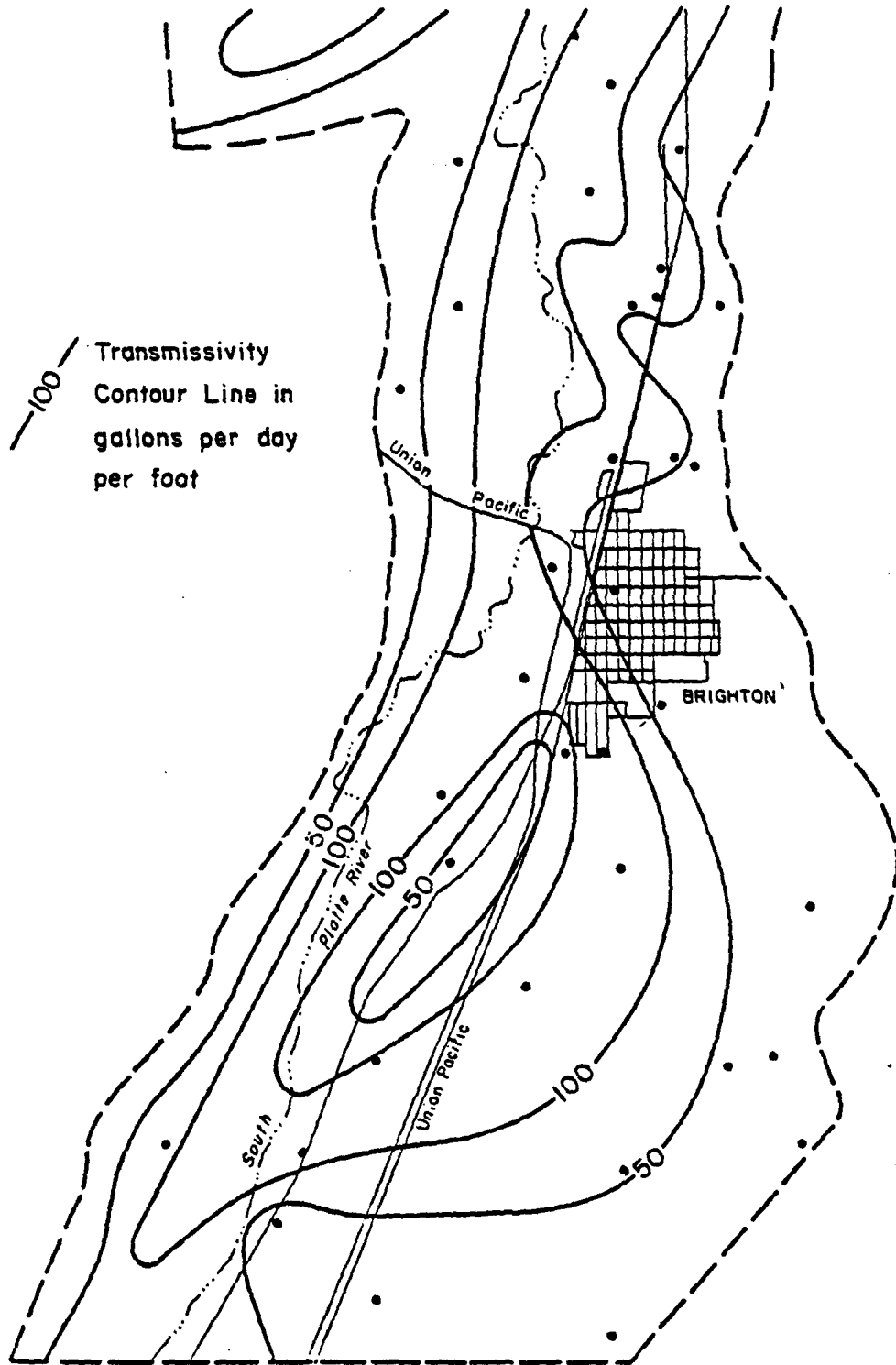


Figure 4.6. Map of Transmissivity Contour Lines for the South Platte Study Area.

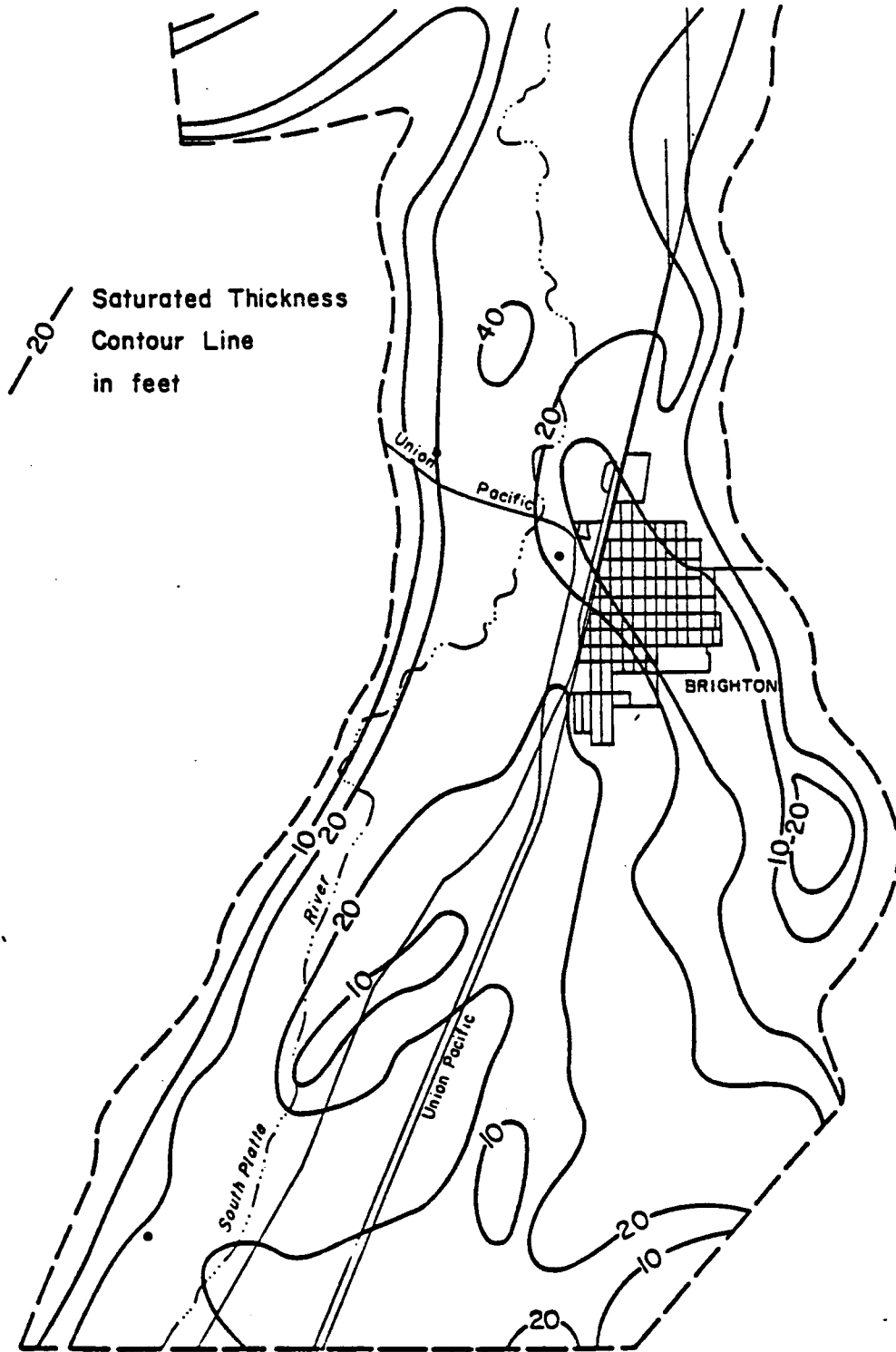


Figure 4.7. Map of Saturated Thickness Contour Lines for South Platte Study Area.

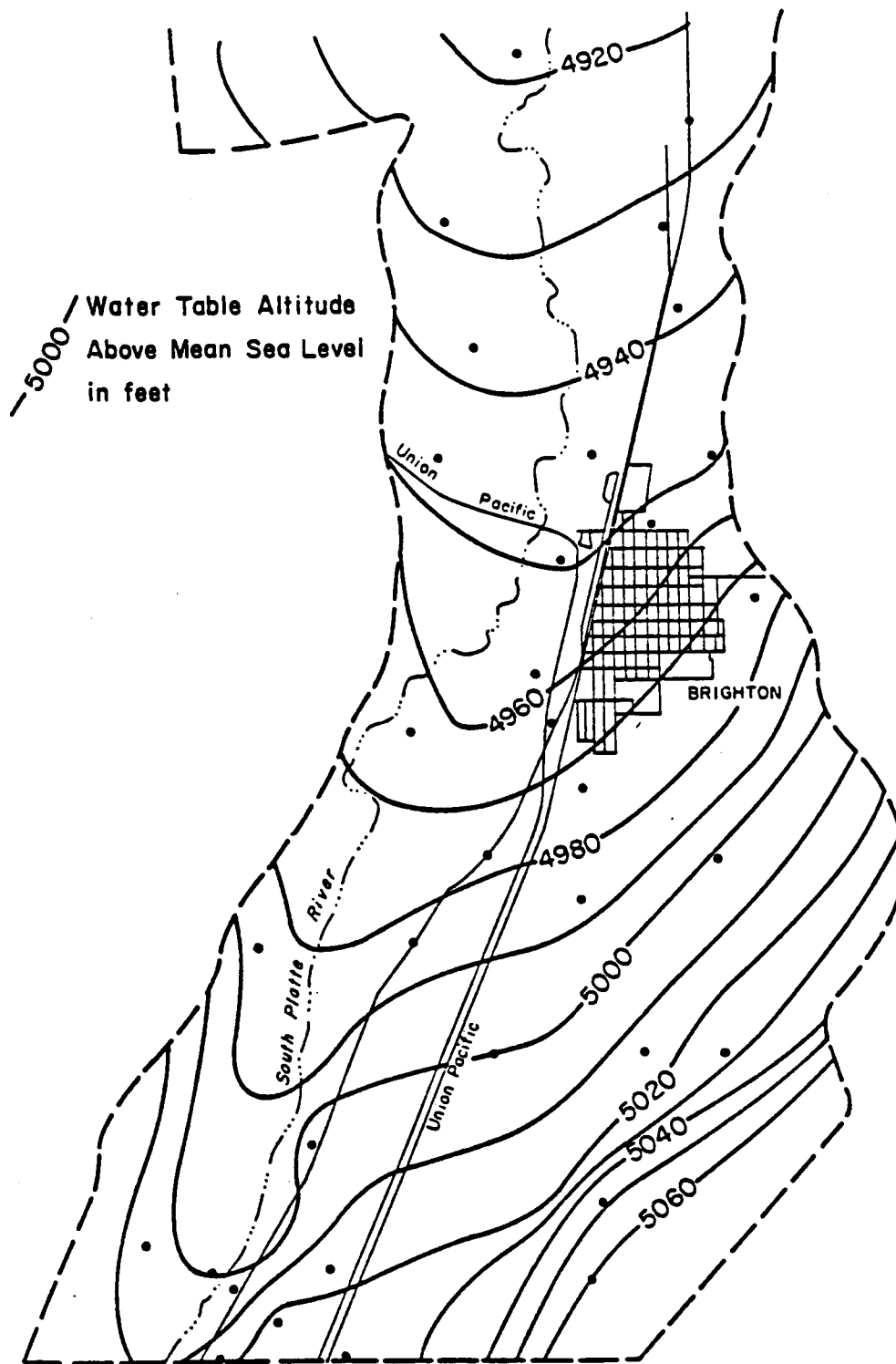


Figure 4.8. Map of Water Table Level Altitude Above Mean Sea Level

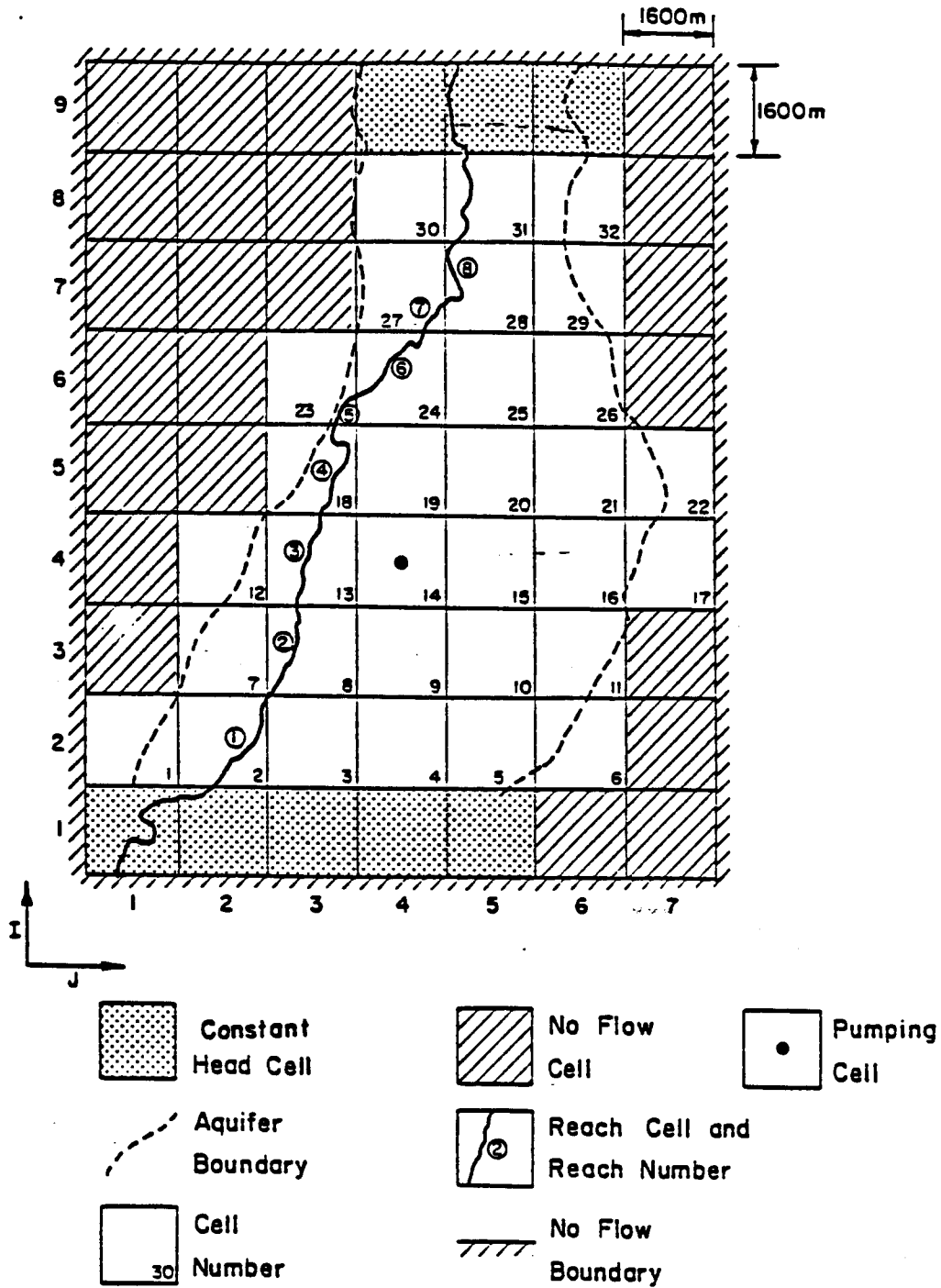


Figure 4.9. Delineation and Discretization of the Hypothetical Stream-Aquifer System.

days (1000 gallons per day per foot is equal to 186.3 square meters per 15 days).

Aquifer Effective Porosity - The value of aquifer effective porosity of the South Platte River basin was taken to be 0.17 as determined by other studies (Restrepo, 1987).

River Reach Transmissivity - The river transmissivity for each reach is expressed as a function of aquifer and river parameters according to Eq. (2.3.a) repeated here for convenience:

$$\Gamma = \frac{T}{e} L \left(\frac{W_p + 2e}{e + 10W_p} \right) \quad (2.3.a)$$

where T is the transmissivity of the aquifer underlying the reach. The estimation of T here is the average transmissivity along the reach from the map, which is different from the average transmissivity of the cell. In Eq. (2.3.a) e is the average saturated thickness of the aquifer along the reach, L is the length of the reach, and the W_p is the wetted perimeter, practically the width of the reach. The length and width of each reach are approximately estimated from areal photographs (TOUPS Corporation, taken in October 1977). The saturated thickness, e, is obtained from Figure 4.7. The values of the reach transmissivity ($m^2/15$ days) calculated by Eq. (2.3.a) as well as the relevant parameters are given in Table 4.4.

9	0	0	0	14904	18630	5589	0
8	0	0	0	15835	18630	5529	0
7	0	0	0	16767	15835	5589	0
6	0	0	2794	18630	17698	6520	0
5	0	0	13041	16767	18630	8383	2794
4	0	5589	18630	16767	18630	8383	1863
3	0	14904	18630	18630	13972	5589	0
2	1863	13041	7452	7452	4657	1863	0
1	18630	13041	9315	7452	4657	0	0
	1	2	3	4	5	6	7

I ↑
J →

Transmissivity Values in m^2 per fifteen days

Figure 4.10. Average Transmissivities (in $m^2/15$ days) for Cells in Grid for South Platte study.

Table 4.4
River Reach Transmissivity and Other Parameters

Parameter	Reach 1	2	3	4	5	6	7	8
Saturated Thickness e (m)	7.6	9.1	6.1	6.1	3.0	9.1	7.6	6.1
Aquifer Transmissivity T ($m^2/15$ day)	16,767	22,356	20,493	18,630	9,315	20,493	20,493	18,630
Width of Reach W_p (m)	57.9	45.7	48.8	42.7	42.7	48.8	54.9	64.0
Length of Reach L (m)	2,092	1,609	1,770	2,011	644	1,931	724	1,207
Reach Transmissivity T ($v^2/15$ days)	575,071	541,934	733,777	778,779	226,357	586,187	245,785	434,614

Time Parameters. According to the user, return flows at every half month interval are desired. The length of the period is 15 days and there are 9 time periods within the irrigation season (about four and half months). In order to have good accuracy, the initial time step Δt_{\min} is selected as 0.01 period and the maximum time step for the first two time periods is set to 0.1 period. The time multiplier factor is 1.5.

Selection of Subsystem Size. By comparison of the results using a (3 by 3), a (5 by 5) or a (7 by 7) subsystem, it is found that to generate the discrete kernels for only 3 periods, a (3 by 3) subsystem is adequate; and to generate the discrete kernels for 9 time periods, a (5 by 5) subsystem is fine. For the purpose of comparisons, three procedures are used with different sizes of subsystems.

Initial Conditions. The initial water table drawdowns of the study area are estimated from Figure 4.8, which depicts the water table contour lines for the study area in March 1968. The average initial aquifer drawdowns for all the cells are shown in Table 4.5. The values are relative values compared to the elevation of 5000 ft, above the sea level selected as datum. For the no-flow cells, all the values are entered as zero and are not needed.

River Stage Drawdowns. River stage drawdowns do vary with time and space. In this hypothetical case, for simplicity, river stage drawdowns for all 9 time periods are assumed to be steady. The values are shown in Table 4.6, relative to the 5000 feet datum above sea level.

Pumping Pattern. In this hypothetical case, a net uniform withdrawal is assumed nonzero only at cell (4,4), which is pumping location 14, and only during the first time period at a rate equal to 10 million $m^3/15$ days.

Table 4.5
Initial Water Table Drawdowns
(in meters)

I	J						
	1	2	3	4	5	6	7
1	-9.14	-6.10	-7.62	-13.72	-19.81	0	0
2	-3.05	-1.52	-3.05	-9.14	-18.29	-19.81	0
3	0	-1.52	0.0	-3.05	-9.14	-18.29	0
4	0	1.52	4.57	3.05	0.0	-7.62	-9.14
5	0	0	7.62	7.62	6.10	0.0	-6.10
6	0	0	10.67	12.80	10.67	6.10	0
7	0	0	0	15.24	15.24	12.19	0
8	0	0	0	18.28	18.28	16.76	0
9	0	0	0	21.34	20.42	19.81	0

Table 4.6
River Stage Drawdowns
(in meters)

Reach	1	2	3	4	5	6	7	8
$\sigma(m)$	-.91	.61	5.18	8.23	11.28	13.41	15.85	15.85

Procedure without Reinitialization. The discrete kernels are generated within a (7 by 7) moving subsystem for 9 time periods for all active cells by program KERGEN. Since a (7 by 7) subsystem is almost big enough to cover the entire study area, it is assumed that the results are equivalent to one without the use of moving subsystems. The return flows for 9 periods are calculated by simulation program KERSIM accounting for the initial water table drawdowns, the river stage drawdowns and pumping from cell (4,4).

Procedure with Reinitialization Every 3 Periods. The discrete kernels are generated within a (3 by 3) moving subsystem for 3 time periods for all active cells by program KERGEN. Then simulation is performed by program KERSIM with reinitialization every 3 time periods.

Procedure with Reinitialization Every Period. In this case it suffices to generate the discrete kernels for one period of time.

Comparison of the Results. Comparison of the results of simulated return flows due to the initial non-equilibrium conditions, river stage drawdowns and net uniform withdrawal in cell (4,4), by the three different calculation procedures, is displayed in Figures 4.11 and 4.12. Return flows for 6 reaches over 9 time periods are plotted. The results by the three procedures are very close.

Comparison of the computer time spent for the three calculation procedures are listed in Table 4.7. There are quite large differences between the procedures using reinitialization and without using reinitialization. This is only a hypothetical case with an area around 32 square miles. For a real study area covering hundreds, even thousands

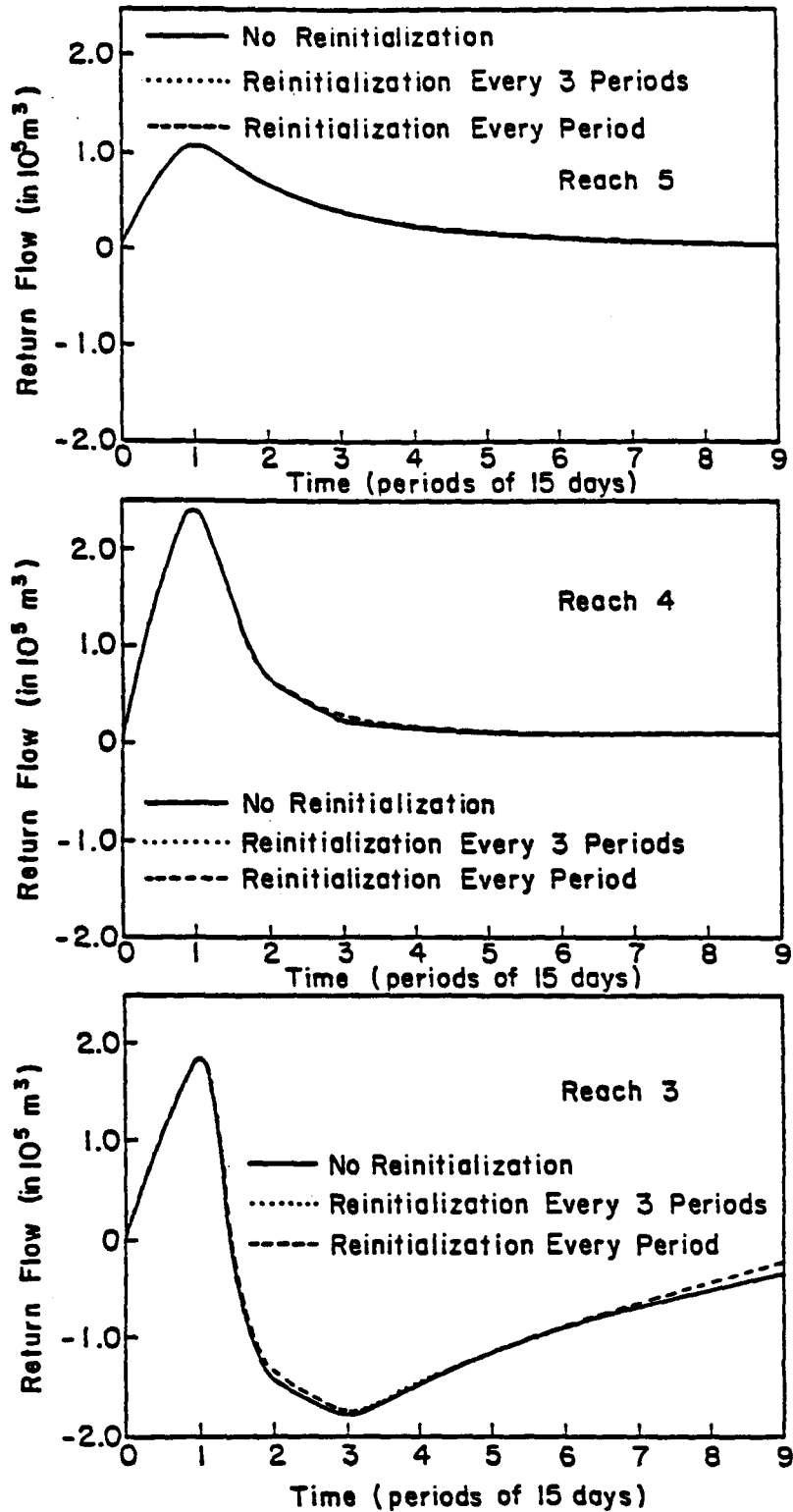


Figure 4.11. Comparison of Return Flows by 3 Procedures (without, with reinitialization every 3 periods or every period). Reaches 3, 4 and 5.

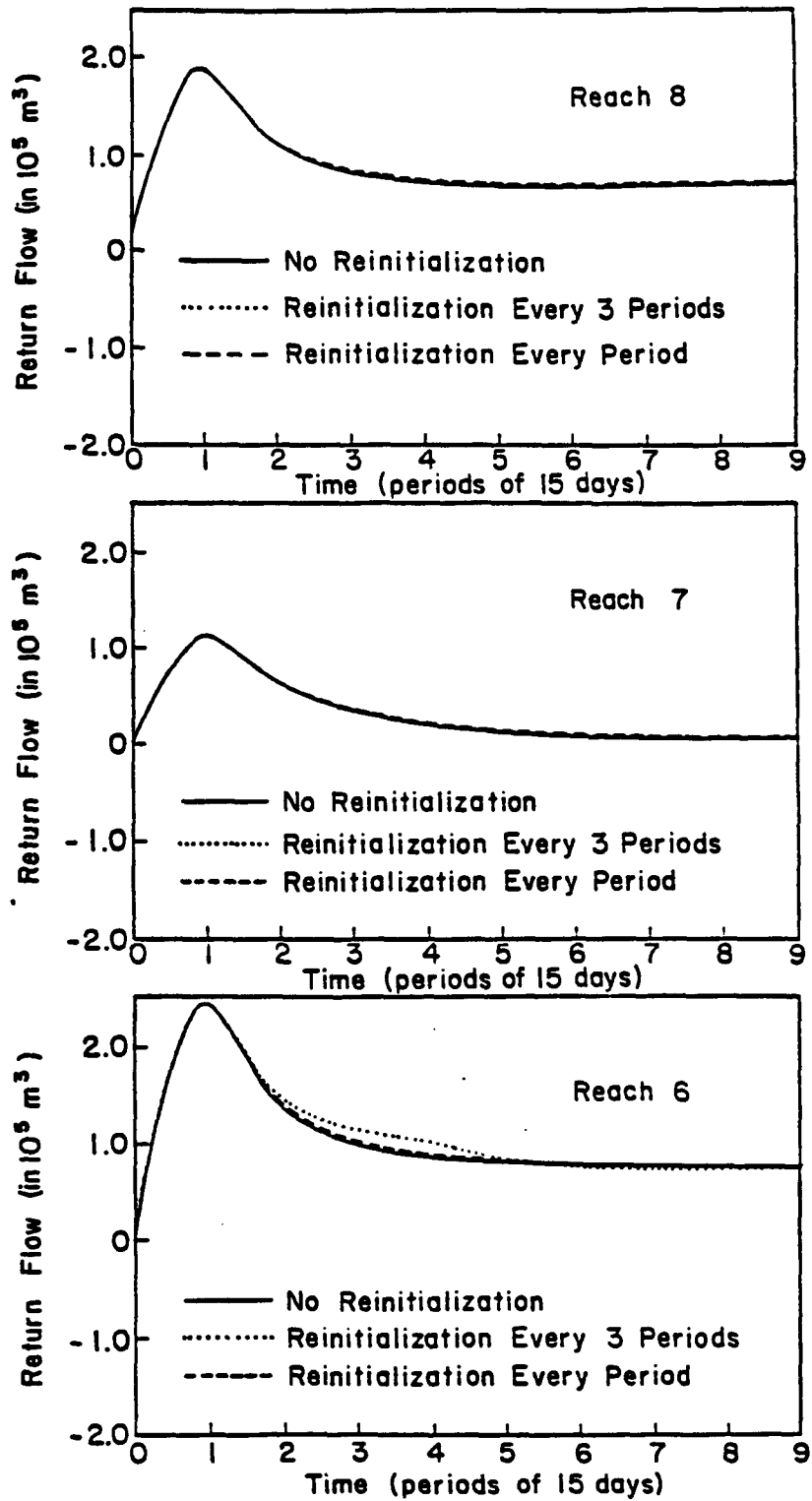


Figure 4.12. Comparison of Return Flows by 3 Procedures (without, with reinitialization every 3 periods or every period). Reaches 6, 7 and 8.

Table 4.7

Comparison of Computer Time for Three Procedures

	No Reinitialization	Reinitialization every 3 periods	Reinitialization every period
	<hr/>	<hr/>	<hr/>
Generation	28.516 cp sec.	2.969 cp sec.	2.133 cp sec.
Simulation	8.462 cp sec.	2.666 cp sec.	2.667 cp sec.
Total	36.978 cp sec.	5.635 cp sec.	4.800 cp sec.

of square miles, the computer time saved by the use of a moving subsystem for the generation and by the use of the sequential reinitialization technique will be tremendous.

From this comparison the conclusion can be drawn that the reinitialization technique is a very cost-effective method with very good accuracy for large scale stream-aquifer problems with long time horizon.

Chapter 5
APPLICATION TO A PORTION OF THE SOUTH PLATTE
STREAM-AQUIFER SYSTEM

For the particular interest on the conjunctive administration of water resources for the South Platte River, this stream-aquifer model has been applied to a portion of the South Platte River to estimate return flows in space and in time. The application includes two parts. The first part consists of the generation of the return flow discrete kernels. These discrete kernels characterize the stream and aquifer physical properties. The second part consists of a simulation of the return flows in terms of these discrete kernels.

PROBLEM STATEMENT

The South Platte flows are sustained by upstream, tributary and aquifer return flows from the alluvial aquifer. The significance of the return flows had already been recognized by the end of the 19th century (Carpenter, 1869; Carpenter, 1916; Parshall, 1922). The historic records show that roughly one third of the streamflow comes from the aquifer. Aquifer return flow is thus an important resource in the Basin and a significant component for the water management in this area. Though it is not possible to measure return flows directly, it is possible to estimate them fairly accurately from the properties (transmissivities) and from the state (river stages, water table elevations) of the system.

The South Platte River partially penetrates a long and narrow alluvial aquifer as it flows from a southwest point to a northeast corner as shown in Figure 4.8. There is permanent hydraulic connection between the river and the aquifer, i.e., there always exists a saturated flow exchange between these two water bodies. Most of the time, the aquifer water table elevation is higher than that of the river free surface and consequently water flows from the aquifer laterally into the river. This flow is called aquifer return flow or, simply, return flow. Sometimes, such as during the flood season, the river level is higher than that of the water table and river water seeps into the aquifer. This flow is called seepage flow and it is a negative return flow. From Figure 4.8, one can see that return flow varies along the river course. In other words return flow varies in space and in time.

It is that variation of the return flows in time and space and its complex relationship with groundwater withdrawals and river flow fluctuations, that makes the administration of water rights for the South Platte particularly difficult. Given the character of Colorado's water law, the "priority" system (first in time, first in right), to allocate the water properly the State Engineer must anticipate the influence of current and past pumpage on current and future return flows and therefore river flows at all surface diversion points.

Figure 5.1 illustrates schematically the need for that estimation of return flows along the river course. There exists downstream a senior irrigation water right diversion whereas a junior diversion is located in the upstream reach of the river. Often during a drought period, the small river flow can only satisfy the downstream senior right. The junior right

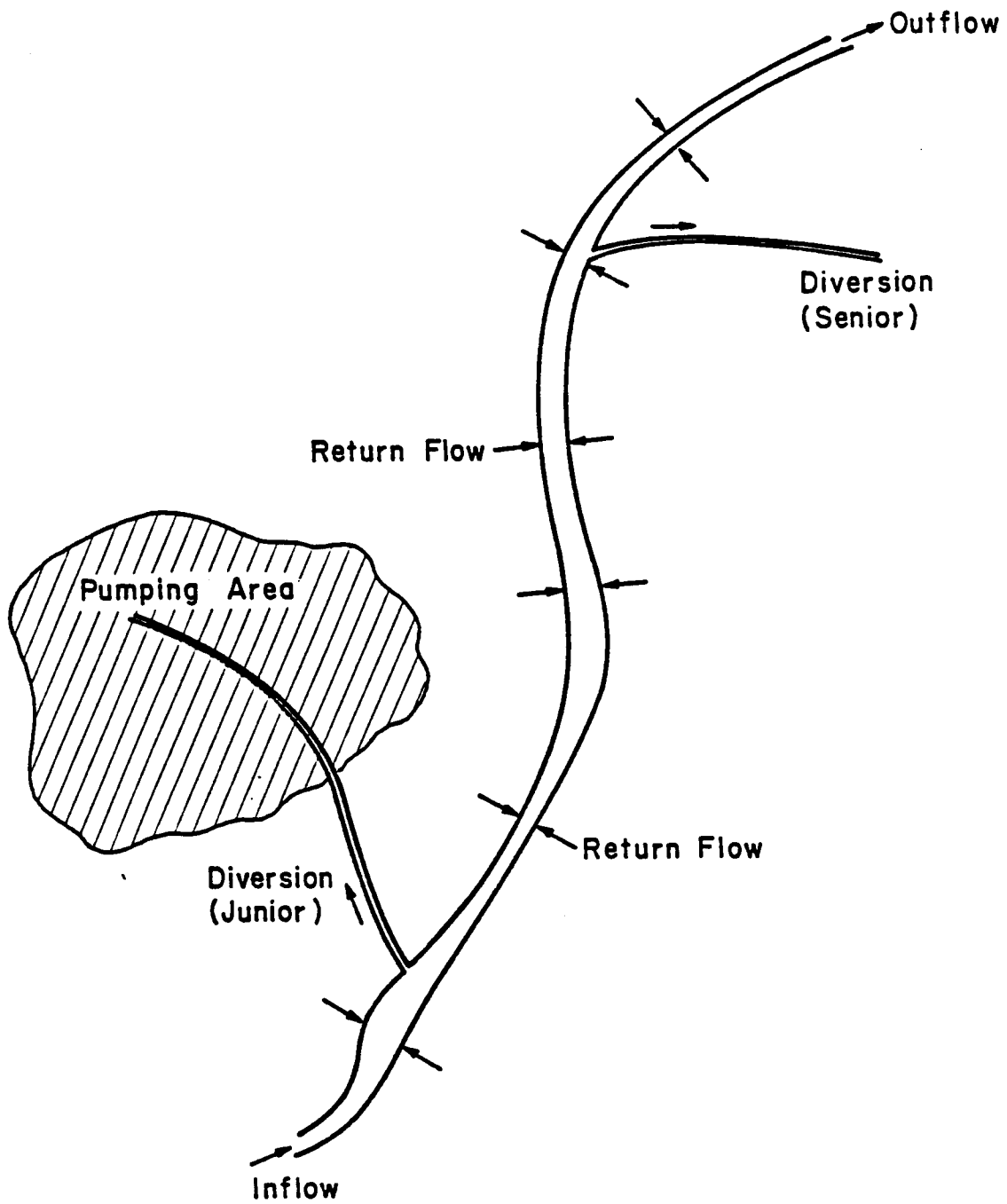


Figure 5.1. Illustration of Necessity to Estimate Return Flow in Space and in Time.

farmers, without a surface water supply, must draw from the groundwater reservoir to irrigate their crops. That action is reasonable. It is in periods of shortage that one draws upon one's reserves. However, legally, these irrigators cannot do so without evidence that their pumpage will not damage the downstream senior right during the irrigation season. Alternately, the junior right holders must have an "augmentation plan" that will deliver, when needed, volume compensation for the damage to streamflow resulting from the pumpage. Of course the parties involved cannot agree to a plan if the extent and location of the damage cannot be estimated realistically in space and in time.

OBJECTIVES OF STUDY

Problems similar to the one just described have been investigated over many years starting with a first rather simple operational model for the description of the 3-way stream-aquifer-well interaction (Morel-Seytoux et al. 1973) and culminating with a very sophisticated and realistic model (Morel-Seytoux and Restrepo, 1986) describing the numerous interactions between hydrology, hydraulic structures (reservoirs, canals, wells) agriculture, irrigation, law, administration, institutions and economics, not to mention politics! Different problems need different methods of solution and it would be foolish to use a complex and therefore rather cumbersome tool to solve a rather simple problem. The purpose of this study was to describe well the stream-aquifer interaction and how it is influenced by both groundwater withdrawal (in a net sense) and river stage fluctuations, and does so in a manner that permits its coupling with management investigations in an easy and cost-effective manner. The key to the successful completion of this task is the development of simple

algebraic relations between the return flows in various reaches and the net withdrawals from groundwater throughout the system.

DESCRIPTION OF THE STUDY AREA

The study area is a part of the South Platte River Basin between the Henderson Gaging Station (near Denver) and the Gaging Station near Kersey (close to Greeley). It is shown in Figure 5.2. The total length of the river in the study area is about 55 miles or 88 km. There are three tributaries that flow into the South Platte River in this area. They are the St. Vrain Creek, the Big Thompson and the Cache La Poudre Rivers. There are 19 diversion ditches, five of which are believed to be inactive.

A finite difference grid system is imposed on the study area, as shown in Figure 5.2. The size of the cell is one mile by one mile (i.e. 1600 m by 1600 m) following the USGS map. With the uniform cell size, the total rectangular area is 42 cells in length and 23 cells in width. Among the $(42)(23) = 966$ cells, only 289 cells are active interior cells, which cover the aquifer, and 27 cells are constant head cells, which are at the interface of the study area and the rest of the aquifer outside the study area. The shaded cells are no-flow cells which actually are not considered in the calculations. The South Platte River in this area is discretized by the finite difference grid into 57 reaches. The tributaries are not considered in the interaction between stream and aquifer. Only the amounts of tributary inflows are accounted in the mass balance. The boundary conditions for the overall rectangular area are no-flow boundaries. The boundary conditions along the natural aquifer

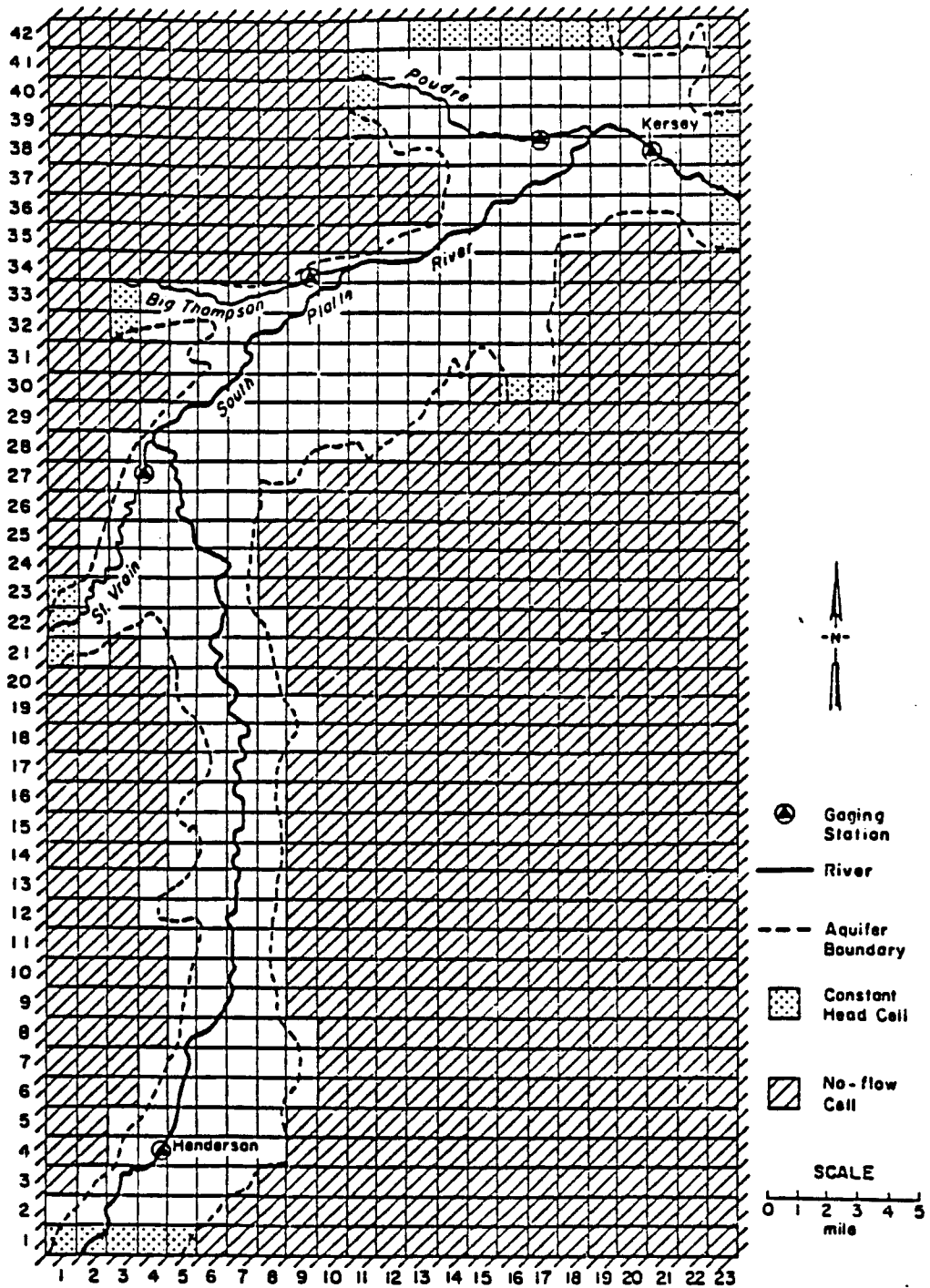


Figure 5.2. The South Platte Valley from Henderson to Kersey and the Finite Difference Grid System.

boundary are no-flow boundaries. Constant uniform heads are imposed as boundary conditions at the interface between a tributary alluvial aquifer and the main South Platte alluvial aquifer as well as at the upper and lower end of the main aquifer in the study area.

For agricultural management, a reasonable time period is 15 days. In one irrigation season there are 8 or 9 time periods. The metric system is used throughout the calculations. The delineation of the study area is based on the map developed in the course of a more comprehensive study (Restrepo, 1987).

GENERATION OF THE RETURN FLOW DISCRETE KERNELS

The drawdown discrete kernels, the return flow discrete kernels and the coefficients needed in the equations for the determination of the artificial pumping rates, required in the simulation, are calculated and saved by program KERGEN. It is based on the following preparation.

Aquifer and Stream Physical Parameters.

The average aquifer transmissivity for each cell is estimated from USGS maps (Albin and Hurr, 1972). The effective porosity is chosen as 0.17 based on previous experience (Restrepo, 1987). The river reach transmissivity is calculated according to Eq. (2.3.a). The sources of data are either from USGS maps or from TOUPS areal photographs.

Determination of the Size of Subsystem.

Within the capability of the program, the discrete kernels can be generated by using subsystems with different sizes or for the whole study area. A test was designed to check which option is more reasonable. For

later economic analysis the discrete kernels for 8 or 9 time periods were required. The generation of the discrete kernels for 9 time periods was tested in four different ways, using the whole system or using (3 by 3), (5 by 5) or (7 by 7) subsystems. Comparisons for accuracy and efficiency in computer time are listed in Table 5.1.

The comparison suggests that a 5 by 5 subsystem is a good option with sufficient accuracy and requiring less computer time. The discrete kernels for both drawdowns and return flows were generated for the whole study area using a moving subsystem of size (5 by 5). The computer time spent on the CYBER 180 was 101.974 cp seconds. Trying to see how much time was saved by this selection, a run with generation of discrete kernels for the whole area without using a subsystem was carried out. The computer time on the CYBER 180 for one set of discrete kernels was about 140 seconds. For completion of the total generation for all the potential excitation cells (289 of them) the computer time would be $(140)(289) = 40,460$ cp seconds. The difference is really tremendous.

Analysis of the Characteristics of the Return Flow Discrete Kernels

As mentioned before, return flow discrete kernels represent the physical characteristics of a stream-aquifer system, they are functions of aquifer properties and river geometric properties. Similar to the unit hydrograph in surface hydrology, which represents the direct runoff response to a unit pulse of effective rainfall for a lumped catchment, the return flow discrete kernel is the stream response to a unit excitation of pumping in the aquifer. More than one unit hydrograph is required however, because the ground water problem is a distributed one. The set

Table 5.1

**Comparison of the Accuracy and Computer Time in Generating
Return flow Discrete Kernels by Different Options
for South Platte Study Area**

Option Number	(1) Whole System	(2) 7 by 7 Subsystem	(3) 5 by 5 Subsystem	(4) 3 by 3 Subsystem
Accuracy (the biggest difference in results compared to Option (1) (percentage)	0.0%	0.001%	0.039%	0.150%
Computer Time (cp second)	33.982	28.516	11.472	3.953

of return flow discrete kernels (as many unit hydrographs as there are combinations of reaches and pumping sites) also gives the spatial distribution of the response of return flow to a unit excitation. This temporal and spatial distribution is a set of return flow discrete kernels due to a unit pulse excitation. For illustration three sets of return flow discrete kernels are selected from the results of the generation phase of the study. The first set of return flow discrete kernels is due to a unit pulse of pumping at pumping site 13 (see Figure 5.3). Pumping cell 13 contains reach 3. Table 5.2 shows that the greatest part of the seepage flow (93%) occurs in reach 3 for nine time periods. It also shows that for these six reaches most of the seepage flow (88%) occurs during the first two periods. The total amount of return flow during the irrigation season (9 periods) is about 97% of the withdrawn volume from

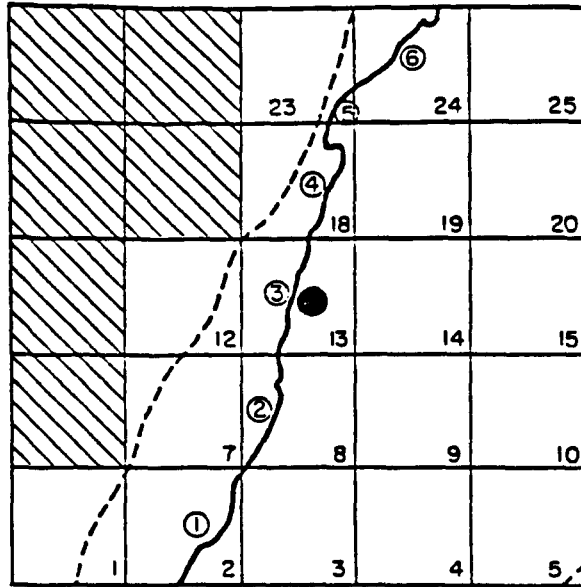


Figure 5.3. Five by Five Subsystem Centered at Pumping Site 13.

Table 5.2

Return Flow Discrete Kernels due to Pumping at Site 13

(in M³/15-day)

	TIME 1	TIME 2	TIME 3	TIME 4	TIME 5	TIME 6	TIME 7	TIME 8	TIME 9	TOTAL
REACH 1	0	-0.00001	-0.00002	-0.00003	-0.00003	-0.00004	-0.00004	-0.00004	-0.00004	
REACH 2	-0.0047	-0.00977	-0.00449	-0.00115	-0.00036	-0.00019	-0.00015	-0.00015	-0.00015	
REACH 3	-0.49704	-0.35868	-0.06886	-0.00615	-0.00109	-0.00062	-0.00054	-0.00049	-0.00044	-0.93391
REACH 4	-0.00503	-0.00913	-0.00322	-0.00034	-0.00009	-0.00008	-0.00008	-0.00008	-0.00008	
REACH 5	0	-0.00002	-0.00002	-0.00001	-0.00001	-0.00001	0	0	0	
REACH 6	0	-0.00001	-0.00004	-0.00005	-0.00007	-0.00007	-0.00008	-0.00008	-0.00008	
TOTAL	-0.50677	-0.37762	-0.07665	-0.00773	-0.00165	-0.00101	-0.00089	-0.00084	-0.00079	
RATIO	88%*		8.4%*		0.3%*		0.2%*		0.1%*	97%*

*Ratio of reach seepage during time interval (2 periods in this case except for last period) over total volume pumped during the pulse (equal to 1 (M³/15-day) by definition). The values are negative because of the algebraic convention that real seepage is negative return flow.

the pumping cell. Figures 5.4 and 5.5 all show that the return flow is very much concentrated both in time and in space. In the jargon associated with the unit hydrograph theory (Morel-Seytoux, 1986), one can say that the memory time and the distance memory are both short.

The second set of return flow discrete kernels is due to pumping at cell 14, which is next to the cell which contains the reach of index 3, in an average sense, 1600 meters away from the river (see Figure 5.6). The temporal and spatial distribution of return flow (see Table 5.3 and Figure 5.7) are quite different from the one due to pumping at site 13.

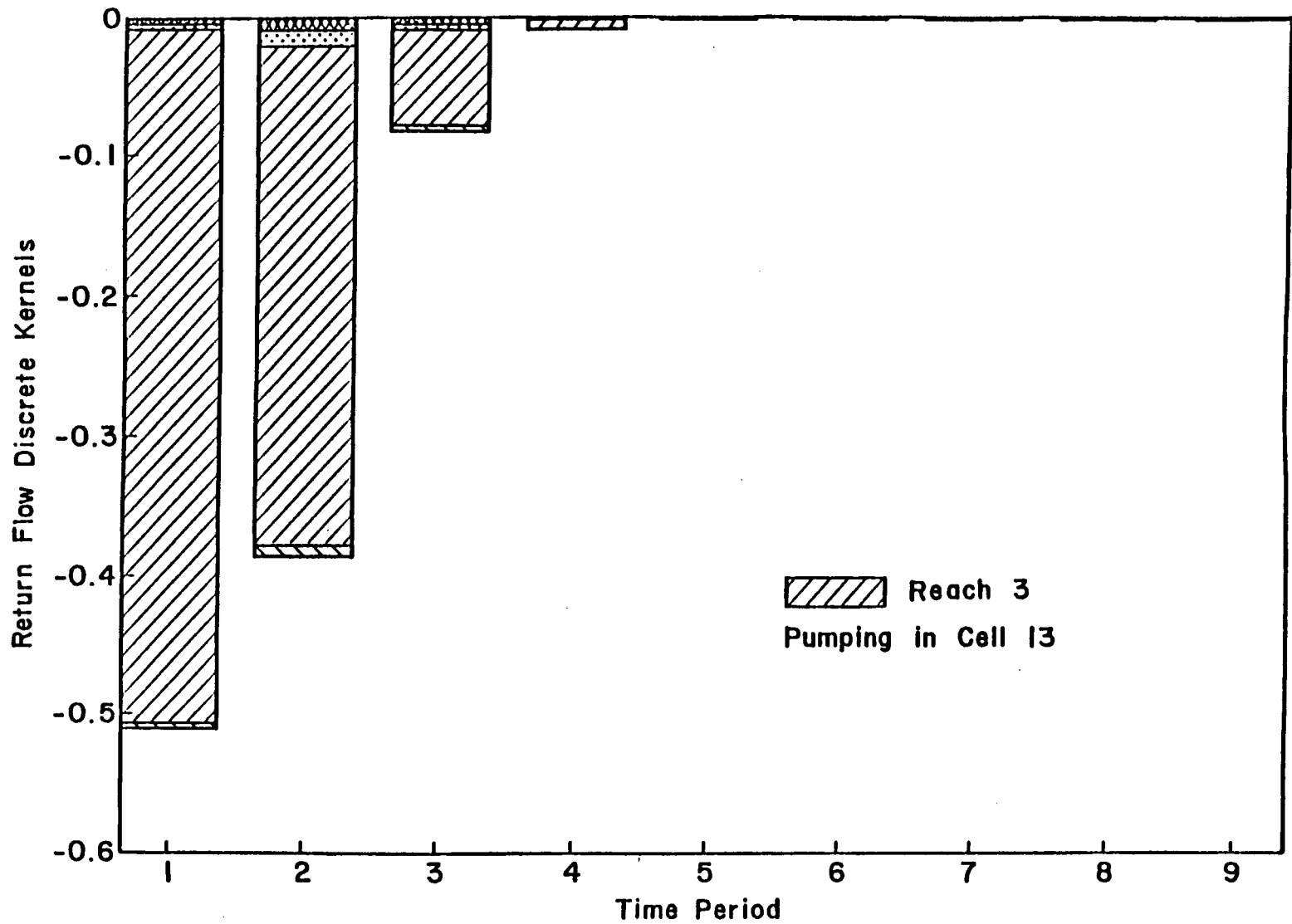


Figure 5.4. Time Evolution of Return Flows in 4 Reaches due to a Unit Pulse of Pumping in Cell 13.

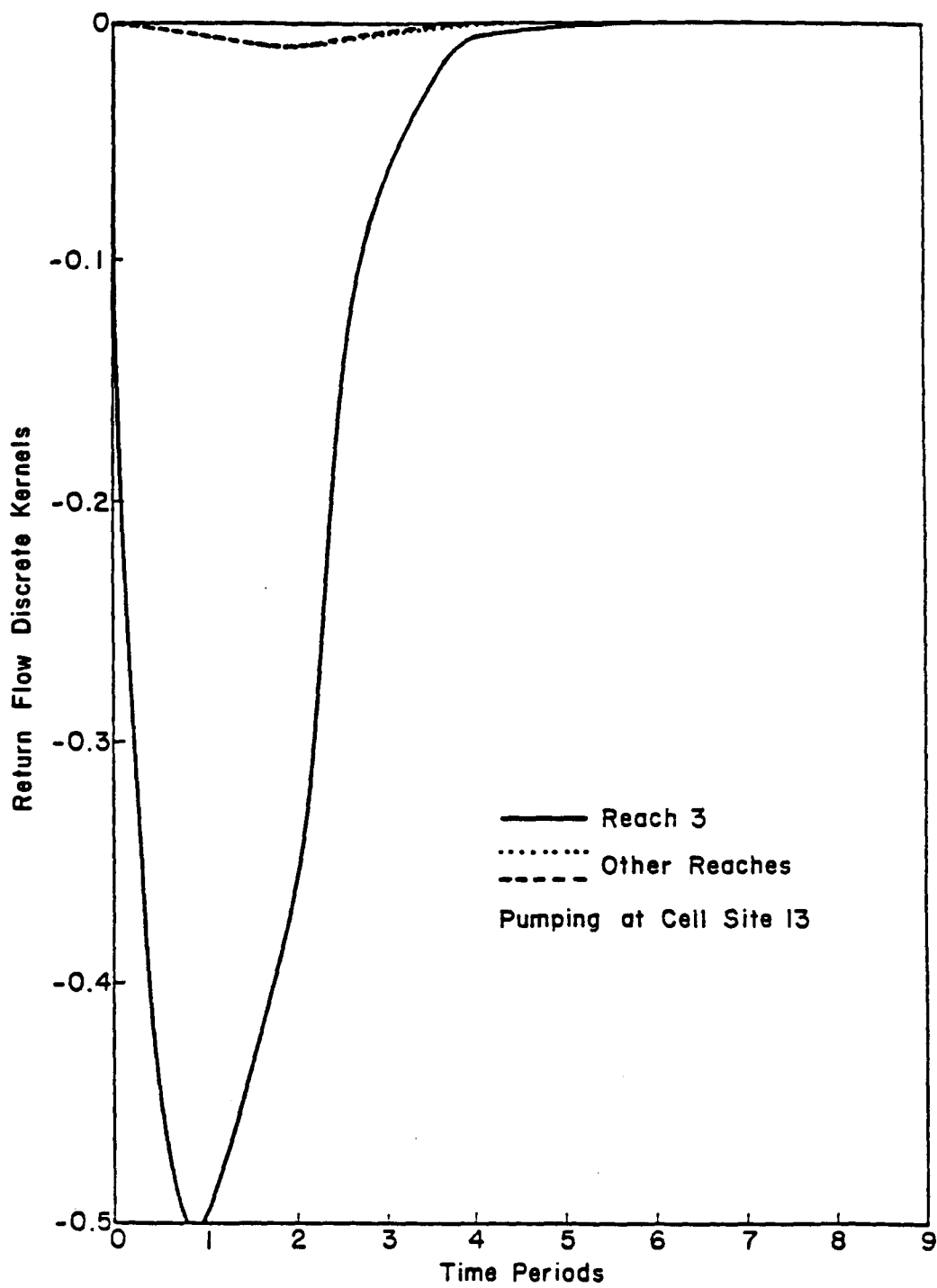


Figure 5.5. Temporal and Spatial Distribution of Return Flow Due to Pumping at Site 13

The cumulative volume of return flow for all six reaches within 9 time periods (the whole irrigation season) is only 24.2% of the volume pumped during the unit pulse. It means that the return flow due to pumping at site 14 will last more than 4 times 4.5 month, i.e., one and a half year, because after the peak during time period 3 return flow is decreasing gradually. Figure 5.7 also shows that the spatial distribution among reaches is not as concentrated as in the previous case with pumping at site 13. As time increases, the proportion of the contributions to return flow by the other reaches increases slightly while the proportion for reach 3 is decreasing. In the language of unit hydrograph theory, the return flow unit hydrograph has a large memory time and a lengthy distance memory.

Table 5.3

Return Flow Discrete Kernels due to Pumping at Site 14

(in M ³ /15-day)										
	TIME 1	TIME 2	TIME 3	TIME 4	TIME 5	TIME 6	TIME 7	TIME 8	TIME 9	TOTAL
REACH 1	.00000	.00000	.00000	-.00001	-.00001	-.00002	-.00003	-.00004	-.00004	
REACH 2	-.00016	-.00113	-.00231	-.00317	-.00365	-.00394	-.00411	-.00420	-.00423	
REACH 3	-.00827	-.02678	-.02772	-.02454	-.02156	-.01899	-.01679	-.01490	-.01327	-.17282
REACH 4	-.00017	-.00108	-.00206	-.00270	-.00299	-.00316	-.00325	-.00329	-.00327	
REACH 5	.00000	.00000	-.00001	-.00002	-.00003	-.00004	-.00004	-.00004	-.00005	
REACH 6	-.00009	-.00071	-.00168	-.00248	-.00296	-.00328	-.00350	-.00363	-.00370	
TOTAL	-.00869	-.02970	-.03378	-.03292	-.03120	-.02943	-.02772	-.02610	-.02174	
RATIO	3.8%*		6.7%*		6.1%*		5.4%*		2.2%*	24.2%*

*Ratio of volume of reach seepage during time interval (2 periods in this case except for period 9) over total volume pumped during the pulse (equal to 1 (M³/15-day) by definition)

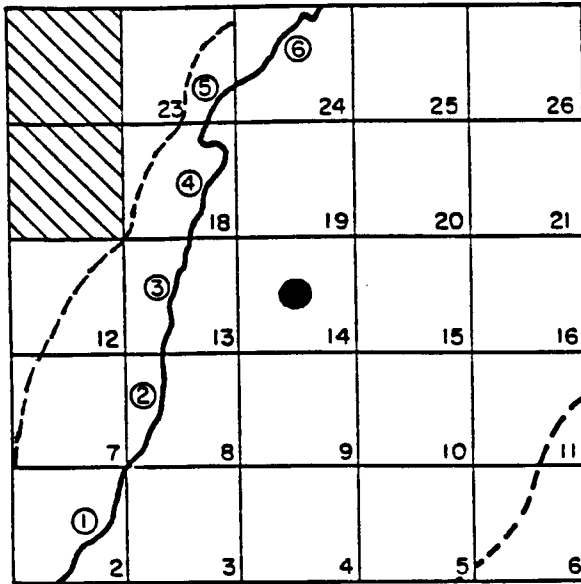


Figure 5.6. Five by Five Subsystem Centered at Pumping Site 14.

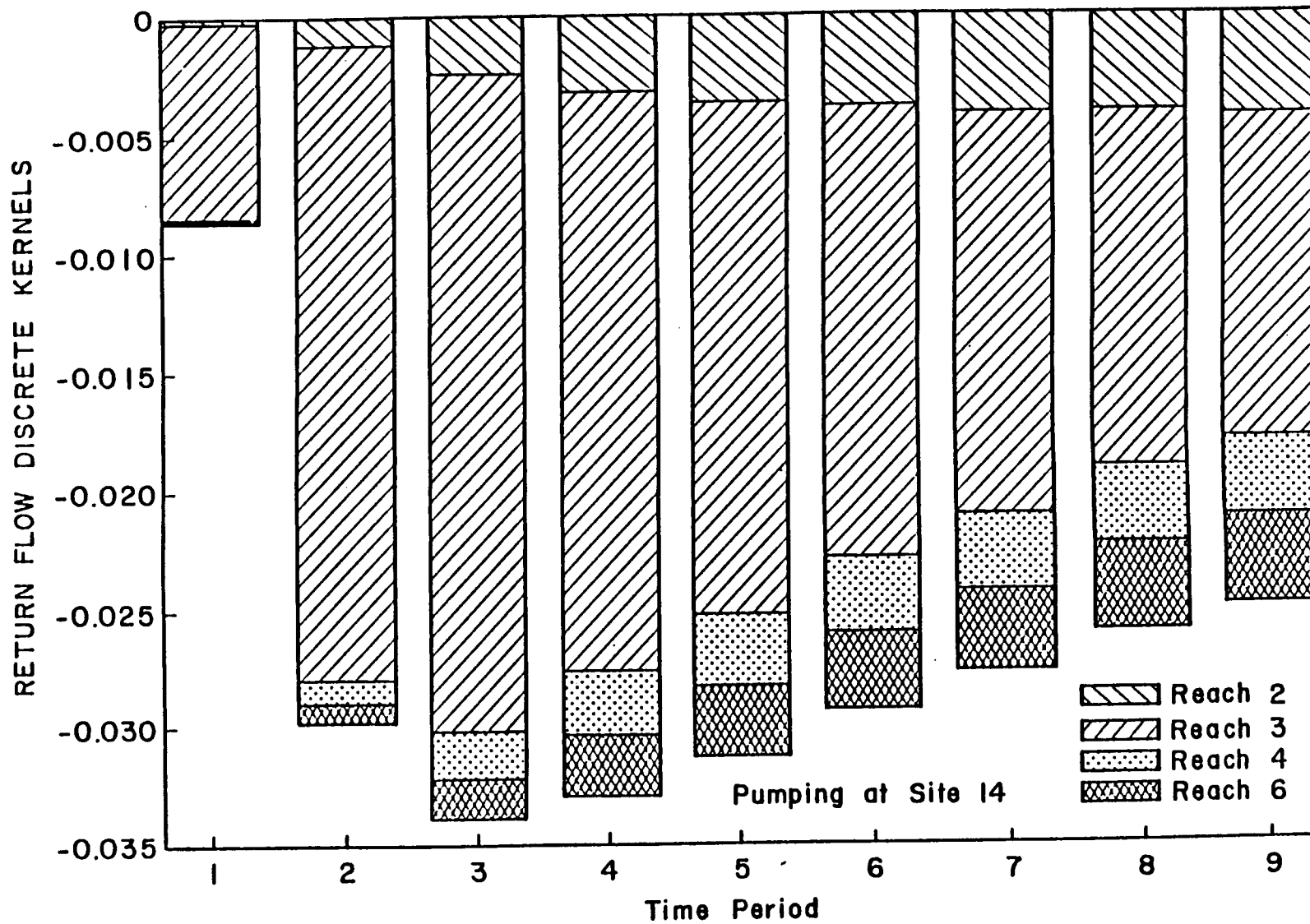


Figure 5.7. Temporal and Spatial Distribution of Return Flow Due to Pumping at Site Indexed 14

A third representative set of return flow discrete kernels is one due to pumping in cell 15, which is two cells away, or on the average, 3200 meters away from the river, as shown in Figure 5.8. From the statistics in Table 5.4, the total return flow within the whole irrigation season is only 4.1%. Figure 5.9 shows that the magnitude of the return flows for all five reaches are all increasing with time even though the rate of increase is decreasing. The spatial distribution is not much concentrated in reach 3 as in the previous two cases. These phenomena show that the influence of the pumping a few miles away from the river is really small but gradually increasing and lasting for a very long time.

Table 5.4

Return Flow Discrete Kernels due to Pumping at Site 15

(in M ³ /15-day)										
	TIME 1	TIME 2	TIME 3	TIME 4	TIME 5	TIME 6	TIME 7	TIME 8	TIME 9	TOTAL
REACH 2	.00000	-.00004	-.00018	-.00038	-.00058	-.00077	-.00096	-.00113	-.00129	
REACH 3	-.00011	-.00084	-.00191	-.00276	-.00324	-.00357	-.00379	-.00393	-.00400	-.02415
REACH 4	.00000	-.00004	-.00019	-.00037	-.00054	-.00070	-.00085	-.00099	-.00111	
REACH 5	.00000	.00000	.00000	.00000	-.00001	-.00001	-.00001	-.00002	-.00002	
REACH 6	.00000	-.00005	-.00025	-.00054	-.00084	-.00114	-.00143	-.00170	-.00196	
TOTAL	-.00011	-.00097	-.00253	-.00405	-.00521	-.00619	-.00704	-.00777	-.00838	
RATIO	0.1%		0.6%		1.1%		1.5%		0.8%	4.1%

*Ratio of volume of reach seepage during time interval (2 periods in this case except for period 9) over total volume pumped during the pulse (equal to 1 (M³/15-day) by definition).

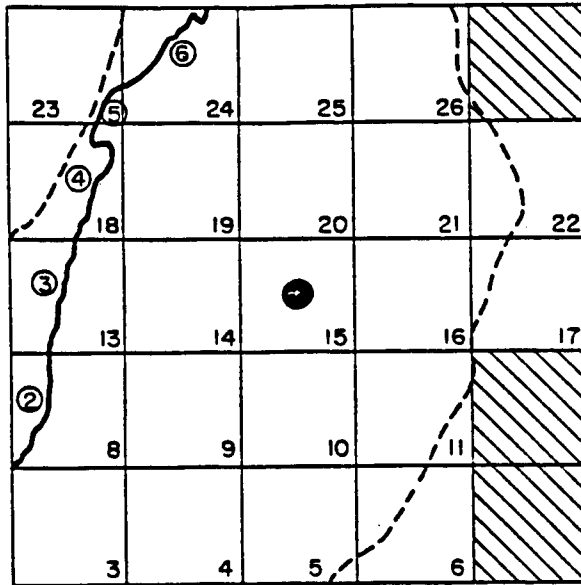


Figure 5.8. Five by Five Subsystem Centered at Pumping Site of Index 15.

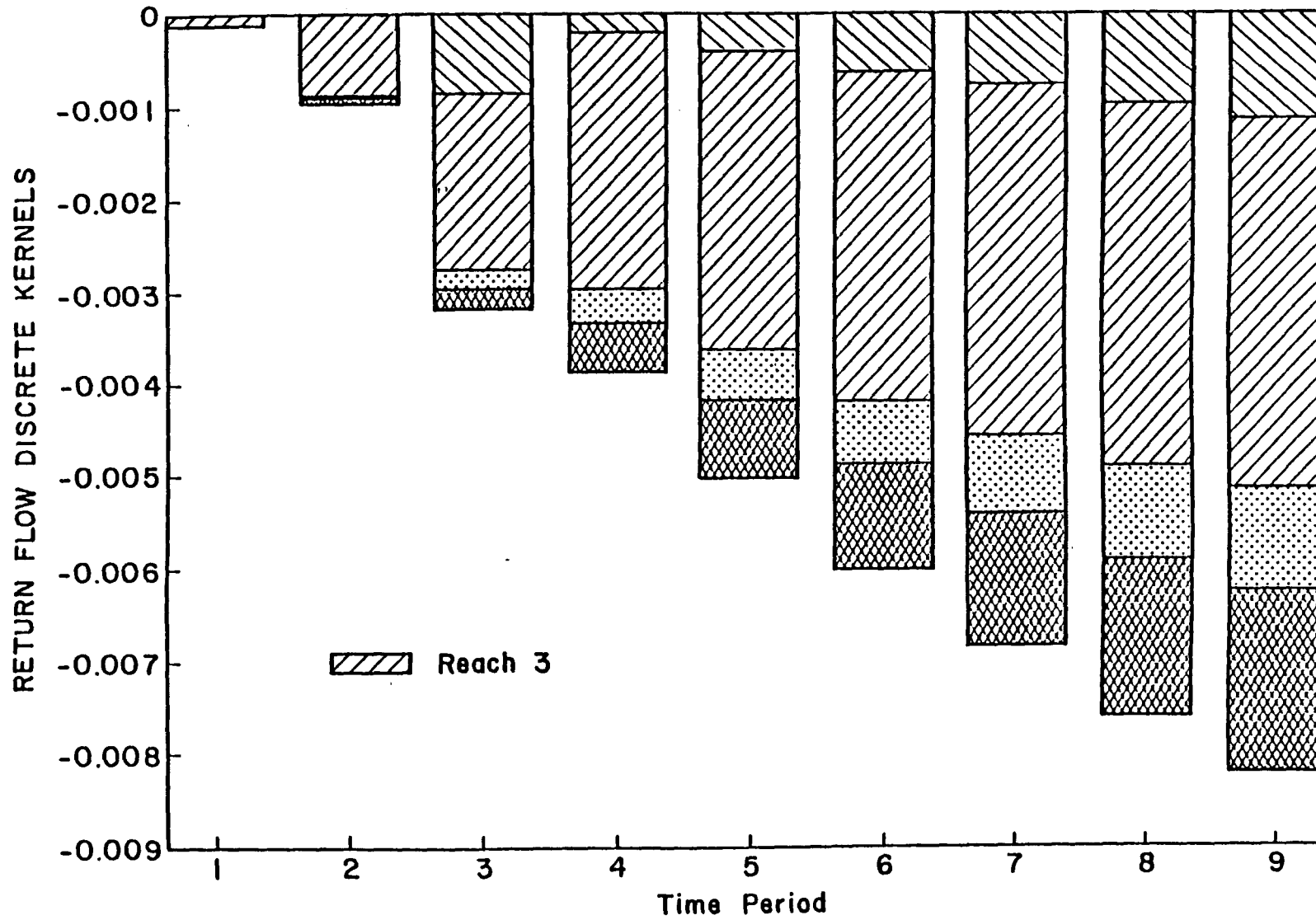


Figure 5.9. Distribution of Return Flows in Different Reaches Due to a Unit Pulse of Pumping at Site 15.

Through the above analysis of the characteristics of return flow discrete kernels, one can find that the prediction of return flows at required time and required reach is available. In other words, the unmeasurable return flow can be predicted by this model.

SIMULATION OF RETURN FLOWS

In order to evaluate the impacts due to changes in political, economical or agronomical policies, a short time simulation for four and half months and five long time simulations for ten years have been conducted on the South Platte River Basin. The emphasis was on the evaluation of return flows under different conditions.

In the South Platte River, the causes of return flows can be classified as three: the initial drawdowns of the water table, the river stage drawdowns, and the net uniform withdrawal from the aquifer, which is an algebraic summation of irrigation water, pumping water, evapotranspiration, seepage from canals, artificial recharge, precipitation, etc. Symbolically, the return flow in reach ρ during time n can be expressed as:

$$Q_{r,\rho}(n) = -\Gamma_{\rho} s_{g(\rho)}^i + \Gamma_{\rho} \sigma_{\rho}(n) + \sum_{i=1}^{N_R} \sum_{j=1}^{N_C} \sum_{\nu=1}^n \epsilon_{\rho,ij} (n-\nu+1) [Q_{ij}(\nu) + \Gamma_{ij} \sigma_{ij}(\nu) + Q_{r,ij}^a - Q_{ij}^a] \quad (5.1)$$

Before running the simulation model KERSIM, these three kinds of excitations were examined based on historical records.

Initial Water Table Drawdowns in the Aquifer

The historical data for water table drawdowns in the South Platte River Basin is available for March 1968. For this reason the simulation horizon for the short time runs was chosen from May to September of 1968, and the long time simulation horizon went from January 1968 to December 1977. The water table contours in March 1968 (Schneider, Jr., 1972) are used as the initial water table conditions for the simulation. The elevation of 5000 feet (1524m) is chosen as the high datum. The water table elevation is converted to drawdowns by comparing the elevation and the datum. The average drawdowns of the water table for all the cells range from -21.3 m to 136.6 m, from upstream to downstream. The initial water table drawdowns show the direction of the ground water flow.

River Stage Drawdowns.

River stage data is not directly available and for this reason daily discharges at Henderson Gaging Station and Kersey Gaging Station were converted into river stages by the analytical rating curve used in SAMSON (Morel-Seytoux, Restrepo, et al, 1985). The Henderson Gaging Station (1968) and Kersey Gaging Station datums are 5005.12 feet (1525.56m) and 4575.77 feet (1394.69m) respectively according to the USGS Water Resources Data for Colorado. The average river stages for each 15 days are calculated for the two gaging stations and interpolated linearly for the 55 reaches in between. The river bed elevations for all the reaches were obtained from the SAMSON data file. The average river stages were added to the reach bed elevations then river water surface elevations were obtained. By comparison with the datum, the average river stage drawdowns are obtained for all the reaches for 240 time periods. The range of the

river stage drawdowns along the river is from about -2.4 m to 128 m. The river stage drawdown almost stays constant over time.

Net Uniform Withdrawal Rates

The net uniform withdrawal rate for each cell is the algebraic summation of all the positive and negative inputs to the cell. Here basically three kinds of input to each cell are considered: pumping water, farm irrigation seepage and canal seepage. The net withdrawal rate patterns in space and in time were provided by Jim Booker (private communication) based on considerations of agricultural requirements and based on availability of water from surface water diversions according to water rights. The proper percentage of the amount of water for evapotranspiration, seepage in the fields and seepage from canals are all considered. The deficit in surface water to meet crop requirements is made up by pumping groundwater. The net withdrawal rates over irrigation season are varied with time and space. A year is roughly divided into 3 seasons. Every season includes 8 time periods (15 days is one time period). After the current irrigation season and before the next irrigation season, the net withdrawal rates are assumed to be zero for all the cells. For the long time simulation, the net withdrawal rate pattern is repeated every year for 10 years.

Short Time Simulation of Return Flows due to Natural Conditions

In an economic, agronomic and legal context while investigating water management strategies, the only controllable variable on the right-hand side of Eq. (3.16) is the net uniform withdrawal, $Q_{ij}(\nu)$, which is to vary

according to the water management strategy. The return flow can be expressed by two terms:

$$Q_{r\rho}(n) = \sum_{i=1}^{N_R} \sum_{j=1}^{N_C} \sum_{v=1}^n \epsilon_{\rho,ij} (n-v+1)Q_{ij}(v) + C_{\rho}(n) \quad (5.2)$$

where the first term on the right-hand side is the return flow due to the net uniform withdrawals. The second term $C_{\rho}(n)$ is the return flow due to the initial conditions and the river stage drawdown fluctuations. Given the assumption that the river stage is not affected by the aquifer, $C_{\rho}(n)$ is independent of the water management strategy. This study utilizes historical data and therefore $C_{\rho}(n)$ can be calculated prior to the investigation of the management problem.

Given the initial conditions, the river stage drawdowns and the net uniform withdrawal everywhere being zero, the simulation model KERSIM is run to calculate the return flows for 9 periods. The return flow variable $C_{\rho}(n)$, for $\rho=1,2,\dots,57$ and $n=1,2,\dots,9$, are obtained. The results show that return flow due to natural conditions is decreasing with time and tends to a steady state. This is a reasonable result. Due to the large dimension of the arrays, KERSIM was run on the Cyber 205. The computer time spent is 21.775 seconds on CYBER 205. The drawdowns of the aquifer at each time period are also calculated and saved. Otherwise the computer time would be much less.

River Mass Balance and Analysis

The available historic data include upstream inflows at Henderson Gaging Station, downstream outflows at Kersey Gaging Station, tributary flows at St. Vrain, Big Thompson and Cache La Poudre Gaging

Stations, and diversion flows at 19 diversion locations (5 of them are always zero). These data were obtained from the SAMSON project data files. The only unknown for the river balance is the return flow because there is no measurement for it. The total historic return flow for the whole river section within the study area can be calculated as:

$$Q_{r,T}(n) = I(n) + \sum_{i=1}^3 Tr_i(n) - \sum_{r=1}^{19} D_r(n) - O(n) \quad (5.3)$$

where $I(n)$ is upstream inflow, $O(n)$ is downstream outflow, $Tr_i(n)$ is tributary flow for tributary i , $i=1,2,3$, $D_r(n)$ is diversion flow for diversion r , $r=1,2,\dots,19$, and $Q_{r,T}(n)$ is the total historic return flow over the entire river section.

In order to check if the simulated return flow due to natural conditions, $C_\rho(n)$, $n=1,\dots,9$; $\rho=1,\dots,57$, is reasonable, the historic return flows $Q_{r,T}(n)$ and the simulated return flows $\sum_{\rho=1}^{57} C_\rho(n)$ are compared. The river mass balance results and the comparison are shown in Table 5.5.

From the comparison several conclusions can be drawn. The simulated return flow due to the natural conditions is decreasing with time and tends toward a steady state. Except for the first time period, the simulated return flow is equal to or less than historical return flow. This is reasonable because the return flows due to irrigation, which is a very important input to the aquifer, during the growing season have not been included.

The big difference between historic return flow and simulated return flow for the first time period may be due to several reasons. The

historic return flow during the first period is much less than the one during other periods because irrigation has just started. The simulated return flow during the first time period is much larger than during other periods because the estimated initial condition brings larger unstable factors at the beginning of the simulation.

The mass balance in Table 5.5 also shows that the historic return flow is of the same order of magnitude as the upstream inflow. This tells that the lateral inflow is as important as upstream inflow for the South Platte River.

Table 5.5
River Mass Balance
(in M³)

PERIOD	Upstream Inflow	St. Vrain	Thompson	Poudre	Outflow	Diversion	Historic Return Flow	Simulated Return Flow
1	.13569E+08	.34717E+07	.10127E+07	.37995E+06	.40466E+07	.22465E+08	.80780E+07	.25276E+08
2	.13933E+08	.44895E+07	.16710E+07	.15585E+07	.12500E+08	.21964E+08	.12812E+08	.13175E+08
3	.13561E+08	.68504E+07	.25885E+07	.66498E+07	.23419E+08	.25166E+08	.18935E+08	.91375E+07
4	.21579E+08	.71783E+07	.36161E+07	.60675E+07	.17814E+08	.35284E+08	.14657E+08	.77216E+07
5	.18102E+08	.66278E+07	.13872E+07	.12013E+07	.66987E+07	.36710E+08	.16090E+08	.70540E+07
6	.14354E+08	.61311E+07	.16882E+07	.10031E+07	.61165E+08	.34712E+08	.17652E+08	.66732E+07
7	.22315E+08	.84064E+07	.18545E+07	.13114E+07	.13138E+08	.35071E+08	.14322E+08	.64221E+07
8	.15213E+08	.62804E+07	.74376E+06	.11156E+07	.13238E+08	.29304E+08	.19189E+08	.62373E+07
9	.12573E+08	.69899E+07	.27891E+07	.12893E+07	.12397E+08	.27290E+08	.16046E+08	.60901E+07

Sensitivity Analysis in Simulation of Return Flows

To study the sensitivity of return flow to errors in the initial water table conditions and river stage drawdown conditions, two runs were made. The first run is made by increasing the aquifer initial drawdowns everywhere by 1.0 meter, and the second run is made by reducing the river stage drawdowns in every reach by 1.0 meter. The return flows for both

cases are all reduced. The results are tabulated in Table 5.6. The results for two cases are almost the same. This is because the effects of increasing aquifer drawdowns and of reducing river stage drawdowns are the same. Both of them are reducing the relative head differences in the aquifer and in the river. However, the change in aquifer drawdowns is for 227 cells while the change in river stage drawdowns is only for 57 reaches. This fact implies that the inaccuracy in the input data in river stage drawdown in one reach obviously will bring more error in result than the one in aquifer drawdown in one cell. From this point of view, the return flow is more sensitive to the input data of river stage drawdowns than aquifer initial conditions.

Table 5.6

Sensitivity Analysis for Return Flows in m³

Time Period	Normal Condition	Increasing Aquifer Drawdown by 1.0 meter	Percentage as compared with normal condition	Reducing River Stage Drawdown by 1.0 meter	Percentage as compared with normal condition
1	.25276E+08	.99346E+07	39%	.99272E+07	39%
2	.13175E+08	.69783E+07	53%	.69646E+07	53%
3	.91375E+07	.58862E+07	61%	.58706E+07	60%
4	.77216E+07	.54336E+07	70%	.54175E+07	70%
5	.70540E+07	.51947E+07	73%	.51783E+07	73%
6	.66732E+07	.50494E+07	76%	.50328E+07	75%
7	.64221E+07	.49499E+07	81%	.49331E+07	81%
8	.62373E+07	.48748E+07	78%	.48579E+07	78%
9	.60901E+07	.48135E+07	79%	.47965E+07	79%

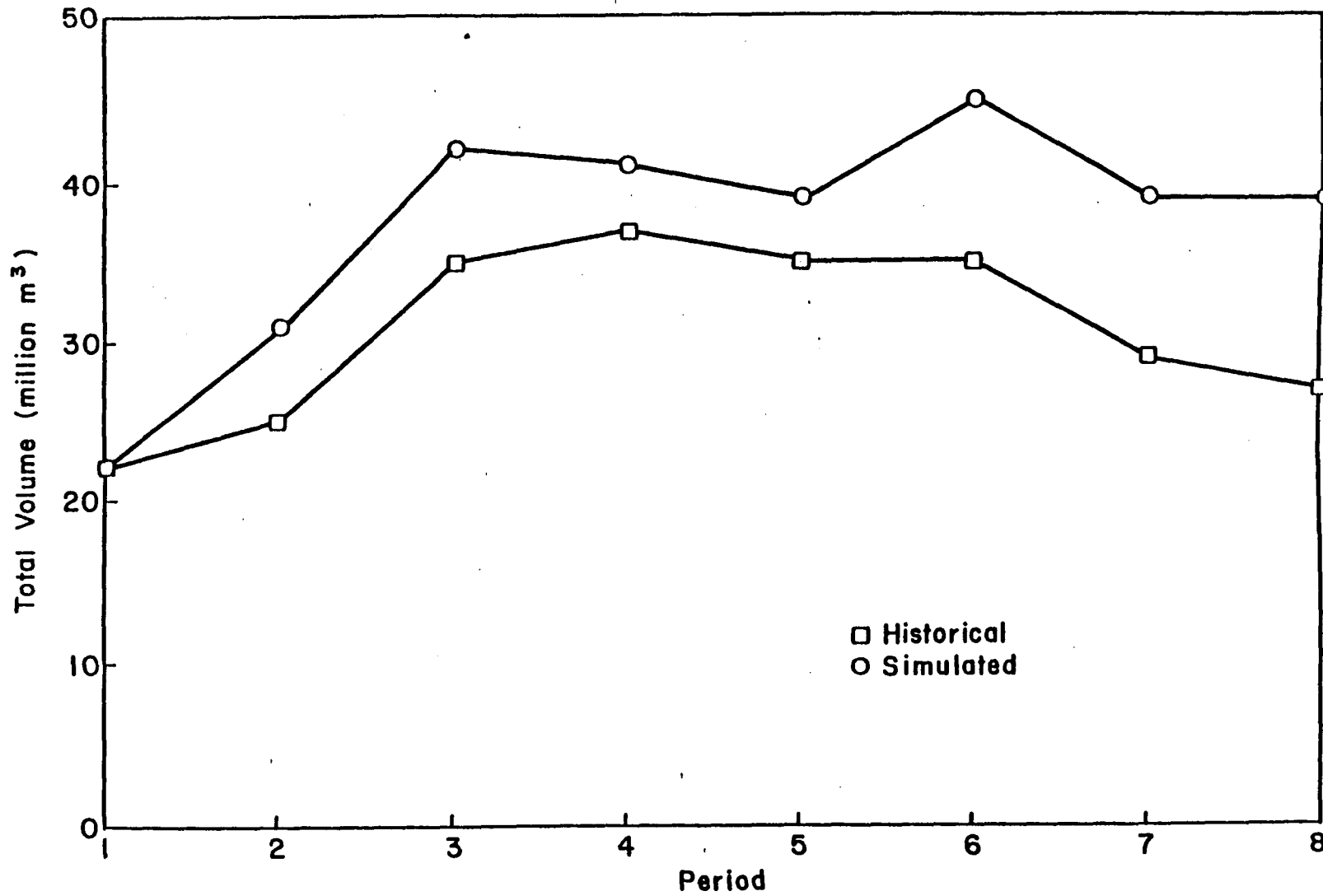


Figure 5.10. Historical and Simulated Diversions for South Platte Basin During the 1968 Irrigation Season.

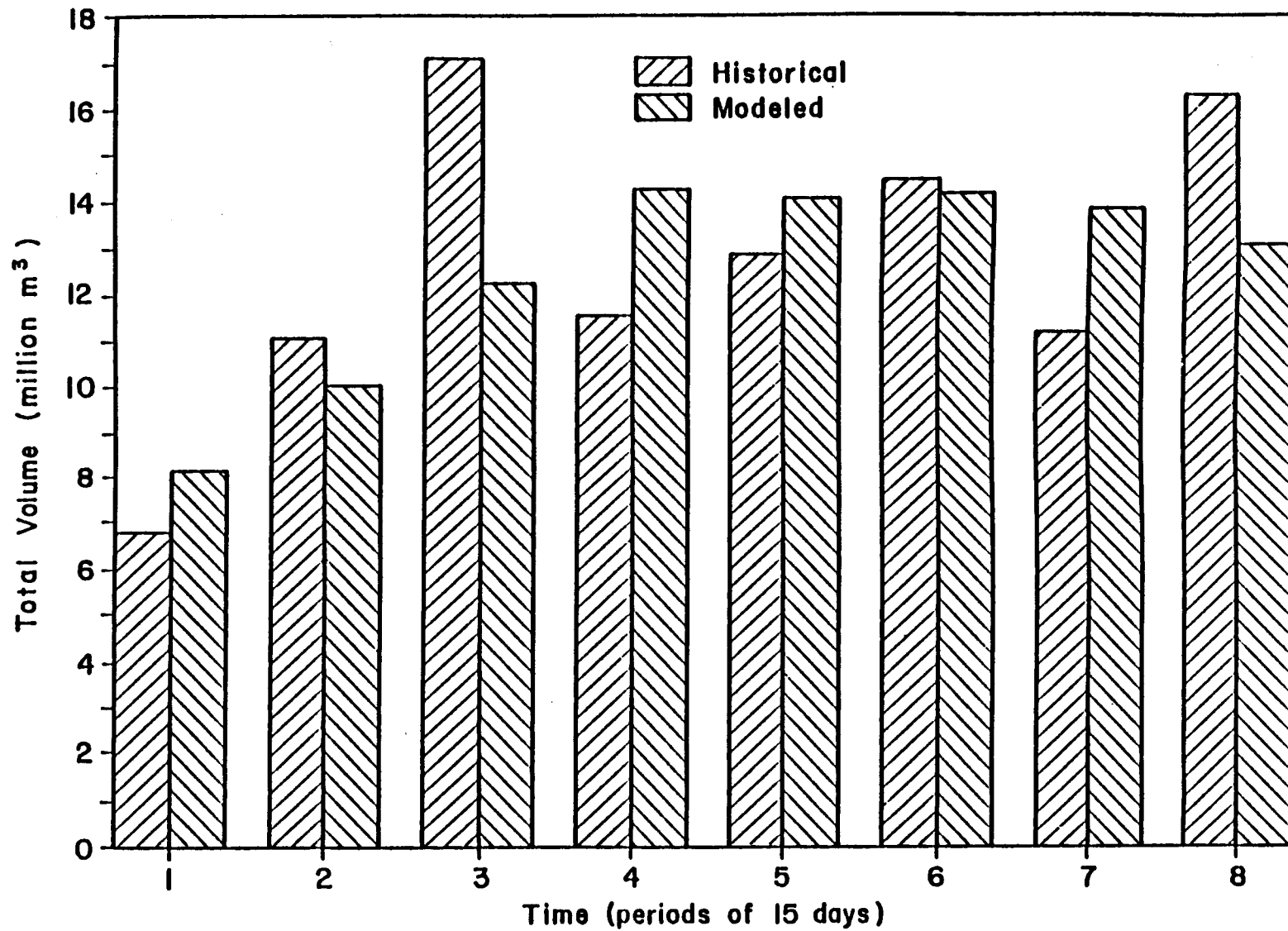


Figure 5.11. Historical and Simulated Total Return Flows for Irrigation Season of 1968 in South Platte Basin.

Long Time Simulation of Return Flows with Different Management Scenarios

The model KERSIM was run for five long time simulations, each of which is for 10 years, with five different scenarios with different economic, legal and agronomic considerations. Different from the short time simulation, the sequential reinitialization technique was used after every 8 time periods up to 240 time periods. The computer time spent on the CYBER 205 for each 10-year simulation is about 200 seconds.

For the basic case simulation, because the simulated diversion flows during the 1968 irrigation season are relatively close to the historical ones as shown in Figure 5.10, the historical and simulated return flows are very close. Figure 5.11 illustrates this fact.

The seasonal total return flow for the whole study area for ten years for this basic case is shown in Figure 5.12. The total return flows for 3 seasons every year are quite different. As expected, during the irrigation seasons, say season 2, 5, 8 ..., etc., the return flow volume reaches its maximum of the year. After the irrigation seasons, say season 3, 6, 9, etc., the amount of return flow drops to a medium value, because there is no irrigation but the influence of irrigation is still felt. For the beginning season of each year, say seasons 4, 7, 10,, etc., the amount of return flow is minimum, because by then the remaining influence of the previous irrigation season is very small. The seasonal total return flow behaves cyclically, much like a sinusoidal curve with period of one year as shown in Figure 5.12.

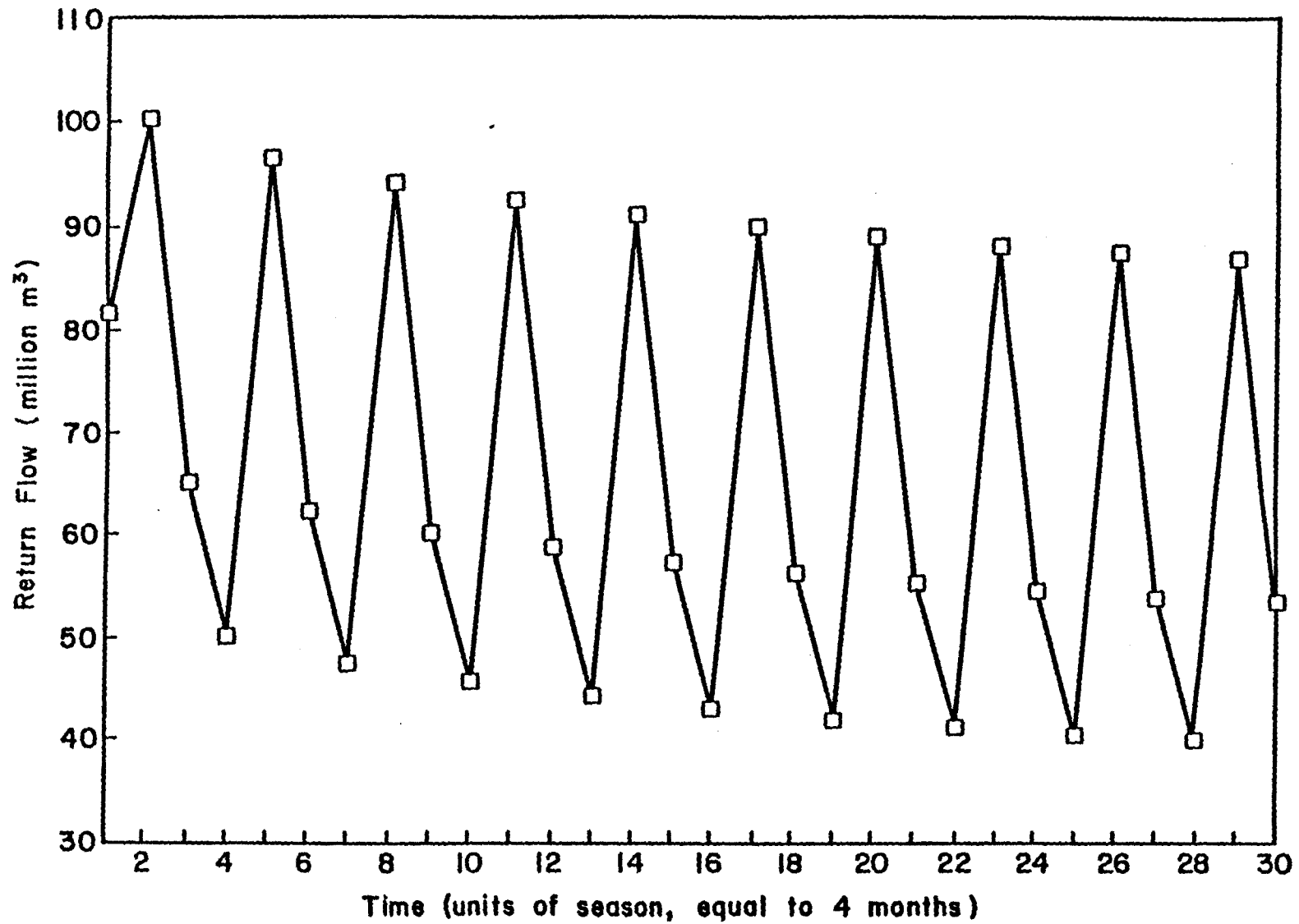


Figure 5.12. Long Term Cyclical Pattern of Seasonal Return Flows in the South Platte Basin.

The seasonal return flow also displays a slight decreasing trend over several years. It seems to level off to a quasi steady-state level. The reason for the decrease at the beginning is probably due to a somewhat erroneous estimation of the initial conditions. The quasi steady-state agrees with the fact that the aquifer water table elevation of the South Platte Basin remains roughly at the same level over the years, as demonstrated by studies carried out by the Climatic Center of CSU. The yearly regular replenishment of the aquifer from irrigation is of course the reason.

The other four simulations were performed for the purpose of evaluation of different management strategies. The analysis of these results is conducted by Jim Booker and Professor Robert A. Young from the Agricultural and Natural Resources Economics Department of Colorado State University. One of them was conducted to evaluate the merit of improved on-farm irrigation efficiency. The traditional irrigation method is ditch siphon, which needs more surface water diversion and causes more seepage. Therefore, it is a method with low efficiency. In order to increase the farm irrigation efficiency, sprinklers were assumed to be used. It needs less surface diversion and causes less seepage. However, after 10 years of simulation, there is about a 35% reduction in return flow from the use of sprinklers. Obviously, this reduction in return flow is due to the reduction in the deep percolation of excess irrigation water to the aquifer. This means that the high irrigation efficiency on individual farms causes the lower efficiency of using water for the study area.

Chapter 6

SUMMARY AND CONCLUSIONS

This study has developed a general methodology for modeling a groundwater system under complex boundary conditions by using the discrete kernel approach. For the particular purpose, this study has applied this method in modeling a stream-aquifer system.

SUMMARY

The aim of modeling a stream-aquifer system is to find out the explicit relationship between input and output of the system in order to conjunctively manage surface and ground waters. The methodology used here is based on the assumption that (1) the groundwater system behaves like a linear system, and the fact that (2) the relationship between the return flow (flux between stream and aquifer) and the head difference between stream and aquifer is linear, a consequence of Darcy's law. Therefore linear system theory has been used throughout the work. The stream-aquifer behavior is described mathematically as a two-dimensional boundary value problem with the presence of the stream introducing a special time-dependent boundary condition of the third type. In particular the principle of superposition, Green's function theory and Duhamel's theorem are used. A finite difference model is used for the numerical generation of the so-called "discrete kernels".

Two kinds of discrete kernels are generated by a finite difference model. One is the aquifer drawdown discrete kernel, which is the response of the aquifer water level at each cell due to a unit pulse of withdrawal excitation. The other is the return flow discrete kernel, which is the response of return flow at each reach due to a unit pulse of withdrawal excitation. These discrete kernels are calculated only once and saved. They are characteristic coefficients which represent the linear relationship between excitations and responses for a particular stream-aquifer system. Simulation or formal mathematical programming optimization for that stream-aquifer system can be easily and cost-effectively implemented for any kind of excitation with any amount of water, at any time and any location.

For cost effectiveness purpose, the technique of sequential reinitialization is used in the model so that the discrete kernels need only be generated within a small "moving" subsystem for a few time periods, which is specially beneficial for a large scale stream-aquifer system to be studied over a long-time horizon.

The accuracy and efficiency of the methodology and computer codes are tested by several illustrative or hypothetical cases. It has been shown that this model is efficient and convenient to simulate the behavior of a stream-aquifer system.

For the specific case of the South Platte River basin, 289 finite difference cells with size of 1 mile by 1 mile are delineated in the area of interest. Of these there are 57 cells which include river reaches. The time period is chosen as 15 days. Thus there are eight time periods within one irrigation season. A "moving" subsystem of 5 by 5 cells is selected because beyond that range the response due to an excitation at

the center of the subsystem is practically negligible. In total 289 times 8 sets of drawdown discrete kernels are generated, each set including 25 drawdown discrete kernels. (57 times 8) sets of return flow discrete kernels are generated simultaneously, each set having no more than 9 non-zero values (depending on the number of reaches included in the subsystem). For such a large scale system with 8 time periods calculation, only 101.974 cp seconds was spent on the Cyber 180/840. With these coefficients saved, the return flows and drawdowns of the aquifer are simulated under natural non-equilibrium conditions for a single irrigation season. The long time (10 years) simulations have also been conducted under different scenarios to evaluate the consequences of changes in political, economical, agronomical and legal policies.

CONCLUSIONS

This section concludes this dissertation in three aspects: the contribution of this study, the applicability and potential uses of this model and recommendations for further study.

Contributions of This Study

It has been realized that the interaction between stream and aquifer, in the case of permanent hydraulic connection, follows the integrated Darcy's law by the previous studies. In previous studies the discrete kernels of drawdowns due to a withdrawal excitation were generated as if the stream did not exist, and in a second step, by superposition, were corrected to reflect the presence of the stream. In this study, this stream-aquifer interaction is simulated directly as a time-dependent third type boundary to an aquifer. Therefore, the solution can be directly

obtained by solution of a boundary-value problem with a boundary of the third type. It makes the concepts clear and straightforward, and the calculation much simpler because the generation of the influence coefficients for drawdowns and for return flows is carried out more effectively in one step.

The discrete kernel approach has been applied in many previous studies of groundwater system or stream-aquifer system. However the boundary conditions in the studies are usually limited in simple and time-independent cases, such as no-flow boundary and constant head boundary. This study develops the methodology to apply the discrete kernel approach in groundwater modeling with complex and time-dependent boundary conditions.

As a powerful assistance, the sequential reinitialization technique has been used in a variety of studies. This study further derives the sequential reinitialization formulas for a stream-aquifer system in a rigorous way instead of only for simple boundary conditions.

Applicabilities And Potential Uses of the Model

This model has a variety of options so it could be used in many different cases. It is particularly suited for modeling a stream-aquifer system where the relationship between stream and aquifer is a permanent hydraulic connection. It is also suited for modeling a groundwater system which is only a part of a large aquifer and the responses of the system does not only depend on the excitations inside the area of interest but also depend on the excitations outside the area of interest. In this case the boundary condition is of the third type. The advantage of this model is the capability to generate the explicit discrete kernels for return

flows or boundary flux. Therefore the influence of the interaction between different water bodies can be directly involved in management.

The results have shown that this stream-aquifer model is really a convenient and cost-effective tool for the evaluation of regional policy variations in a stream-aquifer system. Since this model can detail return flow distributions in space and in time, it can also be used in a regional water resources planning for determination of optimal strategies, such as pumping pattern or artificial groundwater recharge pattern by mathematical optimization. For example, this model has great potential for studies of direct estimation of reductions in return flows in space and in time due to any pattern of withdrawals. The model is potentially a great tool for realistic adjudication and administration of conjunctive water use with full respect for the current water laws.

Recommendation for Further Study

For the current objectives of study, this model does not consider the dynamics in the river and the influence of the aquifer on the river. For further study, these components should be better involved in a more complete stream-aquifer model especially for operation purposes.

REFERENCES

- Albin, Donald R. and Hurr, Theodore R., 1972, "Map Showing Transmissivity of the Valley-Fill Aquifer in the Brighton Reach of the South Platte River Valley, Colorado," USGS, Open-file Map.
- Albin, Donald R. and Hurr, Theodore R., 1972, "Map Showing Transmissivity of the Valley-Fill Valley in the Greeley Reach of the South Platte River Valley, Colorado," USGS, Open-File Map.
- Bear, Jacob, 1979. "Hydraulics of Groundwater," 569 pages, McGraw-Hill Book Company.
- Bouwer, H., 1969. "Theory of Seepage from Open Channel."
- Bouwer, H., 1978. "Groundwater Hydrology," McGraw-Hill Book Company, 480 pages.
- Carpenter, L.G., 1896. "Seepage of Return Water from Irrigation," The Agriculture Experiment Station, Bulletin 33.
- Carpenter, L.G., 1916. "Seepage and Return Waters," the Agriculture Experiment Station, Bulletin 180.
- Carslaw, H. S., 1921. "The Conduction of Heat", MacMillan and Co., pp. 152.
- Carslaw, H.S. and Jaeger, J.C., 1959. "Conduction of Heat in Solids," Oxford, 510 pages.
- Dreizin, Y. C. and Y. Y. Haimes, 1977. "A Hierarchy of Response Functions for Groundwater Management", Water Resources Research, Vol. 13, No. 1, Feb. 1977.
- Glover, R. E. and B.G. Balmer, 1954. "River Depletion Resulting from Pumping a Well near a River", Trans. Amer. Geophys. Union, Vol. 35, No. 3, pp. 468-470.
- Hornberger, G. M., Ebert, J. and Remson, I. "Numerical Solution of the Boussinesq Equation for Aquifer-Stream Interactions." Water Resources Research, Vol. 6, No. 2, pp. 601-608, April 1970.
- Jenkins, C. T., 1968. "Techniques for Computing Rate And Volume of Stream Depletion by Wells", Ground Water, Vol. 6, No. 2, pp.37-46.

- Jenkins, C. T., 1969. "Electric-Analog and Digital-Computer Model Analysis of Stream Depletion by Wells", *Ground Water*, Vol. 6, No. 6, pp. 27-34.
- Illangasekare, T.H., 1978. "Influence Coefficients Generator Suitable for Stream-Aquifer Management," Ph.D. Dissertation, Colorado State University, 1978.
- Illangasekare, T.H., and H.J. Morel-Seytoux, 1982. "Stream-Aquifer Influence Coefficients as Tools for Simulation and Management", *Water Resources Research*, Vol. 18, No. 1, pp. 168-176, Feb. 1982.
- Illangasekare, T.H., Morel-Seytoux, H.J. and Verdin, K.L., 1984. "A Technique of Reinitialization for Efficient Simulation of Large Aquifer Using the Discrete Kernel Approach," *Water Resources Research*, Vol. 20, No. 11, pp. 1733-1742, November 1984.
- Maddock, T., III, 1972. "Algebraic Technological Function from a Simulation Model", *Water Resources Research*, Vol. 8, No. 1, Feb. 1972, pp.120-134.
- Maddock, T., III., 1974. "The Operation of a Stream-Aquifer System Under Stochastic Demands", *Water Resources Research*, Vol. 10, No. 1, Feb. 1974, pp. 1-10.
- Morel-Seytoux, H. J., R. A. Young, and G. Radosevich, 1973. "Systematic design of legal regulations for optimal surface groundwater usage", Final report to OWRR, Colorado Water Resources Research Institute, Completion Report Series No. 53, August 1973, 81 pages.
- Morel-Seytoux, H.J. and Daly, C.J., 1975. "A Discrete Kernel Generator for Stream-Aquifer Studies," *Water Resources Research*, Vol. 11, No. 2, pp. 253-260, April 1975.
- Morel-Seytoux, H.J., 1975. "A Combined Model of Water Table and River Stage Evolution," *Water Resources Research*, Vol. 11, No. 6, December 1975, pp. 968-972.
- Morel-Seytoux, H.J., 1979. "Cost Effective Methodology for Stream-Aquifer Interaction Modeling and Use in Management of Large Scale System." Hydrowar Report, Hydrology Days Publications, 1005 Country Club Road, Fort Collins, Colorado 80524, 60 pages.
- Morel-Seytoux, H. J., T., Illangasekare, M. W. Bittinger and N. A. Evans, 1980. "Potential Use of a Stream-Aquifer Model for Management of a River Basin: Case of the South Platte River in Colorado", *Prog. Wat. Tech.* Vol 13, Cincinnati. pp. 175-187.
- Morel-Seytoux, H.J., 1985. "Conjunctive Use of Surface and Ground Waters," Chapter 3 in *Artificial Recharge of Groundwater*, T. Asano, ed., Butterworth Publishers, Boston, pp. 35-67.
- Morel-Seytoux, H.J., 1985. "Optimal Ground Management," Handout No. F85-632-5 for course CE632, Fall 1985.

- Morel-Seytoux, H. J., 1986. "Engineering Hydrology: Ensemble of Lecture Notes and Class Handouts Developed since 1977." Hydrowar Report, Hydrology Days Publications, 1005 Country Club Road, Fort Collins, Colorado 80524, 300 pages
- Morel-Seytoux, H. J., 1987. "Value and Role of Conjunctive Use of Surface and Ground Waters in River Basin Water Management." Proc. Inter. Symp. on Water for the Future, Rome, April 6-11, 1987. Edited by W. O. Wunderlich and J. E. Prins, A. A. Balkema Publishers, Rotterdam, pp. 515-524.
- Morel-Seytoux, H.J., Restrepo, J.I. and Rathnayake, R.M.D., 1985. S.A.M.S.O.N.: Executive Summary, "Description of Samson Computer System General Flow Chart, Flow Charts for Thirteen Basic Blocks and Subroutine Documentation," October 1985.
- Myers, Glen E., 1971. "Analytical Methods in Conduction Heat Transfer," McGraw-Hill Book Company.
- Necati-Özisik, M., 1968. "Boundary Value Problem of Heat Conduction," International Textbook Company, 505 pages.
- Parshall, Ralph L., 1922. "Return of Seepage Water to The Lower South Platte River in Colorado," Colorado Agriculture Experiment Station, Bulletin 279.
- Peters, G.C. and Morel-Seytoux, H.J., 1977. "User's Manual for DELPET:A FORTRAN IV Discrete Kernel Generator for Stream-Aquifer Studies, HYDROWAR Program," Colorado State University, December 1977.
- Peters, G.C., 1978. "Modeling Aquifer Return Flows And Non-Equilibrium Initial Conditions", Thesis, Colorado State University, Spring, 1978.
- Pinder, S. and Sauer, S. P. "Numerical Simulation of Flood Wave Modification due to Bank Storage Effect." Water Resources Research. 7(1), pp. 63-70, 1971.
- Restrepo, J. I., 1987. "A Surface and Ground Water Model for the Conjunctive Use of a Stream-Aquifer System," Ph.D. Dissertation, Colorado State University, Fort Collins, Colorado, Spring 1987, 226 pages.
- Schneider, Paul A., Jr., 1972. "Map Showing Water-Table Contours of The Valley-Fill Aquifer in the Brighton Reach of The South Platte River Valley, Colorado," March 1968, USGS, Open-File Map, Plate 3.
- Schneider, Paul A., Jr., 1972. "Map Showing Water-Table Contours of The Valley-Fill Aquifer in the Greeley Reach of The South Platte River Valley, Colorado," March 1968, USGS, Open-File Map.
- Schneider, Paul A., Jr., 1972. "Map Showing Saturated Thickness of The Valley-Fill Aquifer in The Greeley Reach of The South Platte River Valley, Colorado," March 1968, USGS, Open-File Map.

- Schneider, Paul A., Jr., 1972. "Map Showing Water-Table Contours of The Valley-Fill Aquifer in The Brighton Reach of The South Platte River Valley, Colorado," March 1968, USGS, Open-File Map.
- Theis, C. V., 1941. "The Effect of a Well on the Flow of a Nearby Stream.", Trans. Amer. Geophys. Union, Part 3, pp. 734-738.
- Verdin, Kristine L., Morel-Seytoux, H.J. and Illangasekare, T.H., "User's Manual for AQUISIM:FORTRAN IV Programs for Discrete Kernel Generation and for Simulation of an Isolated Aquifer Behavior in Two Dimensions," December 1981, HYDROWAR Report, Hydrology Days Publications, Fort Collins, Colorado 80524, 150 pages.
- Young, Robert A., Daubert, John T. and Morel-Seytoux, Hubert J., 1986. "Evaluating Institutional Alternatives for Managing an Interrelated Stream-Aquifer System, American Journal of Agriculture Economics," Vol. 68, No. 4, November 1986, pp. 787-797.
- Zhang, C.- M. and H. J. Morel-Seytoux, 1989. "User's Manual for KERNEL, KERGEN and KERSIM: FORTRAN V Programs for the Simulation of the Behavior of a Stream-Aquifer System in Response to Excitations." Hydrowar Report in preparation, and expected for completion in December 1989.
- Zeta, V. L. and Wiggert, J. M. "Flood Routing in Channels with Bank Storage." Water Resources Research, &(5), pp. 1341-1345, 1971.